Title	Development of Micro/Mesofluidic Chemiluminescence Techniques Using Flow based Technology for Monitoring Selected Trace Heavy Metals in Environmental Samples
Author	Mr.Narin Toakaenchan
Degree of	Doctor of Philosophy in Applied Chemistry
Advisory Committee Chairperson	Assistant Professor Dr.Sakchai Satienperakul

ABSTRACT

The works reported in this thesis covers the application of chemiluminescence techniques to develop two unrelated flow based methods for the determination of arsenic and cadmium in environmental samples. In the first part of this thesis, the simultaneous determination of As(III) and As(V) in aqueous solution, based on the acidic permanganate and luminol chemiluminescence (CL) detection systems, have been applied to a split microfluidics flow injection (μFI) with dual-channel manifolds at rapid sampling rate. The μFI-CL system consisted of two halves of micro-conduit platforms, which ran on a simple device made from small pieces of the laser engraved polymethylmethacrylate (PMMA) and polydimethylsiloxane (PDMS). The specific CL reaction for As(III) was produced by the oxidation of acidic potassium permanganate in the presence of a sodium hexametaphosphate media, while the CL reaction for As(V) was generated based on the oxidation of luminol with a vanadomolybdoarsenate heteropoly acid (AsVMo-HPA) complex in an alkaline solution. The μFI method involved the injection of the mixed standard solution into an acid carrier stream, where it was then splitted and merged with the reagent solutions of each reaction systems on a spiral-designed microfluidic platform. The solution mixtures were passed through each spiral flow channel, where the CL intensity of both resulting reaction mixtures were measured with two photomultiplier tubes. Linear calibrations for As(III) and As(V)were established over the concentration ranges of 20-60 μg L^{-1}. The limits of detection (signal-to-noise ratio of 3) of As(III) and As(V) were found to be 4 μg L^{-1} and the limits of quantification (signal-to-noise ratio of 10) were found to be 10 μg L^{-1}, respectively. The

proposed procedure was successfully applied to determine As(III) and As(V) in ground water samples.

In the second part, a sensitive flow injection chemiluminescence procedure was proposed for determination of cadmium in environmental samples coupled with an off-line preconcentration step. A mini column, packed with polystyrene beads as an adsorption material, was used for the preconcentration of Cd(II) ions based on the complex formation with ammonium pyrolidinedithiocarbamate (APDC). The Cd-APDC complex adsorbed on polystyrene beads was eluted by methanol and subsequently determined by the flow injection chemiluminescence system. The chemiluminescence reaction was based on Cd(II) catalyzing the luminol-H_2O_2 CL reaction in the present of alkaline media. Under the optimum condition a linear calibration graph was obtained over the concentration range 2-6 μg L^{-1}. The limits of detection of cadmium ($3SD_{blank}$ /slope) was found to be 0.6 μg $L^{-1}$and the limits of quantification (10 SD_{blank} /slope) were found to be 2.0 μg L^{-1}, respectively .The proposed procedure was successfully applied for the determination of Cd(II) in contaminated soils from a nearby coal mining area.

For the final part of this thesis a new approach to enhance the electrogenerated chemiluminescence (ECL) of the tris(2, 2′-bipyridyl)ruthenium (II)($Ru(bpy)_3^{2+}$) system was proposed using resonance energy transfer with L-cysteine-capped cadmium telluride quantum dots (CdTe-QDs) in aqueous solution. The oxidative peak signal of $Ru(bpy)_3^{2+}$ occurred at a voltage of 1.10 V, when the potential was cycled between 0.4 and 1.6 V using cyclic voltammetry with a carbon screen-printed electrode (SPEC) in a 0.11 M phosphate buffer at pH 7.50. The L-cysteine-capped cadmium telluride quantum dots (CdTe-QDs) were synthesized and added into the solution of $Ru(bpy)_3^{2+}$ to magnify the ECL sensor. The ECL emission signal was measured by a red-sensitive photomultiplier tube set at a constant potential of 850 V. The extreme enhancement of the ECL intensity was achieved via the energy transfer by the L-cysteine-capped CdTe-QDs. It was found that the induced ECL from the $Ru(bpy)_3^{2+}$CdTe-QDs system was inhibited by the presence of selected nitrofurans. This quenching effect of nitrofuran antibiotics on the anodic ECL of $Ru(bpy)_3^{2+}$CdTe-QDs was found to be selective and concentration dependent and was observed to have a linear relationship over the concentration range 10-100×10^{-6} M. The detection limits were found to be 0.40, 0.73 and 0.60 μM for furaltadone (FTD), furazolidone (FZD) and nitrofurantoin (NFT). In addition, the proposed ECL method was

successfully applied to detect the total residuals of selected nitrofuran residues in animal feed samples with satisfactory results.

ชื่อเรื่อง	การพัฒนาเทคนิคไมโคร/มีโซฟลูอิดิกส์เคมิลูมิเนสเซนซ์ด้วยเทคโนโลยีการวิเคราะห์ โดยอาศัยการไหลสำหรับการติดตามโลหะหนักปริมาณน้อยบางชนิด ในตัวอย่างทางสิ่งแวดล้อม
ชื่อผู้เขียน	นายนรินทร์ ท้าวแก่นจันทร์
ชื่อปริญญา	ปรัชญาดุษฎีบัณฑิตสาขาวิชาเคมีประยุกต์
ประธานกรรมการที่ปรึกษา	ผู้ช่วยศาสตราจารย์ ดร.ศักดิ์ชัย เสถียรพีระกุล

บทคัดย่อ

รายงานในดุษฎีนิพนธ์ฉบับนี้ ประกอบด้วยการศึกษาและพัฒนาระบบการตรวจวัดชนิดโฟลอินเจคชันเคมิลูมิเนสเซนต์สองระบบ สำหรับการวิเคราะห์หาปริมาณสารหนู และ แคดเมียม ในตัวอย่างจากธรรมชาติ

ในส่วนแรกที่ได้ทำการศึกษาคือ การวิเคราะห์ปริมาณสารหนู (III) และ สารหนู (V) ในตัวอย่างน้ำธรรมชาติ ด้วยระบบสปลิทโฟลว์ไมโครฟูอิดิกแบบสองช่องทาง ร่วมกับการตรวจวัด เคมิลูมิเนสเซนต์แบบระบบสองช่องสัญญาณ โดยอุปกรณ์ไมโครฟูอิดิกโฟลว์เซลล์ประกอบด้วยแผ่นวัสดุ 2 ชิ้น แต่ละชิ้นจะมีท่อขนาดเล็กรูปก้นหอย แผ่นวัสดุสร้างมาจากแผ่นโพลีเมทิลเมทะคริเลต (PMMA) และ แผ่นโพลีไดเมทิลไซลอกเซน (PDMS) ท่อขนาดเล็กและรูปแบบของก้นหอยสร้างด้วยเทคนิคแกะสลักด้วยเลเซอร์ เมื่อสารละลายมาตรฐานและตัวอย่างผสม ถูกฉีดเข้าสู่กระแสตัวพาในสภาวะที่เป็นกรด จะถูกแบ่งออกเป็นสองส่วน โดยส่วนแรกจะเกิดปฏิกิริยากับสารละลายโปแทสเซียมเปอร์แมงกาเนตในสภาวะกรด ภายใต้กระแสตัวพาโซเดียมเฮกซะเมตตาฟอสเฟต และไหลผ่านเข้าสู่ไมโครฟูอิดิกโฟลว์เซลล์ ตรวจวัดด้วยหลอดขยายสัญญาณชนิดไวต่อแสงสีแดง ในส่วนที่สองถูกผสมกับรีเอเจนต์แอมโมเนียมโมลิบเดต และแอมโมเนียมเมตะวานาเดต ในสภาวะด่าง เกิดเป็นสารประกอบเชิงซ้อนวานาโดโมลิบโดอาร์ซีเนตเฮทโทโรโพลีแอซิด (AsVMo-HPA) กราฟมาตรฐานสำหรับสารหนู (III) และ สารหนู (V) มีช่วงเป็นเส้นตรง ในช่วงความเข้มข้น 20-60 ไมโครกรัมต่อลิตร ค่าขีดจำกัดต่ำสุดของการตรวจวัด (3 เท่าของส่วนเบี่ยงเบนมาตรฐานที่ได้จากสัญญาณรบกวน)สำหรับสารหนู (III) และ สารหนู (V) มีค่าเท่ากับ 4.0 ไมโครกรัมต่อลิตร ค่าขีดจำกัดของการวิเคราะห์ปริมาณ (10 เท่าของส่วนเบี่ยงเบนมาตรฐานที่ได้จากสัญญาณรบกวน) สำหรับสารหนู (III) และ สารหนู (V) มีค่าเท่ากับ 10.0ไมโครกรัมต่อลิตร

วิธีการที่พัฒนาขึ้นสามารถนำไปตรวจวิเคราะห์หาปริมาณสารหนู (III) และ สารหนู (V) ที่ตกค้างในตัวอย่างน้ำผิวดินได้

ระบบโฟลอินเจคชันเคมิลูมิเนสเซนต์ที่สอง ที่ได้พัฒนาขึ้นร่วมกับกระบวนการเพิ่มความเข้มข้น ใช้สำหรับวิเคราะห์ หาปริมาณแคดเมียม ที่ตกค้างในตัวอย่างทางสิ่งแวดล้อม โดยทำการบรรจุเม็ดพอลีสไตรีนลงในคอลัมน์ขนาดเล็กเพื่อทำหน้าที่เป็นตัวดูดซับ สารประกอบระหว่างแคดเมียมไอออนและ APDC จะถูกชะออกมาด้วยเมทานอล หลังจากนั้นจึงทำการวิเคราะห์ด้วยเทคนิคของโฟลอินเจคชันเคมิลูมิเนสเซนต์ปฏิกิริยาเคมิลูมิเนสเซนต์ เกิดจากปฏิริยาเร่งระหว่างแคดเมียมไอออน กับ ลูมินอล ไฮโดรเจนเปอร์ออกไซด์ ภายใต้สภาวะด่าง ภายใต้สภาวะที่เหมาะสม ได้กราฟมาตรฐานเป็นเส้นตรงในช่วงความเข้มข้น 2-6 ไมโครกรัมต่อลิตร ค่าขีดจำกัดต่ำสุดของการตรวจวัด (3 เท่าของส่วนเบี่ยงเบนมาตรฐานที่ได้จากสัญญาณรบกวน/ความชัน) มีค่าเท่ากับ 0.6 ไมโครกรัมต่อลิตร ค่าขีดจำกัดของการวิเคราะห์ปริมาณ (10เท่าของส่วนเบี่ยงเบนมาตรฐานที่ได้จากสัญญาณรบกวน/ความชัน) มีค่าเท่ากับ 2.0 ไมโครกรัมต่อลิตร วิธีการที่พัฒนาขึ้นสามารถนำไปตรวจวิเคราะห์หาปริมาณแคดเมียมที่ตกค้างในตัวอย่างดิน ที่พบการปนเปื้อนจากแหล่งเหมืองได้

ในส่วนสุดท้ายที่ได้ทำการศึกษาวิธีการวิเคราะห์ปริมาณสารกลุ่ม ไนโตรฟิวราน ด้วยเทคนิคอิเลคโครเคมิลูมิเนสเซนต์ (ECL) จากปฏิกิริยาของ ทริส(2,2′-ไบไพริดิล)รูทีเนียม (**II**)และ แอล-ซิสเตอิน-ควอนตัมดอท โดยงานวิจัยนี้ได้ทำการสังเคราะห์แอล-ซิสเตอิน-ควอนตัมดอท และได้เติมลงไปในสารละลายของ ทริส(*2,2*'-ไบไพริดิล)รูทีเนียม(**II**) ในสารละลายฟอสเฟตบัฟเฟอร์ pH 7.5 เมื่อให้ศักย์ไฟฟ้าตั้งแต่ +0.4 - +1.6 โวลต์ ด้วยเทคไซคลิกโวลแทมเมตรี พบว่า ที่ศักย์ไฟฟ้าเท่ากับ 1.1 โวลต์ จะเกิดออกซิเดชันพีค พร้อมกับเกิดการคายแสงออกมา ซึ่งสามารถวัดแสงดังกล่าวด้วยหลอดขยายสัญญาณแสง ที่ศักย์ไฟฟ้าเท่ากับ 850 มิลลิโวลต์ ปริมาณแสงที่เพิ่มขึ้นเกิดการจากการถ่ายโอนพลังงานของแอล-ซิสเตอิน-ควอนตัมดอทที่เติมลงไป

จากปฏิกิริยาอิเลคโครเคมิลูมิเนสเซนต์ ของ ทริส(*2,2*'-ไบไพริดิล)รูทีเนียม(**II**) และ แอล-ซิส*เ*ตอิน-ควอนตัมดอท พบว่าเมื่อมีสารกลุ่ม ไนโตรฟิวราน ปริมาณแสงที่เกิดขึ้นจากปฏิกิริยาดังกล่าวมีค่าลดลง ซึ่งอาจเกิดจากระบวนการยับยั้งในปฏิกิริยาอิเลคโครเคมิลูมิเนสเซนต์ภายใต้สภาวะที่เหมาะสมดังกล่าวจะทำให้สามารถทำการวิเคราะห์สารกลุ่มไนโตรฟิวรานได้ในช่วงความเป็นเส้นตรงอยู่ในช่วง 10-100$\times10^{-6}$ โมลาร์ ค่าขีดจำกัดต่ำสุดของการตรวจวัด ฟูรัลทาโดน (FTD) ไนโตรฟูแรนโตอิน (FZD) และ ไนโตรฟูราโซน (NFT) มีค่าเท่ากับ 0.40 0.73 และ 0.60 ตามลำดับวิธีการดังกล่าวนี้สามารถนำไปตรวจหาปริมาณสารตกค้างกลุ่มไนโตรฟิวราน ในตัวอย่างของอาหารสัตว์ได้

ACKNOWLEDGEMENTS

I would like to express my sincere appreciation to all who gave me the support to complete this thesis.

First of all, I would like to express my sincere gratitude and appreciation to Assistant Professor Dr. Sakchai Satienperakul, my supervisor, for his kind supervision, encouragement and inspiring discussions throughout the years of my studies. To my advisory committee, Assistant Professor Dr. Sirirat Phaisansuthichol, Assistant Professor Dr. Pusit Pookmanee, Dr. Tanin Tangkuaram, Dr. Supaporn Sangsrichan, Dr. Ratchadaporn Puntharod and Dr. Surasak Kuimalee many thanks for their invaluable guidance during my study at Maejo University. And to the examination chairperson, Associate Professor Dr. Boonsom Liawruangrath for her vital helpful suggestions and helpful review to complete this thesis.

My sincere acknowledgement are extended to the financial supports form the National Research Council of Thailand (NRCT) and the Faculty of Science, Maejo University.

To the Department of Primary Industries and Mines Region 3 Chiang Mai, Dr. Ponlayuth Sooksamiti, for providing soil samples used in this work.

Thanks are also expressed all staff members of the Department of Chemistry, Faculty of Science, Maejo University for providing help one way or another that contributed to the success of this work.

Finally, I wish to express my heartfelt gratitude to my father, mother and family for their source of inspiration, tender love, care and endless encouragement throughout the long years of my study.

Narin Taokaenchan

APPENDIX

APPENDIX A

VITA

VITA

Name **Mr. Narin Taokaenchan**

Date of Birth **14 October 1978**

Research Work and Awards

Publications

1. Narin Taokaenchan, Tanin Tangkuaram, Pusit Pookmanee and Sakchai Satienperakul. 2012. Microfluiddic chmiluminesceence device for Arsenic (III) determination in Thai traditional herbs. PACCON 2012 proceeding book.
2. Narin Taokaenchan, Rudchadaporn Puntharod, Tanin Tangkuaram, Pusit Pookmanee, Sirirat Phaisansuthichol, Supaporun Sangsrichan and Sakchai Satienperakul. 2014. Specific speciation of As(III) and As(V) in aqueous solution by a split microfluidic chemiluminescence system. Journal of Flow Injection Analysis. Vol. 31, No. 1. 27-37.
3. Narin Taokaenchan, TaninTangkuaram, Pusit Pookmanee, Sirirat Phaisansuthichol, Surasak Kuimalee and Sakchai Satienperakul. Enhanced electrogeneratedchemiluminescence of tris(2,2′-bipyridyl)ruthenium(II) system by L-cysteine-capped CdTe quantum dots and its application for the determination of nitrofuran antibiotics. 2015. Biosensors and Bioelectronics. Accepted.

Presentations

International Conference

1. Narin Taokaenchan, Tanin Tangkuaram, Pusit Pookmanee and Sakchai Satienperakul. 2012. Microfluiddic chmiluminesceence device for Arsenic (III) determination in Thai traditional herbs. Pure and Applied Chemistry International Conference, January 11-13, The Empress Chaing Mai hotel. Thailand.
2. Narin Taokaenchan, Tanin Tangkuaram, Posit Pookmanee, Sirirat Phaisalsuthichol, Supaporn Sangsrichan and Sakchai Satienerakul. 2012. Simultaneous determination of arsenite and arsenate in aqueous solution by a split flow injection chemiluminescence system. SPEC 2012 : Shedding New Light on Disease conference, November 11-16, Chiang Mai, Thailand.
3. Narin Taokaenchan, Tanin Tangkuaram, Pusit Pookmanee, Sirirat Phaisalsuthichol, and Sakchai Satienperakul. 2013. Electrochemiluminescence from tris(2,2′-bipyridyl) ruthenium (II) in the presence of L-cysteine-capped CdTe quantum dots and its application for the determination of selected nitrofurans antibiotic residues. ASEAN^{+}. 2013. The 2nd Regional Symposium on Biosensors, Biodiagnostics and Biochips. December 11-13, Mae Fah Luang University, Thailand.
4. Narin Taokaenchan, Ratchadaporn Puntharod, Tanin Tangkuaram, Pusit Pookmanee, Sirirat Phaisalsuthichol, Supaporn Sangsrichan and Sakchai Satienperakul. 2014. Specific speciation of As(III) and As(V) in aqueous solution by a split microfluidic chemiluminescence system. International Symposia on Research towards Green Innovation. January 14. Chiang Mai, Thailand.

5. Narin Taokaenchan, Tanin Tangkuaram, Pusit Pookmanee, Sirirat Phaisalsuthichol, and Sakchai Satienperakul. 2014. Enhanced electrogeneratedchemiluminescence of tris(2,2′-bipyridyl)ruthenium(II)system by L-cysteine-capped CdTe quantum dots and its application. Biosensors. 2014 : 26th Anniversary World Congress on Biosensors, 23-27 May 2014, Melbourne, Australia.

APPROVAL SHEET

GRADUATE SCHOOL, MAEJO UNIVERSITY

THE DEGREE OF DOCTOR OF PHILOSOPHY IN APPLIED CHEMISTRY

Title

DEVELOPMENT OF MICRO/MESOFLUIDIC CHEMILUMINESCENCE TECHNIQUES USING FLOW BASED TECHNOLOGY FOR MONITORING SELECTED TRACE HEAVY METALS IN ENVIRONMENTAL SAMPLES

By

NARIN TAOKAENCHAN

APPROVED BY

Advisory Committee Chairperson ..... S. Satienperakul

(Assistant Professor Dr.Sakchai Satienperakul)

14 / NOV / 2014

Advisory Committee Member ..... P. Sirirat

(Assistant Professor Dr.Sirirat Phaisansuthichol)

14 / NOV / 2014

Advisory Committee Member ..... Pusit Pookmanee

(Assistant Professor Dr.Pusit Pookmanee)

14 / NOV / 2014

Advisory Committee Member ..... Tanin Tangkuaram

(Dr.Tanin Tangkuaram)

14 / NOV / 2014

Advisory Committee Member .....

(Dr.Supaporn Sangsrichan)

14 / Nov. / 2014

Chairperson, Committee on Philosophy of Science ..... Tanin Tangkuaram

Program in Applied Chemistry

(Dr.Tanin Tangkuaram)

14 / NOV / 2014

CERTIFIED BY GRADUATE SCHOOL ..... J. Varith

(Assistant Professor Dr.Jatuphong Varith)

14 / NOV / 2014

CHAPTER 1

INTRODUCTION

1.1 Flow injection analysis (FIA)

Flow injection analysis (FIA) is a simple, rapid, and versatile technique that is now firmly established, with widespread application in quantitative chemical analysis. This is apparent from the number of related papers that have appeared in the technical press since 1975, and since then the scope of the method has grown at an unprecedented rate. Over 10,000 papers devoted to FIA have been published in scientific journals up to now. The designation of FIA was proposed in 1975 by Ruzicka and Hansen (Ruzicka and Hansen, 1975). The inclusion of the term injection in the name of this technique occurred because the technique originally entailed using a syringe to inject a sample through a septum into a reagent flow. Currently, rotation valves are mainly used for this purpose. FIA may be defined as the sequential insertion of discrete sample solution into an unsegmented continuously flowing stream with subsequent detection of the analyte. Even this definition, however, is frequently made obsolete by new developments. The first definition, given by Ruzicka and Hansen was "A method based on injection of a liquid sample into a moving unsegmented continuous stream of a suitable liquid. The injected sample forms a zone, which is then transported toward a detector that continuously records the absorbance, electrode potential, or any other physical parameter, as it continuously changes as a result of the passage of sample material through the flow cell".

The concept of FIA depends on a combination of three factors: reproducible sample injection volumes, controllable sample dispersion, and reproducible timing of the injected sample through the flow system. Except for detector warm-up, the system is ready for instant operation as soon as the sample is introduced. FIA offers several advantages in term of : considerable decrease in sample (normally using 10 to 50 μL) and reagent consumption, high sample throughput (50 to 300 samples per hour) reduced residence times (reading time is about 3 to 40 s), shorter reaction times (3 to 60 s), easy switching from one analysis to another (manifolds are easily assembled and/or exchanged), reproducibility (usually less than 2% RSD), reliability, low carry over, high degree of flexibility, and ease of automation. Perhaps the most compelling advantage of the FIA technique is the great reproducibility in the results obtained by this

technique that can be set up without excessive difficulties and at very low cost of investment and maintenance. These advantages have led to an extraordinary development of FIA, unprecedented in comparison to any other technique.

1.1.1 Principle of the FIA

The three principles or cornerstones of FIA were identified by Ruzicka and Hansen as sample injection, controlled dispersion of the injected sample zone, and reproducible timing of the movement of the injected zone from the injection point to the detector. More recent developments of FIA showed that sample injection should be understood in a much broader sense. It follows that neither the timing of zone movement nor the control of dispersion should be restricted to those of injected samples. Although dependent on the other two principles, the central issue of FIA is the control of dispersion, which is the very basis for extraction of analytical data under non equilibrium conditions.

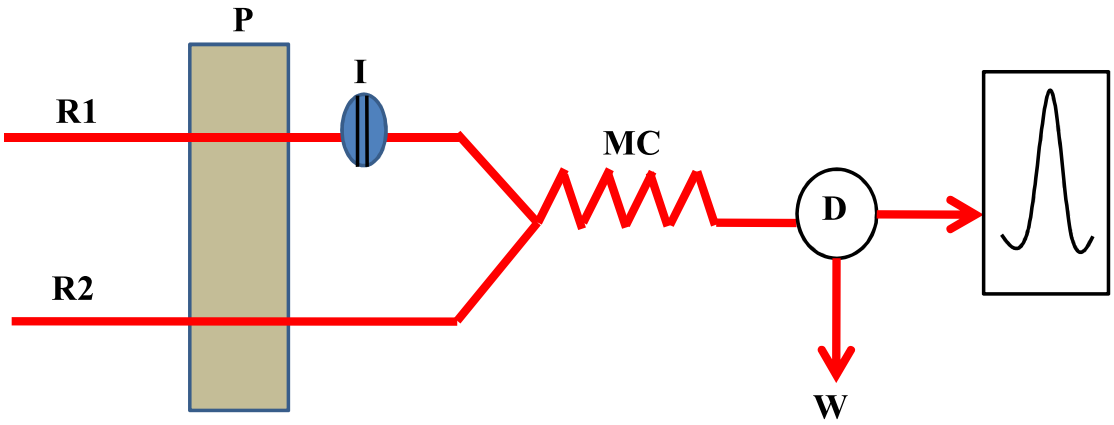

Figure 1 Schematic diagram of the basic FIA system (R1 = reagent 1, R2= reagent 2, P= pump, I= sample injection, MC= mixing coil, D= detector and W= waste)

In the simplest form of FIA the sample is injected into a continuous flow of reagent solution (carrier), dispersed, and transported to detector. Sample flow injection analysis dispersion is controlled through the suitable choice of the injected sample volume, flow rate of carrier, length of the reaction coil, and diameter of the tubing used. A schematic diagram of the basic FI system is shown in Figure 1.

1.1.2 Dispersion in the FIA

As stated previously, the control of dispersion is the most important aspect of FIA systems. The dispersion of a fluid zone reproducibly introduced into a non-segmented flow stream (carrier) during transport of the zone to the detector is the most important physical phenomenon in all FIA systems. The specific feature of dispersion processes in FIA is that they are reproducible and controllable through the manipulation of flow parameters and geometrical dimensions of flow conduits. The driving forces active in dispersion of the injected zone into the carrier stream are molecular diffusion and convection, but the effects of convection dominate, and the effects of molecular diffusion may be neglected in most cases. Convection occurs both as result of linear flow-rate differences of fluid elements located at different points along the radial axis of the conduit and as a result of secondary flows created by centrifugal forces perpendicular to the flow direction in non-straight conduits. A convex parabolic front of the injected zone and a concave parabolic tailing edge are developed with penetration into the carrier stream, the extent increasing with the distance traveled. Thus, under the specific conditions applied in FIA and with a fixed conduit, the acting forces are well under control, so that no random turbulence occurs. The result is that perfectly reproducible concentration time relationships may be obtained which, when recorded and superimposed, precisely overlap each other to form a single curve. This provides the basis for extracting reproducible readout under both FIA physically and chemically non-equilibrium conditions. The dispersion process typical of FIA system is shown in Figure 2.

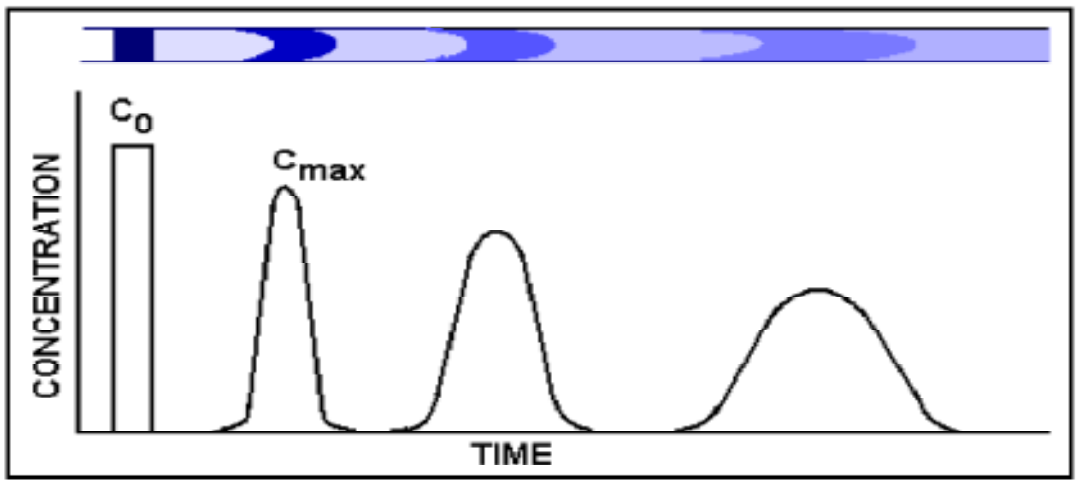

Figure 2 The dispersion process typical of FIA system

The injected fluid zones in a non-segmented flow stream can be manipulated reproducibly to produce various degrees of dispersion. In order to provide a quantitative criterion evaluating the extent of dispersion, the term dispersion coefficient (D) was introduced that being defined as the ratio of the concentration of the constituent of interest in a fluid element of the injected zone before and after dispersion, expressed by:

$$D = C_0/C \quad (1)$$

Where C_0 is the original concentration of the constituent in the solution before dispersion and C is the concentration of that fluid element of the dispersed fluid zone from which analytical readout is extracted. When the fluid element with the highest concentration is used for readout, above equation 1 is expressed as: Flow Injection Analysis.

$$D = C_0/C_{max} \quad (2)$$

Where C_{max} is the concentration of the constituent at peak maximum. D is a dimensionless value, which is equivalent to the dilution factor of the fluid element under consideration. For example, if the sample is diluted 1:1 by carrier, thus the dispersion coefficient is 2. FI systems are categorized into high, medium, and low dispersion systems depending on the degree of dispersion of the injected zone at the read out point. Systems with D above 10 are classified as high, those between 2 and 10 as medium, and those below 2 as low dispersion system. The main experimental parameters influencing the dispersion of an injected fluid zone include sample volume, flow rate of carrier and merging fluid streams, geometrical dimensions and configuration of transport conduits and on line reactor, and pattern of flow segmentation in system with two immiscible phases. The volume of the injected fluid zone, which most cases is the sample, is important factor influencing its dispersion. The dispersion decreases with an increase in sample volume. Ruzicka and Hansen stated that dispersion diminishes with a decrease in flow rate. This happens because decreasing flow rates increase the retention time of the sample awaiting transport to the detector. In this phase the reaction between sample and reagent almost reaches the equilibrium. Hence, the peak signal will be higher in a slower flow rate.

1.2 Micro flow injection analysis (µFIA)

A FIA system lends itself for miniaturization. With miniaturization some disadvantage of a FIA system can be overcome while keeping the advantages. A µFIA system reduces the amount of reagent used, speeds up the sample processing and makes the system portable. A µFIA also call Lab on the Chip is dedicated to the total sequence of lab processes to perform chemical analysis, whereby sample pre-treatment, separation and detection were miniaturized and incorporated within a microfluidic device. Micro fluidics is quickly developing science targeting the manipulation of miniature amounts of fluids, mainly for fast biochemical analysis. More precisely, microfluidics deals with moving gaseous or liquid fluids in cavities and channels tens or hundreds of micrometers in size. Microfluidic channels, often etched into silicon, can be less than 100 nm wide. Typical sizes for micorfluidic chips are usually of the order 1-50 cm^3, with channel width and depth dimensions ranging between 5-100 µm and fluid volumes handled between 0.01-10 µL. The microfluidic system is a system in which may or may not have integrated electronics, analyte by controlling the flow of liquid or gases through a series of tiny channels.

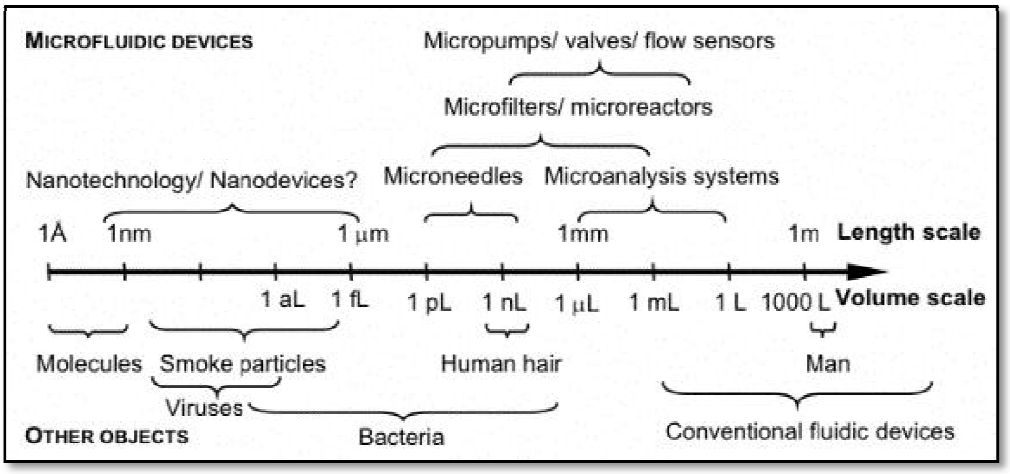

Figure 3 Microfluidic devices dimension (Nguyen and Wereley, 2006)

Recently, these microfluidic systems have been integrated with biosensing devices to perform ELISA (Eteshola and Leckband, 2001; Giri and Dutta, 2014), electrochemical sensing (Karuwan et al., 2011; Park et al., 2013), DNA detection (Javanmard and Davis, 2011; Kim et al., 2013; Wang et al., 2014) and many procedures. The reduction of the amount of solvents required in sample pre-treatment; and the reduction in the amount and the toxicity of solvents and reagents employed in the measurement step, especially by automation and miniaturization have reduced the adverse environmental impact of analytical methodologies (Czugala et al., 2013; Date et al., 2012; Jing et al., 2007; Kim et al., 2013; Li et al., 2007; Marle and Greenway, 2005). At the same time, a wide variety of detection, including absorbance (Date et al., 2012; Kee et al., 2008), fluorescence (Wang et al., 2014), chemiluminecence (Fan et al., 2014; Gao et al., 2008; Kamruzzaman et al., 2012; Lv et al., 2003; Wei et al., 2006; J. Yu et al., 2011) and elctrochemiluminescence (Delaney et al., 2013; Pittet et al., 2008; Yin et al., 2005). Thus, various kinds of microfluidic devices have been fabricated, the same as Figure 4.

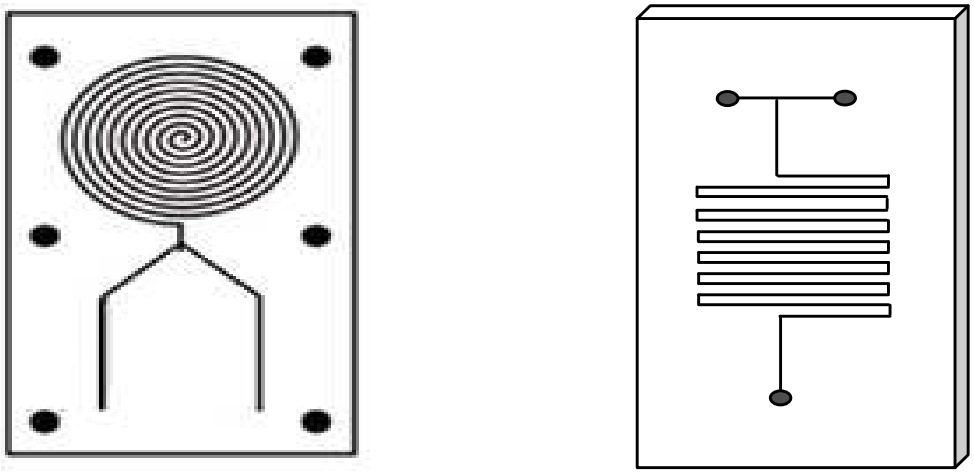

Figure 4 Fabrication of microfluidic devices (a. spiral platform b. square platform)

1.2.1 Frabrication techniqus for microfluidics

The science of miniaturization was initially fueled by the microelectronics industry during the development of miniature silicon-based electronic devices. Techniques for silicon microfabrication and miniaturization were then extended to the fabrication of mechanical devices that become known as microelectro mechanical system (MEMS), MEMS are also referred to as micromachines (in Japan), or Micro Systems Techonology – MST (in Europe).

Microfluidics is a specialty area that has grown out of mergine MEMS technology with the physics of fluid dynamics, chemistry and increasingly the biological sciences. The fabrication propose used for microfluidic device are the subset of MEMS. The common thread binding these disparate application themes is the ability to manufacture devices and systems using batch microfabrication processes. MEMS are made up of components between 1 to 100 micrometers in size (i.e. 0.001 to 0.1 mm) and MEMS devices generally range in size from 20 micrometers (20 millionths of meter) to millimeter. At these size scales, the standard constructs of classical physics are not always useful. The potential of very small machines was of classical physics are not always useful. The potential of very small machines was appreciated. MEMS technology can be implemented using a number of different materials and manufacturing techniques, depending on target device. MEMS are made using the same standard process steps used in integrated circuit manufacturing, including photolithography, wet and dry etching, oxidation, diffusion, low-pressure chemical vapor deposition (LPCVD) and sputter deposition. Some unit process, such as plating, molding and substrate bonding are generally used in MEM (MEMS and Nanotechnology Exchange, 2014) As a general rule, the choice of fabrication method for microfluidic device is determined by several factors, such as available technologies and equipment, cost speed fabrication capabilities (e.g. desired feature size and profile) and the preferred material substrate.

1.2.2 Materials for fabricating microfluidic devices

Microfluidic device have been fabricated from a variety of materials, including silicon, glass metals, ceramics hard plastic and polymer (e. g. polymethyl metacrylate (PMMA), polyamide (PA), polypropylene (PP) and polysulfone (PS))

In past years, the microfluidics has moved from predominantly silicon and glass structures towards polymers due to their ease of manufacturing and moderate cost. PDMS has gained a lot of attention in various analytical applications. Poly (dimethysiloxane) known as PDMS has become an important material in various fields over the years. Some of its applications include mold-release agents, waterproofing, and biomedical products (Kuncova-Kallio and Kallio, 2006). Lately, it became a popular material also in the microengineering. It was discovered as a stamping tool for micropattern transfer during soft lithography and as a fast prototyping material. The latter application has brought it to attention of various BioMEMS developers and nowadays many of the devices are actually manufactured in PDMS. Some of the PDMS applications in BioMEMS include PCR (Kim et al., 2006; Ranjit Prakash et al., 2006; Trinh et al., 2014), DNA microarrays (Cretich et al., 2008; Koo et al., 2011; Yu et al., 2003), capillary electrophoresis (CE) (Schöning et al., 2005; Yassine et al., 2008; Zhang and Gong, 2014), and various other separation and point-of-care devices. In microfluidic analytical systems, the PDMS typically serves as a material, in which the microchannels are manufactured (Gao e al., 2005; Kang and Park, 2005; Xiang et al., 2006).

1.3 Detection methods in the FIA

The method of detection in flow injection should be wisely chosen using a detector that monitors the events occurring in the measuring system as closely as possible. Such detection methods would include molecular spectroscopy (Marcos et al., 2004; Purohit and Devi, 1997), atomic spectroscopy (Fang et al., 1986; Tyson, 1988) and enzymatic methods of detection (Kurtz and Crouch, 1991; Pais et al., 2013; Pohlmann et al., 1990). These methods however are broad and are beyond the scope of this study, and hence shall not be discussed in detail. Nevertheless, more specific methods under molecular spectroscopy and electrochemical detection such as chemiluminescence and electrochemiluminescence are of significance in this study. Details regarding these methods are discussed in the succeeding paragraphs.

1.3.1 Chemiluminescence

The term of chemiluminescence (CL) can define as the emission of ultraviolet, visible or infra-red radiation from a molecule or atom as the result of the transition of an electronically excited state, having been produced as a consequence of a chemical reaction. This chemical reaction produces energy in sufficient amount to induce the transition of an electron from its ground state to an excited electronic state. This electronic transition is often accompanied by vibrational and rotational changes in the molecule. In organic molecules, transitions from a π bonding to a π^* anti-bonding orbital ($\pi \rightarrow \pi^*$) or from a non-bonding to an anti-bonding orbital ($n \rightarrow \pi^*$) are most frequently encountered (Dodeigne et al., 2000). When the reaction occurs in a living system or it is derived from one, the process is called bioluminescence (BL). Luminescent reactions has been observed since ancient time, luminous animals are known in the Greek civilisation, however the first report of artificial chemiluminescence occurred in 1669. The German physician, Henning Brand, isolated from urine a substance that glowed continuously in the dark. He called the substance "phosphorus mirabilis", and it is better known today as white phosphorus (Barnett and Lewis, 1996). In the 19th century it was found that rather simple organic compounds could also give rise to chemiluminescence. Radziszewski observed the green light emission when oxygen was bubbled into an alkaline ethanolic solution of 2,4,5-triphenylimidazole (lophine) (Isacsson and Wettermark, 1974). This discovery was published in the year 1877. The term chemiluminescence was first coined in 1888 by Eilhardt Weidemann, as a part of his classification of "cold light" (luminescence). Forty years later, Albrecht in 1928 reported the luminescent properties of 5-amino-2,3-dihydrophtalazine-1,4-dione (luminol). Early research on CL was mainly focused on the observation of a reaction and investigation of the mechanism and the analytical applications of the phenomenon appeared in the literature in 1960s (Palilis and Calokerinos, 2000).

Nowadays, a lot of inorganic and organic CL reaction are known. A typical CL reaction would be (Townshend, 1990):

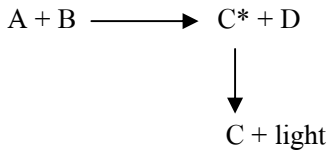

where (*) indicates an electronically excited state. Sometimes, The excited product (C*) is an ineffective emitter, but it can transfer the excitation energy to an efficient fluorophore (F) added to the system:

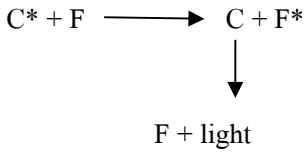

Now, the emission is identical with the fluorescence of F and we can classify that as indirect, sensitived, or energy transfer chemiluminescence. The light emission generated from a chemical reaction requires no light source for excitation, the analytical signal appears out of an essentially black background, and the only background signal is that of the photomultiplier tube's dark current. Analytically, the CL reactions are attractive due to:

(a) Excellent sensibility and excellent detection limits because there is absence of source noise and scatter.

(b) Sometimes high selectivity due to the limited number of available reactions.

(c) Simple, robust and inexpensive instrumentation suitable to both batch and flow analytical techniques. Furthermore, the introduction of flow injection analysis has made CL methods even more attractive because it is possible to mix sample and reagent rapidly with high reproducibility.

Chemiluminogenic reactions mainly occur in solution and in the gas phase. The most common or well known solution phase systems involve luminal (or its derivatives), oxalate esters, lucigenin (N,N‘-dimethyl-9-9‘-diacridinium nitrate) or its derivatives, ruthenium tris-bipyridine and luciferin. Gas phase examples include the ozone- and fluorine- induced, sodium

vapor, and chlorine dioxide chemiluminescence detectors for gas chromatography (Van et al., 2014). A brief of reaction presented in each phase will be discussed as follow.

1.3.1.1 Liquid-phase method

1.3.1.1.1 Luminol (5-amino-2,3-dihydro-1,4 - phthalazinedione)

Luminol reacts with oxidants like hydrogen peroxide (H_2O_2) in the present of a base and a metal catalyst to product an excite state product (3-aminophthalate, 3-APA) with gives off light at approximately 425 mn. The luminol reaction are as follow Figure 5.

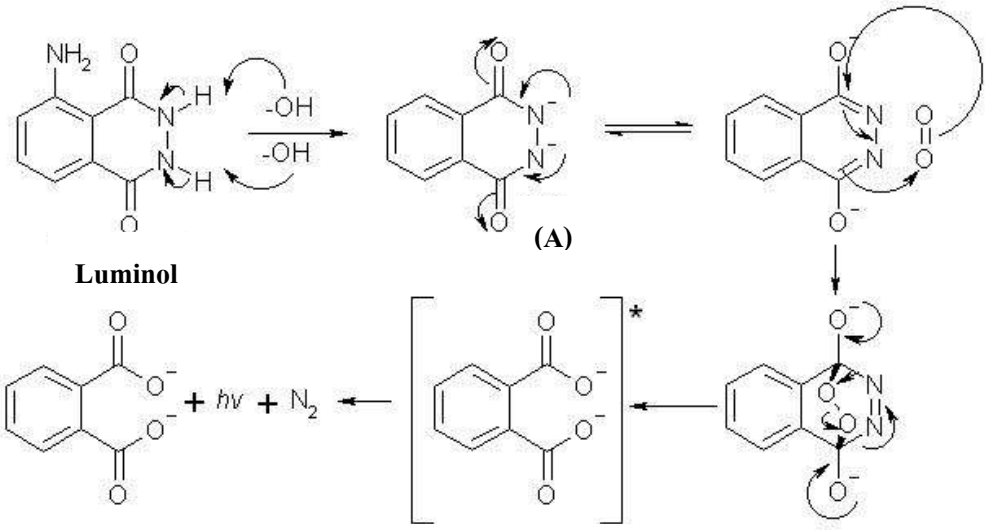

Figure 5 The mechanism of luminol (Fleming, 2014)

1.3.1.1.2 Potassium permanganate ($KMnO_4$)

A possible CL mechanism proposed by Aly (Aly et al., 1998) may be attributed to the following reactions:

$$\text{analyte} + MnO_4^- + 8H^+ \longrightarrow \text{Oxidized analyte*} + Mn^{2+} + 4\,H_2O \qquad (3)$$

In the presence of a fluorophore, the energy resulting from the redox reaction can be effectively transferred to quinine which in turn generates CL emission.

$$\text{Oxidized analyte*} + \text{fluorophore} \longrightarrow \text{Oxidized analyte} + \text{fluorophore*} \qquad (4)$$

$$\text{fluorophore}^* \longrightarrow \text{fluorophore} + \text{light} \qquad (5)$$

1.3.1.1.3 tris(2,2‘-bipyridyl)ruthenium (III)

Since the initial discovery of $Ru(bpy)_3^{2+}$ chemiluminescence, its utility has been applied to the production of reactive oxidant, $Ru(bpy)_3^{3+}$, followed by reduction, by an analyte species, to produce an emission of light (Aly et al., 2000):

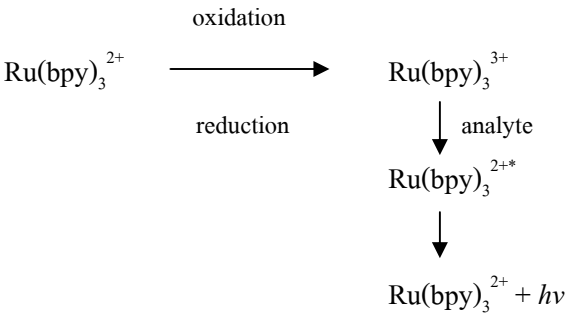

1.3.1.2 Gas phase Method

Gas phase methods have been used with gas chromatography, supercritical fluid chromatography, and many no chromatographic gas phase detectors in which fast response is required. One of the olderst known chemiluminescencet reactions is that of elemental white phosphorus oxidizing in moist air, producing a green glow. This is a gas-phase reaction of phosphorus vapor, above the solid, with oxygen producing the excite states $(PO)_2$ and HPO.

Another gas phase reaction is the basis of nitric oxide detection in commercial analytic instruments applied to environmental air quality testing. Ozone is combined with nitric oxide to form nitrogen dioxide in an activated state.

$$NO + O_3 \longrightarrow NO_2^* + O_2 \qquad (6)$$

The activated NO_2^* luminescence broadband visible to infrared light as it reverts to a lower energy state. A photomultiplier and associated electronics counts the photons which are proportional to the amount of NO present.

1.3.2 Electrochemiluminescence, ECL

Electrogenerated chemiluminescence, also called electrochemiluminescence and abbreviated as ECL, is the generation of light emitting species from electrochemical oxidation and reduction at an electrodes surface (Richter, 2004). A voltage or voltage pattern applied to the electrode causes electron transfer at the electrode's surface to form intermediates. These intermediates react to produce an excited state molecule near the electrode. As the excited molecule returns to the ground state, energy is released in the form of light. This can be seen in the following general mechanism for light emission by ECL.

$$A + e^- \rightarrow A^{\bullet -} \quad \text{(reduction potential)} \quad (7)$$

$$D \rightarrow D^{\bullet +} + e^- \quad \text{(oxidation potential)} \quad (8)$$

$$A^{\bullet -} + D^{\bullet +} \rightarrow A^* + D \text{ (or } D^* + A) \quad (9)$$

$$A^* \text{ (or } D^*) \rightarrow A \text{ (or D)} + h\nu \quad (10)$$

In this scheme, A is an electron acceptor, which is reduced at the electrode's surface, and D is an electron donor, which is oxidized at the electrode's surface. A square wave potential pattern is applied to the electrode with voltages chosen to reduce A and oxidize D. Note that the electron donor and acceptor may be a different molecule or the same molecule.

ECL (Wikipedia: the free encyclopedia, 2014) is usually observed during application of potential (several volts) to electrodes of electrochemical cell that contains solution of luminescent species (polycyclic aromatic hydrocarbons, metal complexes, quantum dots or nanoparticles) in aprotic organic solvent (ECL composition). In organic solvents both oxidized and reduced forms of luminescent species can be produced at different electrodes simultaneously or at a single one by sweeping its potential between oxidation and reduction. The excitation energy is obtained from recombination of oxidized and reduced species.

1.3.2.1 Principles of ECL

ECL is a means of converting electrical energy into light. It involves the production of reactive intermediates from stable precursors at the surface of an electrode. These intermediates then react under a variety of conditions to form excited states that emit light.

For example, ECL from $Ru(bpy)_3^{2+}$ (Figure 6) was first reported in 1972 (Tokel and Bard, 1972) in acetonitrile (MeCN) using tetrabutylammonium tetrafluoroborate ($TBABF_4$) as the electrolyte. ECL was generated by alternate pulsing of an electrode potential to form oxidized $Ru\text{-}(bpy)_3^{3+}$ and reduced $Ru(bpy)_3^{+}$:

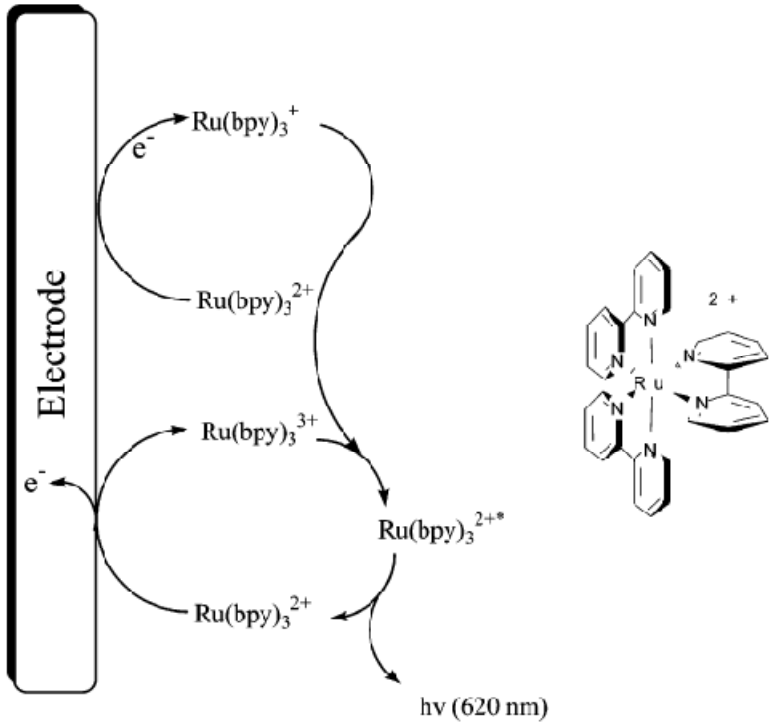

Figure 6 Structure of $Ru(bpy)_3^{2+}$ and proposed mechanism for $Ru(bpy)_3^{3+}$ / $Ru(bpy)_3^{+}$ ECL system (Tokel and Bard, 1972).

$Ru(bpy)_3^{\bullet 2+}$ represents the excited molecule that emits light, and $h\nu$ is a photon of light. The excited state formed in this ECL reaction is similar to that formed during photo excitation (i.e., photoluminescence or PL). In PL, an electron is excited from metal based dπ orbitals to ligand-base dπ* orbitals (a metal-to-ligand charge-transfer (MLCT) transition)(Roundhill, 1994). The excited electron then undergoes intersystem crossing to the lowest triplet states of $Ru(bpy)_3^{\bullet 2+}$ from where emission occurs. The MLCT excited state may be formed in ECL if an electron is transferred to the π* orbital of one of the bipyridine ligands. $Ru(bpy)_3^{\bullet 2+}$ can then decay to the ground state, producing the same luminescence as obtained from photoluminescence spectroscopy.

It is also important to distinguish ECL from chemiluminescence (CL). Both involve the production of light by species that undergo highly energetic electron-transfer reactions. However, luminescence in CL is initiated and controlled by the mixing of reagents and careful manipulation of fluid flow. In ECL, luminescence is initiated and controlled by switching an electrode voltage.

1.3.2.2 General reaction mechanisms

1.3.2.2.1 Annihilation ECL

The first detailed studies on ECL involved electrontransfer reactions between an oxidized and a reduced species, both of which were generated at an electrode by alternate pulsing of the electrode potential (Santhanam and Bard, 1965; Visco and Chandross, 1964). This approach is typically called “annihilation”, and a general mechanism is outlined below:

$$A - e^- \longrightarrow A^{\bullet +} \text{ (oxidation at electrode)} \quad (11)$$

$$A + e^- \longrightarrow A^{\bullet -} \text{ (reduction at electrode)} \quad (12)$$

$$A^{\bullet -} + A^{\bullet +} \longrightarrow A^{\bullet} + A \text{ (excited-state formation)} \quad (13)$$

$$A^{\bullet} \longrightarrow A + h\nu \text{ (light emission)} \quad (14)$$

For example, the potential of the working electrode is quickly changed between two different values to generate the oxidized, $A^{\bullet+}$, and reduced, $A^{\bullet-}$, species (eq 11 and 14, respectively) that will react near the electrode surface to form the emissive state, $A^{\bullet}$ (eq13).

1.3.2.2.2 Coreactant ECL

It is also possible to generate ECL in a single potential step using a coreactant. A coreactant is a species that, upon oxidation or reduction, produces an intermediate that can react with an ECL luminophore to produce excited states. Usually, this occurs upon bond cleavage of the coreactant to form strong oxidants or reducants. For example, oxalate ion ($C_2O_4^{2-}$) was the first coreactant discovered (Rubinstein and Bard, 1981) and is believed to produce the strong reductant $CO_2^{\bullet-}$ upon oxidation in aqueous solution:

$$C_2O_4^{2-} - e^- \longrightarrow [C_2O_4^{\bullet-}] \longrightarrow CO_2^{\bullet-} + CO_2 \qquad (15)$$

The oxidizing potential can also oxidize an ECL luminophore, such as D, where D is, for example, $Ru(bpy)_3^{2+}$.

$$D - e- \longrightarrow D^{\bullet+} \qquad (17)$$

$D^{\bullet+}$ and $CO_2^{\bullet-}$ may then react to produce an excited state capable of emitting light.

$$CO_2^{\bullet-} + D^{\bullet+} \longrightarrow D^{\bullet} + CO_2 \qquad (18)$$

$$D^{\bullet} \longrightarrow D + h\nu \qquad (19)$$

Oxalate is often referred to as an “oxidative” or “oxidative-reductive” coreactant due to its ability to form a strong reducing agent upon electrochemical oxidation. In coreactant ECL the electrode typically only oxidizes *or* reduces the reagents in a *single* potential step, whereas in annihilation schemes a double-potential step (e.g., oxidation followed by reduction) is required to generate the highly energetic precursors.

1.3.2.2.3 Cathodic luminescence

Light emission has also been observed at oxide covered metal (such as aluminum and tantalum) electrodes under various conditions (Gaillard et al., 1999; Kankare et al., 1992; Kulmala et al., 1999; Sung et al., 1998). For example, emission from Dy(III), Sm(III), and Tb(III) has been observed at oxide-covered aluminum electrodes during the reduction of hydrogen peroxide, persulfate, or oxylate in aqueous solution (Kankare et al., 1992). It was proposed that this type of high-voltage cathodic luminescence results from the injection of hot electrons into the aqueous electrolyte solution with the possible formation of hydrated electrons (Kankare et al., 1992; Kulmala et al., 1999). Subsequent studies in non aqueous solution have provided experimental evidence for the production of hot electrons in an acetonitrile solution from a Ta_2O_5-covered Ta electrode (Gaillard et al., 1999; Sung et al., 1998). Although this method is often called “electrogenerated chemiluminescence”.

1.4 Preconcentration in flow-based system

Despite the selectivity and sensitivity of analytical techniques such as FAAS, ETAAS, ICP-OES, and ICP-MS, LC-UV, LC - MS techniques, there is a critical need for the separation and preconcentration of trace analytes from matrices prior to their determination, due to their frequent presence at low concentrations in environmental samples and higher matrix interferences. Sample preparation processes including separation and preconcentration have a direct impact on trueness, precision and detection limits for many analytical methods. This process is also the rate determining step of the analytical method.

Automatic methods are one of the more interesting and attractive topics in the analytical chemistry of today. One of these methods are the continuous flow techniques which are greatly used by the scientific community all over the word. This is easy to understand because these technique offer many advantages, especially their versatility (flow analysis can be couple to any analytical technique). Moreover, conventional methods can be quickly carried out by flow injection; so, usually 100 samples per hour can be analyzed with good precision and accuracy. Moreover, a decrease in both sample and reagent consumption is achieved and also less handing is required. Various improvements in flow-injection systems involving on-line separation and preconcentration.

Preconcentration techniques used in conventional batch procedures for low metal concentration samples are time consuming and they need a large handing. The use of flow injection in the preconcentration of samples allows to avoid these disadvantages and moreover the sensitivity of flow injection analysis is increased. The samples size for this purpose can be increase from μL to mL. For this reason the scientific literature concerning this topic has increased in recent year (Carbonell et al., 1992). There are many solid materials available with different properties which are suitable for preconcentration applications, including silica gel, inorganic oxides, activated carbon and crosslinked polystyrenes .

Adsorption of analyte to solid surface depends on the interaction forces formed between the analyte in the sample and the properties of the solid sorbent. Many kinds of analytes can be retained on the solid material but in most cases their chemical properties cannot be changed. Therefore, the analyte modification is not feasible and it is recognized independent variable in this process. Another factor is the solid material upon which the adsorption takes place. Indeed not the whole solid material participates in the adsorption process but mostly its surface since adsorption process is surface phenomenon. Solid surface is the interaction point between the dissolved analyte in the sample and the functional groups in the sorbent. Thus the best way to improve adsorption is to select suitable solid material that can be chemically changed in its surface so that it becomes able to strongly and/or selectively attract the analyte component from the sample.

1.4.1 C_{18}-bonded silica gel

Despite the large variety of bonded phases available, octadecyl-bonded silica has currently become the most popular phase used. Numerous applications has been reported the use of C_{18}-silica. Bare C_{18}-silica can also retain a fraction of inorganic trace elements, probably due to the presence of silanol groups on its surface. However, in practice, due to its hydrophobic character, C_{18}-silica is not well suited for retention of trace element species, as the latter are often polar or ionic. Retention on C_{18}-silica may be improved by addition of a ligand reagent to the sample before its percolation through the sorbent. An alternative approach is to form the complex by passing the sample through a C_{18}-silica containing the immobilized reagent. Octadecyl bonded silica, modified by suitable ligands has been successfully used for the separation and sensitive

determination of metal ions. Despite their broad application to trace element preconcentration, bonded silica phases (either C18-silica or functionalized-silica gel) present the drawback of a limited range of pH that can be used, as in acidic (below 2 to 4) and basic (above 8) pHs hydrolysis may occur, which changes the interactions that occur between the sorbent and the trace elements.

For determination metal, an application of FI couple with preconcentration method have been studied in many research such as Hassan (Karami et al., 2004) was determination of Bi^{3+}, Cd^{2+}, Co^{2+}, Cu^{2+}, Fe^{3+}, Ni^{2+}, Pb^{2+} and Zn^{2+} in aqueous samples by inductively coupled plasma-atomic emission spectrometry. Fang (Fang et al., 1990) was determination lead in sea water by on-line sorbent extraction pre-concentration system for graphite furnace atomic absorption spectrometry

A CL micro-flow system combined with on-line solid phase extraction (SPE) was presented based on the use of C18 bonded silica for determination of some β-lactam antibiotics (penicillin, cefradine, cefadroxil, cefalexin) in milk. It is based on the enhancement effect of β-lactam antibiotics on the luminol-$K_3[Fe(CN)_6$) signal in CL system. The micro-flow system was fabricated from two PMMA plates (50 mm × 40 mm × 5 mm) with the micro channels of 200 μm wide and 150 μm deep. C18-modified silica gel was packed into the micro channel (length: 10 mm; width: 1 mm; depth: 500 μm) to serve as SPE device (Liu et al., 2007). María E et al (Salinas-Vargas and Cañizares-Macías, 2014) was determination of caffeine in coffee based on the solid phase extraction (SPE) coupled to a flow injection. A C_{18} reverse-phase mini-column was coupled to a continuous flow manifold to carry out the on-line SPE and the quantification of caffeine from aqueous extracts.

1.4.2 Polystyrene polymers

Polystyrene polymers are considered an interesting and alternative material over the common sorbents such as Amberlites XAD-2 and XAD-8 or C_{18}-silica when they have high cross-link structure. In some cases, this material is employed when addition of a reagent to the sample is required to form complexes that are further retained on the hydrophobic sorbent (Kumagai et al., 1998). Moreover, Dmitryenko and coworker have studied the sorption of oxytetracycline and chlorotetracycline by sulphonated polystyrene resins. They investigated effect of the structure of the ion-exchange resin on the sorption process. Evidence has been obtained for the aggregation of these ions in the resin. It was found that the variations in the degree of crosslinking of the resin structure and the concentration of the functional groups have significant effect on the selective behaviour of the resin towards these antibiotics (Dmitryenko and Hale, 1965). Hafez (Hafez et al., 2001) was determination mercury in environmental samples using chemically modified chloromethylated polystyrene-PAN (ion-exchanger) and its determination by cold vapour atomic absorption spectrometry.

1.4.3 Carbon sorbents

Activated carbon is prepared by low-temperature oxidation of vegetable charcoals. Because of their large surface areas (300–1000 m^2g^{-1}), these sorbents are well-recognized for their very strong sorption both for trace organic compounds and trace elements. There is evidence of types of adsorption sites on activated carbons are reported. Firstly, adsorption through van der Waals forces enabled by graphite-like basal planes, especially π-electron interactions. Secondly, ionic interaction of hydrogen bonding that may take place through polar groups like carbonyls, hydroxyls and carboxyls. Consequently, trace elements may be directly adsorbed on activated carbon. The major drawback when utilizing activated carbons is their heterogeneous surface with active functional groups those often lead to low reproducibility. Fortunately, along with the development of polymer materials and bonded phases, a new generation of carbon sorbents appeared in the 1970s and 1980s with a more homogeneous structure and more reproducible properties.

Another kind of carbon sorbents is the graphitized carbon blacks which are obtained by heating carbon blacks at 2700–3000 °C in an inert atmosphere. These sorbents are nonspecific and non-porous (surface area about 100 m^2g^{-1}). Also, due to the presence of positively charged chemical heterogeneities on their surface, they are considered to be both reversed phase sorbents and anion-exchangers (Camel, 2003). Carbon sorbents have been extensively used in the past few years for the SPE of polar organic pollutants from water samples (Masqué et al., 1998), while in trace elements SPE is still rare. The main limitations are possible irreversible retention of analytes, which may be overcome by elution in the backflush mode, and poor mechanical stability. Already many years ago removal of antibiotics from water samples by activated carbon is well known. One of these conventional drinking water treatment processes by activated carbon were evaluated under typical water treatment plant conditions to determine their effectiveness in the removal of some common antibiotics. Carbadox, sulfachlorpyridazine, sulfadimethoxine, sulfamerazine, sulfamethazine, sulfathiazole, and trimethoprim were exmined. The study shows that these antibiotics could be effectively removed using processes already in use in many water treatment plants. However, additional work is needed on the by-product formation and the removal of other classes of antibiotics (Adams et al., 2002). For heavy metal , Daorattanachai (Daorattanachai et al., 2005) was determination Cd(II), Cu(II), Ni(II), and Zn(II) from aqueous solution by column solid phase extraction (SPE) technique. Trace metal ions in aqueous solution were quantitatively sorbed onto ammonium pyrrolidinedithiocarbamate impregnated activated carbon (APDC-AC) packed in a SPE column. The sorbed metals were eluted with 1 M nitric acid in acetone solution and analyzed by flame atomic absorption spectrometry.

1.4.4 Divinylbenzene-vinylpyrrolidone copolymers

Sorbents made of divinylbenzene-vinylpyrrolidone copolymers have recently been developed, such as Oasis HLB. The hydrophilic *N*-vinylpyrrolidine affords good wettability of the resin, while the hydrophobic divinylbenzene provides reversed-phase retention of analytes. This sorbent has been successfully applied to the determination of polar organic compounds in water samples. It is more convenient to use, compared to classical sorbents, as it can dry out during the extraction procedure without reducing its ability to retain analytes. In addition, it is stable over the entire pH range.

A sorbent cartridge based on this copolymer has been applied for the simultaneous determination of BLAs (penicillin G, amoxicillin, ampicillin, penicillin V, oxacillin, cloxacillin, dicloxacillin and nafcillin) in wastewater. The method is based on SPE and high performance liquid chromatography with UV-DAD. The SPE cartridge (Oasis MAX, vinylpyrrolidone and divinylbenzene polymer) have been used for sample clean up and preconcentration (Benito-Pena et al., 2006).

CHAPTER 2

Review of Related Literature

Environmental pollution are worldwide problems. The progress of industries and the environmental impacts of irrigations has led to increased emission of pollutants into ecosystems. Since the industrial revolution, the production of heavy metals such as lead, copper, and zinc has increased exponentially. The major sources of heavy metal pollutants are metal mining, metal smelting, metallurgical industries, and other metal-using industries, waste disposal, corrosions of metals in use, agriculture and forestry, fossil fuel combustion, and sports and leisure activities. Heavy metal contamination affects large areas worldwide. Hot spots of heavy metal pollution are located close to industrial sites, around large cities and in the vicinity of mining and smelting plants. Agriculture activities in these areas faces major problems due to heavy metal transfer into crops and subsequently into the food chain.

Therefore the World Health Organization (WHO), Codex and Thailand government have concerned and set a maximum residuals limit (MRL) for control level of heavy metalscontamination in environmental, as show in Table 1.

Table 1 The MRL of heavy metal in environmental

Heavy metals	maximum residuals limit (MRL)			
	Soil*	Surface water*	Underground water**	Drinking water **
1. Arsenic	3.9	0.01	0.01	0.05
2. Cadmium and compounds	37	0.05	0.003	0.005
3. Hexavalent Chromium	300	0.05	0.05	0.05
4. Mercury and compounds	23	0.002	0.001	0.002
5. Lead	400	0.05	0.01	0.05

*(mg kg^{-1}), **(mg L^{-1})

The increasing on human population contributing greater contamination in environment and bring to many problems. The major problem is an antibiotic contamination in food since many antibiotics are used worldwide as feed additives for the purpose of livestock health maintenance. The use of antibiotics in food-producing animals may lead to residues in livestock products and was banned all of product from EU countries.

The EU have set the maximum residuals limit (MRL) for control level of antibiotics contamination in food and feed as show in Table 2.

Table 2 The MRL of antibiotic in food and feed

Sample types	Antibiotic	MRL
1. Milk	- Aminoglycosides,sulfonamides,phenicols, Fluoroquinolones	100–1500 μg L^{-1}
	- Sulfonamides	100 μg L^{-1}
2. Egg	- Fluoroquinolones	50- 200 μg kg^{-1}
3. Fish	- Fluoroquinolones	600 μg kg^{-1}
	- Tetracyclines	100 μg kg^{-1}
	- Nitroffurans	banned
4. Feed	Nitrofurans:	banned
	- furazolidone,	
	- furaltadone	
	- nitrofurantoin	
	- nitrofurazone	

2.1 Heavy metals

Heavy metal is a member of a loosely-defined subset of elements that exhibit metallic properties. It mainly includes the transition metals, some metalloids, lanthanides, and actinides. Many different definitions have been proposed some based on density, some on atomic number or atomic weight, and some or toxicity. There is no standard definition assigning metals as heavy metals. Some lighter metals and metalloids are much toxic and thus are termed heavy metals, which some heavy metals, such as gold, typically are not toxic. Most heavy metals have a high atomic number, atomic weight and a specific gravity greater than 5.0.

Heavy metals are found naturally in the earth, and become concentrated as a result of human caused activities. Common sources are from mining and industrial wastes; vehicle emissions; lead-acid batteries; fertilizers; paints and treated woods.

2.1.1 Arsenic

2.1.1.1 Physical and chemical properties

Arsenic appears in three allotropic forms: yellow, black and grey; the stable form is a silver-gray, brittle crystalline solid. It tarnishes rapidly in air, and at high temperatures burns forming a white cloud of arsenic trioxide. Arsenic is widely distributed in the earth's crust and present at an average concentration of 2 mg kg^{-1}. It occurs in trace quantities in all rock, soil, water and air. Arsenic can exist in four valency states: –3, 0, +3 and +5. Under reducing conditions, arsenite (As(III)) is the dominant form; arsenate (As(V)) is generally the stable form in oxygenated environments. Elemental arsenic is not soluble in water. Arsenic salts exhibit a wide range of solubilities depending on pH and the ionic environment. There are many arsenic compounds of environmental importance, are shown in Figure7.

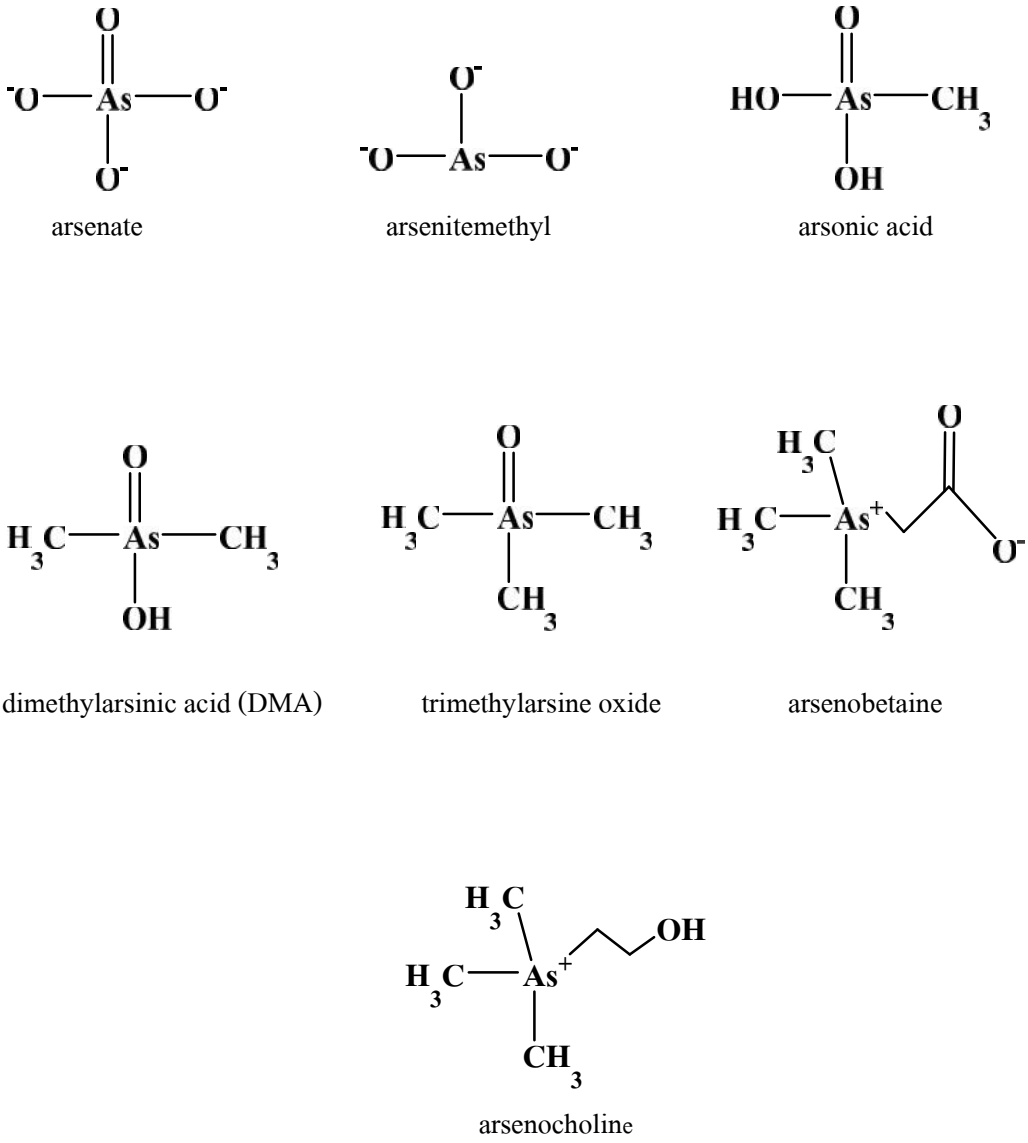

Figure7 Arsenic compounds commonly detected in the environment

Under oxidizing and aerated conditions, the predominant form of arsenic in water and soil is arsenate. Under reducing and waterlogged conditions (< 200 mV), arsenite should be the predominant arsenic compounds. The rate of conversion is dependent on the redox potential (Eh) and pH of the soil as well as on other physical, chemical and biological factors. In brief, at moderate or high Eh, arsenic can be stabilized as a series of pentavalent (arsenate) oxyanions, H_3AsO_4, $H_2AsO_4^-$, $HAsO_4^{2-}$ and AsO_4^{3-}. However, under most reducing (acid and mildly alkaline) conditions, arsenite predominates. A pH and Eh diagram are shown in Figure 8.

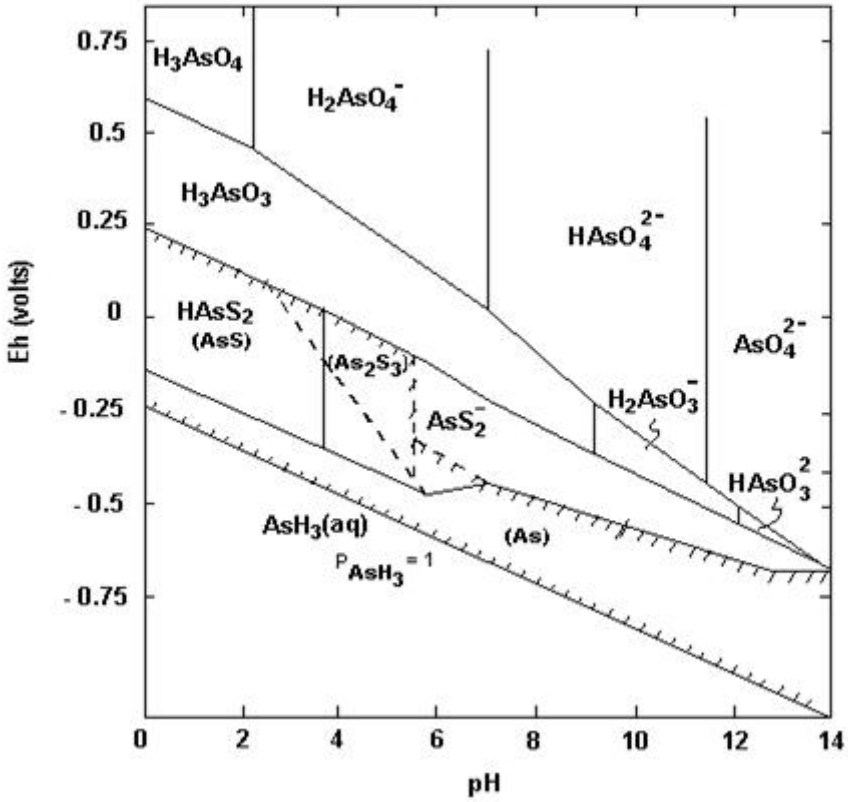

Figure 8 The Eh-pH diagram for arsenic at 25 °C and on atmosphere with total arsenic 10^{-5}mol L^{1}

2.1.1.2 Toxicity

Arsenic is one of the most toxic elements that can be found on earth crust. Despite their toxic effect, inorganic arsenic bonds occur on earth naturally in small amounts. Humans may be exposed to arsenic through food, water and air. The most toxicologically potent arsenic compounds are in the trivalent oxidation state. This has to do with their reactivity with sulfur containing compounds and generation of reactive oxygen species (ROS). However, humans are exposed to both trivalent and pentavalent arsenic.

Exposure to inorganic arsenic can cause various health effects, such as irritation of the stomach and intestines, decreased production of red and white blood cells, skin changes and lung irritation. It is suggested that the uptake of significant amounts of inorganic arsenic can intensify the chances of cancer development, especially the chances of development of skin cancer, lung cancer, liver cancer and lymphatic cancer. Chronicarsenic poisoning results from drinking contaminated well water over a long period of time. The World Health

Organization recommends a limit of 0.01 mg L^{-1} (10 ppb) of arsenic in drinking water. This recommendation is established based on the limit of detection of available testing equipment at the time of publication of the WHO water quality guidelines. Mining techniques such as hydraulic fracturingmay mobilize arsenic in groundwater and aquifers due to enhanced methane transport and resulting changes in redox conditions, and inject fluid containing additional arsenic.

Arsenic contamination of natural waters, tap water and ground water has become an issue of growing concern, particularly in Southeast Asia such as Bangladesh, India, Nepal and Thailand.

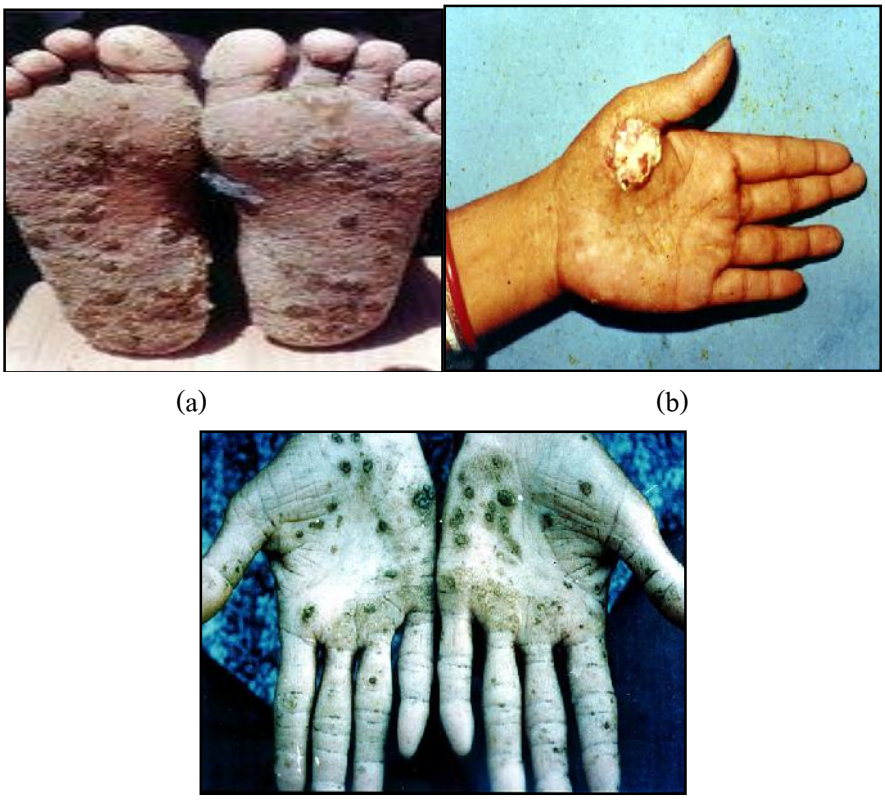

(a) (b)

(c)

Figure 9 Illustration of skin cancer caused by arsenic (Wordbank, 2008)

a: Arsenic lesions on feet, b: Arsenic lesions on hand, cancer and c: Keratoses on hand

In Thailand, arsenic contamination was found in Ronphibun District, Nakhon Si Thammarat Province in 1987 (Sukreeyapongse et al.). People live near or in old tin mine area were sick, their skin became black and were diagnosed as skin cancer.

Figure 10 A map of arsenic groundwater contamination in Southeast Asia (Kim et al., 2011)

2.1.1.3 The analytical techniques for arsenic analysis

There are variety of instrumental techniques for the determination of arsenic in various biological matrix. These include atomic absorption spectrometry (AAS) (Behari and Prakash, 2006; Husakova et al., 2007; Macedo et al., 2009), atomic fluorescence spectrometry (AFS) (Barra et al., 2000; Keller et al., 2014), inductively coupled plasma with optical emission spectrometry (ICP-OES) (Welna and Szymczycha-Madeja, 2014), inductively coupled plasma with atomic fluorescence spectrometry (ICP-AFS) (Hueber and Winefordner, 1995; Koh et al., 2005), inductively coupled plasma with mass spectrometry (ICP-MS)(Milstein et al., 2002; Moreira et al., 2011) and voltammetry (Garlaschelli et al.). Some of these techniques (e.g. ICP-MS) can serve as element-specific detectors when coupled to chromatographic separation techniques (e.g. HPLC and GC). The summary of difference techniques for determine arsenic is given in Table 3

Table 3 Analytical methods used for arsenic determination

No.	Detection method	Species	Samples	Detection limit	Preconcentration/separation	Reference
1.	AAS-VGA	total arsenic	Tab water	-	-	Behari et al, 2006
2.	AAS-HG	total arsenic As(III)	Phosphate fertilizer	0.1 $\mu g\ L^{-1}$	-	Macedo et al., 2009
3.	AAS	total arsenic	Beer	1.6 $\mu g\ L^{-1}$	-	Husakova et al, 2007
4.	AFS-IC-HG	As(III) As(V)	Sulfide water	1-3 $\mu g\ L^{-1}$	IonPac AS16 4×250mm	Keller et al, 2014
5.	AFS	As(III) As(V)	Soil	0.006 $\mu g\ g^{-1}$	-	Barra et al, 2000
5.	Anodic Stripping Voltammetry	As(V)	Industrial waste	1.1 $\mu g\ L^{-1}$	-	Garlaschelli et al, 2013

VGA = vapor generation assembly HG= hydride generation IC= ion chromatography

Table 3 (continue)

No.	Detection method	Species	Samples	Detection limit	Preconcentration/separation	Reference
7.	ICP-OES-HG	As(III)	Fruit juice	0.66 μg L^{-1}	-	Welna et al, 2014
		As(V)		0.65 μg L^{-1}		
8.	ICP-AES-HG	As(III)	Water	0.70 μg L^{-1}	-	Hueber et al, 1995
9.	ICP-AES-HG	As(III)	herbicide, pesticide,	-	yeast-immobilized column	Koh et al, 2005
		As(V)	and cigarette	-		
10.	HPLC-IC-MS	As(III)	white wine	0.10 μg L^{-1}	Anion exchange: Hamilton PRP-	Moreira et al, 2011
		As(V)		0.21 μg L^{-1}	X100 (250 mm×4.1, 10 μm)	
		DMA		0.12 μg L^{-1}		
		MMA		0.15 μg L^{-1}		
11.	HPLC-IC-MS	As(III)	drinking water	0.03 μg L^{-1}	Anion exchange: Hamilton PRP-	Milstein et al, 2002
		As(V)		0.06 μg L^{-1}	X100 (250 mm×4.1, 10μm)	
		DMA		0.03 μg L^{-1}		
		MMA		0.06 μg L^{-1}		

2.1.2 Cadmium

2.1.2.1 Physical and chemical properties

Cadmium is a lustrous, silver-white, ductile, very malleable metal. Its surface has a bluish tinge and the metal is soft enough to be cut with a knife, but it tarnishes in air. It is soluble in acids but not in alkali. It is a metal with an oxidation state of +2. It is chemically similar to zinc and occurs naturally with zinc and lead in sulfide ores but it forms more complex compounds.

Cadmium metal has specific properties that make it suitable for a wide variety of industrial applications. These include: excellent corrosion resistance, low melting temperature, high ductility, high thermal and electrical conductivity. Cadmium is also present as an impurity innon-ferrous metals (zinc, lead, and copper), iron and steel, fossil fuels (coal, oil, gas, peat, andwood), cement, and phosphate fertilizers. In these products, the presence of cadmium generallydoes not affect performance; rather, it is regarded as an environmental concern. Cadmium is also produced from recycled materials (such as Ni–Cd batteries and manufacturing scrap) and some residues (e.g. cadmium-containing dust from electric arc furnaces) or intermediate products. Recycling accounts for approximately 10-15% (IARC Monographs on the Evaluation of Carcinogenic Risks to Humans, 2012)of the production of cadmium in developed countries. Synonyms, trade names and molecular formulae for cadmium, cadmium–copper alloy, and some cadmium compounds are presented in table 4. The cadmium compounds shown are those for which data on carcinogenicity or mutagenicity were available or which are commercially important compounds. It is not an exhaustive list, and does not necessarily include all of the most commercially important cadmium-containing substances.

Table 4 Chemical names, synonyms, and molecular formula of cadmium and cadmium compounds

Chemical name	Synonyms	Formula
Cadmium	Cadmium metal	Cd
Cadmium acetate	Acetic acid, cadmium salt; bis(acetoxy)-cadmium; cadmium (II) acetate; cadmium diacetate; cadmium ethanoate	$Cd(CH_3COO)_2$
Cadmium carbonate	Carbonic acid, cadmium salt; cadmium carbonate ($CdCO_3$); cadmium monocarbonate	$CdCO_3$
Cadmium chloride	Cadmium dichloride; dichlorocadmium	$CdCl_2$
Cadmium hydroxide	Cadmium hydroxide ($Cd(OH)_2$); cadmium Dihydroxide	$Cd(OH)_2$
Cadmium nitrate	Nitric acid, cadmium salt; cadmium dinitrate; cadmium (II) nitrate	$Cd(NO_3)_2$
Cadmium stearate	Cadmium distearate; cadmium octadecanoate; cadmium(II) stearate; octadecanoic acid, cadmium salt; stearic cid, cadmium salt	$Cd(C_{36}H_{72}O_4)$
Cadmium sulfate	Cadmium monosulfate; cadmium sulfate; sulfuric acid, cadmium salt (1:1)	$CdSO_4$
Cadmium sulfide	Cadmium monosulfide; cadmium orange;cadmium yellow	CdS
Cadmium oxide	Cadmium monoxide	CdO

2.1.2.2 Toxicity

Cadmium enters the air, it binds to small particles. It falls to the ground or water as rain or snow, and may contaminate fish, plants, and animals. Improper waste disposal and spills at hazardous waste sites may cause cadmium to leak into nearby water and soil. Cadmium released into the atmosphere by smelting or mining or some other processes, cadmium compounds can be associated with respirable-sized airborne particles and can be carried long distances. It is deposited onto the earth below by rain or falling out of the air. Once on the ground, cadmium moves easily through soil layers and is taken up into the food chain by uptake by plants such as leafy vegetables, root crops, cereals and grains.

Having skin contact with cadmium is not known to cause health problems, but the following exposures to cadmium can cause serious health problems:

- Breathing air that contains high levels of cadmium
- Eating food containing high levels of cadmium, such as shellfish, liver, kidney, potatoes, and leafy vegetables
- Drinking water contaminated with cadmium
- Breathing in cigarette smoke, which doubles the average daily intake of cadmium

Cadmium is extremely toxic, with acceptable levels one tenth that of most of the other toxic metals. Its effects are many, but it mainly affects the kidneys, the cardiovascular system, and is related to cancer. It also ages the skin. Cadmium also contributes to many mental illnesses, particularly violence and other related disorders of behavior and mental attitude. Cadmium is so toxic to the brain that it causes what might be called ‘a small rebellion’ in the tissues of the brain, which results in violent thoughts. Cadmium is involved in all of the major diseases of our time, including cancer, diabetes, arthritic syndromes, heart disease, kidney disease, and others. One reason may be that cadmium replaces zinc in the body. Zinc is required for over 100 or more critical enzymes. These include enzymes needed for proper immune system activity, digestion, cardiovascular health, and much more.

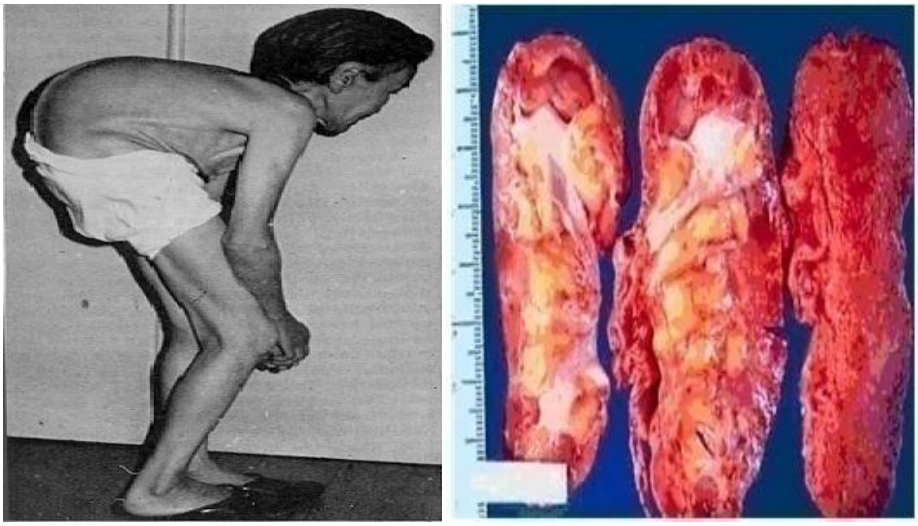

(a) (b)

Figure 11 Illustration of Itai Itai disease (a) Patient suffering from prolonged exposure to cadmium (Cornell university genetically engineered machines, 2009) (b) kidney of patent of Itai Itai disease (Kanazawa, 2014)

Many health agencies have set exposure standards designed to protect the general public from excess cadmium exposure from various sources. For example: Food and Drug Administration (FDA) set the maximum limit of cadmium in bottled water at 0.005 mg L^{-1}. The Environmental Protection Agency (EPA) has established limits on the quantity of cadmium that can be discharged into water or disposed of as solid wastes from factories that manufacture or employ cadmium. It is considering regulations that would limit the amount of cadmium that could be emitted into outside air. EPA has also established an interim Maximum Contaminant Level (MCL) of 0.01 mg L^{-1} (10 µg L^{-1}) for cadmium in drinking water. It has proposed a Maximum Contaminant Level Goal (MCLG) of 0.005 mg L^{-1}(5 µg L^{-1}). The Agency for Toxic Substances and Disease Registry (ATSDR) has set achronic durational oral minimal risk level (MRL) of 0.0002 mg/kg/day of cadmium based on its renal effects. This MRL standard states how much cadmium can be taken in orally chronically without risk of adverse health effects (ATSDR 1999) and World Health Organization (WHO) set a tolerable weekly intake for cadmium at 0.007 mg/kg/body weight.

In the Mae Sot district, Tak Province and Na-Noi district, Nan Province Thailand, cadmium contamination were reported in soil and rice due to river water contamination suspected from upstream mining activity, by the Thai Ministry of Agriculture in 2003. In the polluted area, Nishijo (Nishijo et al., 2014) was reported that 90% of the rice grain samples were contaminated with Cd at the level greater than 0.2mg kg^{-1} (ppm) and 85% of the surveyed paddy soil samples had a Cd concentration that was greater than 3mg kg^{-1}.

2.1.2.3 The analytical techniques for cadmium analysis

A wide variety of modern instrumental techniques are extensively employed for the detection and determination of trace cadmium. Despite the selectivity and sensitivity of analytical techniques such as flame atomic absorption spectrometry (FAAS) (An-Na and Yun-Fei, 2011; Cancela, 2006; Valfredo Azevedo Lemos and Baliza, 2005; Valfredo A. Lemos et al., 2000), graphite furnace atomic absorption spectrometry (GFAAS) (Minamisawa et al., 2006; Tokman and Akman, 2004), electrothermal atomic absorption spectrometry (ETAAS) (Ivanova et al., 1998; Xu et al., 2000), inductively coupled plasma optical emission spectrometry (ICP-OES) (Castro et al., 2008; Costa et al., 2002; Lara et al., 2001; Marchisio et al., 2005) and inductively coupled plasma mass spectrometry (ICP-MS) (O'Sullivan et al., 2013) techniques. There is a critical need for the preconcentration and separation of trace metals prior to their determination, due to their frequent presence at low concentrations in environmental samples. Accurate analysis of various complex samples (natural water, tap water, waste water, geological samples and industrial effluents), especially at trace levels, is one of the most difficult and complicated analytical task. The summery of method for determination a trace cadmium were listed in the Table 5.

Table 5 Analytical methods used for cadmium determination after selected preconcentration steps

No.	Technique	Samples	Preconcentration sorbent	Chelating material	Detection limit	Reference
1.	FAAS	certified reference materials	2-(2-benzothiazolylazo)-2-*p*-cresol (BTAC)	-	0.27 μg L^{-1}	Lemos et al., 2000
2.	FAAS	Water	Amberlite XAD-2	2-aminothiophenol (AT)	0.14 μg L^{-1}	Valfredo et al., 2005
3.	FAAS	Milk products	Chelite P	aminomethylphosphoric acid (AMPA)	0.014 g μg^{-1}	Cancela et al., 2006
4.	FAAS	Drinking water	Hair	ammonium diethyldithiophosphate (APDC)	0.77 μg L^{-1}	An-Na etal., 2011
5.	GFAAS	Water	Zeolite A4	-	0.02 μg L^{-1}	Minanisawa et al., 2006
6.	GFAAS	Water	Chromosorb-107	ammonium diethyldithiophosphate (APDC)	1.2 μg L^{-1}	Tokman et al., 2004
7.	ETAAS	Water	C_{18}	ammonium diethyldithiophosphate (APDC)	0.5 ng L^{-1}	Xu et al., 2000
8.	ETAAS	Blood	knotted reactor (KR)	Ammonium diethyldithiophosphate (DDPA)	0.2 ng L^{-1}	Ivanova et al., 1998

Table 5 (continue)

No.	Technique	Matrix	Sorbent	Chelating material	Detection limit	Reference
9.	ICP-OES	Saline matrices	1, 10-phenanthroline	Dithizone	30 µg L^{-1}	Costa et al., 2002
10.	ICP-OES	Tea	polyurethane foam	2-(5-bromo-2-pyridilazo)-5-diethylaminophenol (5-Br-PADAP)	4.0 µg L^{-1}	Marchisio et al., 2000
11.	ICP-OES	Wine	knotted reactor (KR)	2-(5-bromo-2-pyridylazo)-5-diethylaminophenol	5 ng L^{-1}	Lara et al., 2001
12.	ICP-OES	Water	silica gel	2-aminothiazole	0.27 µg L^{-1}	Castro et al., 2008
13.	ICP-MS	Water	minodiacetate	-	2.7 pM	O'Sullivan et al., 2013

2.2 Antibiotics

Antibiotics or antimicrobials are natural compounds made by microorganisms, which may be used to destroy bacteria that cause infections and diseases. A wide variety of antibiotics are used in agriculture and medicine alike. They are classified based on their chemical composition as well as the class of microorganisms against which they are effective with. Antibiotic studies demonstrate that preventative treatment may effectively control disease in livestock. Hence, recognizing the potential economic gains, the use of antibiotics in farming practices has expanded rapidly over the years. Although most countries have banned the antibiotics chloramphenicol and nitrofurans from animal food production due to their toxicity to humans, traces of the drugs have been detected in shrimp and other aquaculture products. Chloramphenicol can cause potentially fatal aplastic anemia and leukemia, and nitrofurans are carcinogenic. Therefore, the seafood industry fully supports regulations that control the drugs to assure wholesome foods for consumers.

There are various antibiotics available and they come in various different brand names. Antibiotics are usually grouped together based on how they work. Each type of antibiotic only works against certain types of bacteria or parasites. This is why different antibiotics are used to treat different types of infection. The main types of antibiotics include:

- Penicillins, for example: penicillin V, flucloxacillin, and amoxicillin.
- Cephalosporins, for example:cefaclor, cefadroxil, cefalexin.
- Tetracyclines, for example: tetracycline, doxycycline, and minocycline.
- Aminoglycosides, for example: gentamicin, amikacin, and tobramycin.
- Macrolides, for example: erythromycin, azithromycin, and clarithromycin.
- Clindamycin.
- Sulfonamides and trimethoprim, for example: co-trimoxazole.
- Metronidazole and tinidazole.
- Quinolones, for example: ciprofloxacin, levofloxacin, and norfloxacin.
- Nitrofurans, for example: furaltadone, furazolidone,nitrofurazone and nitrofurantoin.

In this research, nitrofuransincluding furaltadone (FTD), furazolidone (FZD) and nitrofurantoin (NFT) areof interested. The structures of these antibiotics are show in Figure 12.

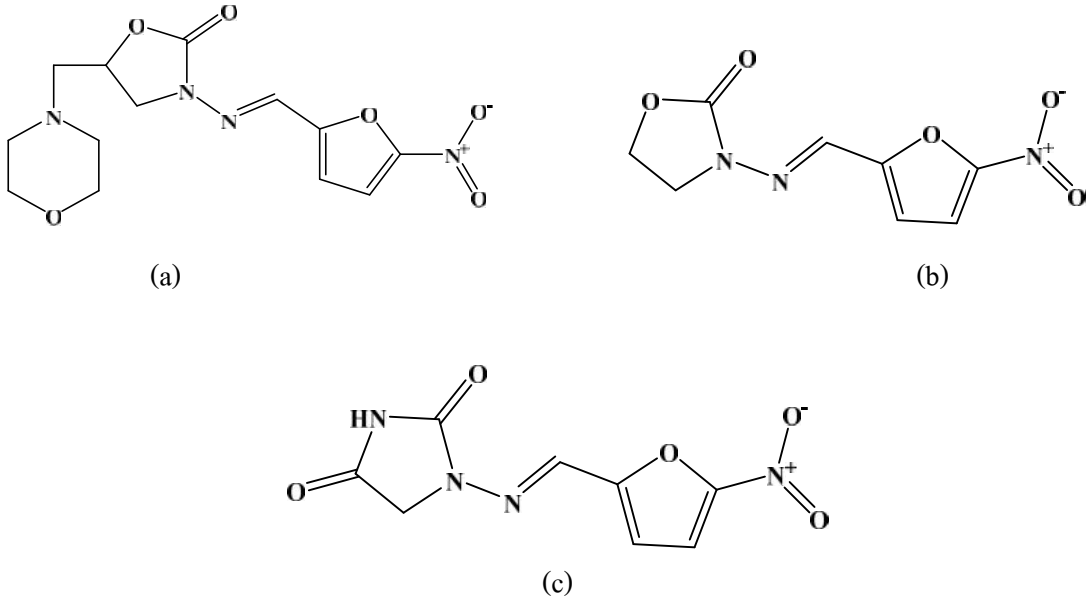

Figure12 Chemical structure of nitrofuran; a furaltadone , b furazolidone and c nitrofurantoin

Nitrofurans were widely used as feed additives in food-producing animals like poultry, swine, cultured fish and shrimps, for treatment and prevention of various gastrointestinal infections caused by bacteria or protozoa and as growth promoters. These compounds are rapidly metabolized *in vivo*, leading to a significant decrease of their parent compounds levels in plasma.

2.2.1 Furaltadone

Furaltadone belongs to the class of 5-nitrofuran antibiotics and has been widely and effectively used for the prevention and treatment of gastrointestinal infections caused by Escherichia coli and Salmonella spp. in cattle, pigs and poultry. It was also used as a growth promoter in food-producing animals. However, both WHO and the European Union (EU) are unable to assign a maximum residue limit for furaltadone because of the potential carcinogenic effects of its residues on human health. As a consequence, the administration of furaltadone to food-producing animals has been prohibited.

2.2.2 Nitrofurantoin

Nitrofurantoin (NFT) is bactericidal to many gram positive and gram-negative pathogens. It is readily absorbed from the gastrointestinal tract and is used in the treatment of urinary tract infections. It is used to treat urinary infections and can be administered orally or parenterally. *E coli, Staphylococcus aureus, Streptococcus pyogenes*and *Erobacteraerogenes*are usually susceptible, while *Proteus* species, *Pseudomonas aeruginosa* and *Streptococcus faecalis*are usually resistant. NFT is a synthetic nitrofuran derivative antibacterial agent. It is used for treatment of initial or recurrent urinary tract infections caused by susceptible pathogens. Adverse effects may include nausea, vomiting, loss of appetite, diarrhea, chest pain, chills, cough, fever, troubled breathing, sore throat, unusual weakness, dizziness, drowsiness, headache, and brownish discoloration of urine.

2.2.3 Furazolidone

Furazolidone (FZD) was added to Annexe 4 of Regulation 2377/90 on 26 June 1995. This decision was taken because furazolidone residues, at whatever limit, in foodstuffs of animal origin constitute a hazard to the health of the consumer. It is known to be a genotoxic carcinogen and insufficient data are available concerning the identity and toxic potential of compounds released from boundfurazolidone residues. Furazolidone therefore joins the other nitrofuran drugs; growth promoting hormones, such as diethylstilboestrol and trenbolone; and other antibacterial compounds, such as chloramphenicol, which are banned in the EU. It is often added to feeds to stimulate growth and prevent and control a number of diseases in animals.

2.2.4 The analytical technique for nitrofurans analysis

Several analytical techniques have been reported to determine nitrofuran residues in various sample matrices have been developed such as the enzyme-linked immunosorbent assay(ELISA) (Jester et al., 2014; Li et al., 2010), liquid chromatography with diode array (LC-DAD) (Barbosa et al., 2007; Degroodt et al., 1992; Wang and Zhang, 2006), liquid chromatography with mass spectrometry LC-MS (Ardsoongnearn et al., 2014; Mottier et al., 2005), and flow injection chemiluminescence (FI-CL) (Liu et al., 2012; Thongsrisomboon et al., 2010) as depicted in Table 6.

Table 6 Analytical methods used for nitrofurans determination

No.	Techniques	Analyte	Samples	Detection limit	Reference
1.	ELISA	Furazolidone	Fish	0.05 ng g^{-1}	Jester et al., 2014
		Furaltadone		0.2 ng g^{-1}	
2.	ELISA	Furazolidone	Animal feed	12.5 ng mL^{-1}	Li et al., 2010
		Furaltadone		16.0 ng mL^{-1}	
		Nitrorurantoin		15.6 ng mL^{-1}	
		Nitrofurazone		6.0 ng mL^{-1}	
3.	LC-DAD	Nitrofurazone	Animal feed	51 µg kg^{-1}	Barbosa et al., 2007
		Furazolidone		47 µg kg^{-1}	
		Furaltadone		98 µg kg^{-1}	
		Nitrorurantoin		76 µg kg^{-1}	
4.	LC-DAD	Furazolidone	Animal feed	1.0 mg kg^{-1}	Wang et al., 2006
		Furazolidone		2.0 mg kg^{-1}	
		Furaltadone		1.0 mg kg^{-1}	
5.	LC-DAD	Nitrofurazone	Meat and fish	1.0 µg kg^{-1}	Degroff et al., 1992
		Furazolidone		2.0 µg kg^{-1}	

Table 6 (continue)

No.	Techniques	Analyte	Samples	Detection limit	Reference
6.	LC-MS/MS	Nitrofurazone	Meat	0.11 µg kg^{-1}	Mottier et al., 2005
		Furazolidone		0.12 µg kg^{-1}	
		Nitrofurantoin		0.21 µg kg^{-1}	
7.	LC-MS/MS	Nitrofurazone	Feed water	0.25µg L^{-1}	Ardsoongnearn et al., 2014
		Furazolidone		0.002 µg L^{-1}	
		Furaltadone		0.002µg L^{-1}	
		Nitrorurantoin		0.04 µg L^{-1}	
8	LC-MS/MS	Nitrofurazone	Animal feed	0.2 mg kg^{-}	Wang et al., 2006
		Furazolidone		0.1 mg kg^{-1}	
		Furaltadone		0.1 mg kg^{-1}	
9.	FI-CL	Furaltadone	Animal feed	0.83 mg L^{-1}	Thongsrisomboon et al.,
		Nitrorurantoin		0.83 mg L^{-1}	2010
		Nitrofurazone		0.83 mg L^{-1}	
10.	FI-CL	Furaltadone	Animal feed	$2x10^{-7}$ g mL^{-1}	
		Furazolidone		$4x10^{-7}$ g mL^{-1}	Liu et al., 2012
		Nitrorurantoin		$8x10^{-7}$ g mL^{-1}	

CHAPTER 3

Specific Speciation of As(III) and As(V) in Aqueous Solution by a Split Microfluidic Chemiluminescence System

3.1 Introduction

Arsenic is a naturally occurring element present in the environment in both organic and inorganic forms. Inorganic arsenic is considered to be the most toxic form of the element, and arsenic contamination of ground water is found in many countries throughout the world, including China, Bangladesh, Vietnam and Thailand. The present of arsenic in natural water is of concern because of its toxicity and possible carcinogenic activity, and the biological effects of arsenic are significantly altered by its oxidation state as well as by its complexation with organic materials. Depending on the environment, inorganic arsenic can exist in two different oxidation states As(III) and As(V) in natural water, although As(V) is thermodynamically favored. Because of its ability to form complexes with certain co-enzymes, however, As(III) is more toxic to animal and plants than is As(V). The USEPA reduces the maximum permissible level (MPL) of arsenic in drinking water from 50 to 10 μg L^{-1} (Agency, 2013). Current arsenic detection always relies on large apparatus including atomic absorption spectrometry (AAS) (APHA, 2005), hydride generation atomic fluorescence spectrometry (HGAFS) (Cava-Montesinos et al., 2003; M. Featherstone et al., 1998; Yan et al., 2002; Zhang et al., 2010), inductively coupled plasma atomic emission spectrometry (ICP-AES) (Jitmanee et al., 2005; Morita et al., 1981; Sheppard et al., 1994) and inductively coupled plasma mass spectrometry (ICP-MS) (Beauchemin et al., 1989; Heitkemper et al., 2001; Villadangos et al., 2010). The USEPA approved spectrometric methods are all based on atomic spectrometry, which can readily provide detection limits in the sub-microgram per liter range, but the instrumentations are bulky, expensive, and require large amounts of pure gas in addition to the high cost of consumables. Hence, the alternative, portable and sensitive equipment is continually demanded for on-site measurement.

Microfluidic devices currently present unique advantages for sample handling, reagent mixing, separation, and detection. Microfluidic channel dimensions typically range from 1 to 1000 μm in width and height and require between 100 nL and 10 μL of sample and reagents. In addition to obvious advantages that are associated with smaller sample, reagent and waste volumes required which is ideal for handling costly and difficult-to-obtain samples and reagents. The materials used to construct microfluidic devices vary, depending on the application; however, the vast majorities are constructed of glass, silicon, polymers or even filter paper using photolithography to define hydrophobic micro-channels. One particular polymer that has recently been used extensively is poly(dimethylsiloxane), or PDMS since PDMS is a transparent, elastomeric polymer that can be fabricated rapidly by laser engraving with features having dimensions as small as 10 nm. The elastomeric nature of PDMS makes it a great sealant, since often the adhesion due to conformal surface contact with a smooth, flat surface is enough to seal meso- or even microchannels for low pressure applications (Duffy et al., 1998; Ng et al., 2002).

During the past decades, there have been word-wide efforts to develop miniaturized instrumentation for chemical analysis. However, the utilization of microfluidics in the attempts for the determination of arsenic has rarely appeared. One attempted had been reported by Matusiewicz (Matusiewicz and Slachcinski, 2012). Only few reports exploited the use of CL detection to determine inorganic arsenic spices and most of them were based on a flow injection (FI) system (Li and Hak Lee, 2005; Lomonte et al., 2007).

In this present work, the integration of a microfluidic device with chemiluminescence(CL) detection for the determination of As(III) and As(V) in aqueous samples is proposed. Since, CL provides high sensitivity and selectivity, white is a simple and inexpensive optical instrumentation. The acidic permanganate and luminal chemiluminescence detections have been allocated for our system. The sandwich type microfluidics chip consisted of two halves of spiral conduit platforms where the CL reaction for As(V) was generated based on the oxidation of luminol with a vanadomolybdo arsenate heteropoly acid (AsVMo-HPA) complex in an alkaline solution. On the other hand the CL reaction for As(III) was produced by the oxidation of acidic potassium permanganate in the presence of a sodium hexameta phosphate media.

3.2 Research methodology

3.2.1 Reagent and solution

All chemicals used as list in Table 8 are analytical reagent (AR) grade, and all standard and reagent solutions were prepared with deionized water.

Table 7 Chemical reagent and their manufactures for determination of As(III) and As(V)

	Reagent	Grade	Manufactures	Country
1.	Ammonium metavanadate (NH_4VO_3)	AR	BDH	UK
2.	Ammonium molybdate ($(NH_4)_6Mo_7O_{24}.4H_2O$)	AR	BDH	UK
3.	Copper (II) sulphate monohydrate ($CuSO_4.5H_2O$)		Ajax	Australia
4.	Formaldehyde (CH_2O)	AR	BDH	UK
5.	Iron (III) nitrate nonahydrate ($Fe(NO_3)_3.9H_2O$)	AR	QReC	New Zealand
6.	Iron (II) sulphate hetahydrate ($FeSO_4.7H_2O$)	AR	MercK	Germany
7.	Luminol ($C_8H_7N_3O_2$)	HPLC	Sigma-Aldrich	USA
8.	Magnesium sulfate ($MgSO_4$)	AR	Sigma-Aldrich	USA
9.	Manganese (II) sulfate monohydrate ($MnSO_4.H_2O$)	AR	Ajax	Australia
10.	Potassium permanganate ($KMnO_4$)	AR	Ajax	Australia
11.	Rhodamine B ($C_{28}H_{31}ClN_2O$)	HPLC	Fluka	USA
12.	Sodium arsenite ($NaAsO_2$)	HPLC	Ajax	Australia
13.	Sodium arsenate monohydrate ($Na_2HAsO_4.H_2O$)	HPLC	Ajax	Australia
14.	Sodium chloride (NaCl)	AR	Lab scan	Ireland
15.	Sodium fluoride (NaF)	AR	Riedel-de Haen	USA
16.	Sodium hexametaphosphate $(NaPO_3)_6$	AR	Sigma-Aldrich	USA
17.	Sodium hydroxide (NaOH)	AR	Lab scan	Ireland
18.	Sodium nitrate (Na_2NO_3)	AR	Sigma-Aldrich	USA
19.	Sodium nitrite ($NaNO_2$)	AR	Sigma-Aldrich	USA
20.	Sodium phosphate dibasic (Na_2HPO_4)	AR	CARLO ERBA	Italy
21.	Sodium sulfate (Na_2SO_4)	AR	Sigma-Aldrich	USA
22.	Sulfuric acid (H_2SO_4)	AR	J.T baker	Poland

3.2.2 Standard preparation

As(III) and As(V) stock solution (1,000 mg L^{-1}) were prepared by dissolving 0.1734 g of $NaAsO_2$ and 0.4160 g of $Na_2HAsO_4.H_2O$ in 100 mL of deionized water, respectively. The As(III) and As(V) stock solutions were kept in a sealed container in a refrigerator at 4 °C when not in use. Standard solutions of As(III) and As(V) (4-60 μg L^{-1}) were made up by making appropriate dilution of As(III) and As(V) stock solution in 6.0 mM sulfuric acid solution.

3.2.3 Reagent preparation

Potassium permanganate stock (1.0×10^{-2} M) was prepared by dissolving 0.1578 g of $KMnO_4$ in 100 mL deionized water. Rhodamine B solution (100 mg L^{-1}) was prepared by dissolving 0.01 g of $C_{28}H_{31}ClN_2O_3$ in 100 mL deionized water.

The stock solution of luminol (1.0×10^{-2} M) was prepared by dissolving 0.0886 g of luminol in 50 mL of 0.1 M NaOH solution. Ammonium metavanadate solution (0.1 M) was prepared by dissolving 1.17 g of NH_4VO_3 in 0.02 M sulfuric acid solution. Ammonium molybdate solution (0.1M) was prepared by dissolving 12.40 g of $(NH_4)_6Mo_7O_{24}.4H_2O$ in 0.02 M sulfuric acid solution.

The carrier stream solution (C) was a 6.0 mM of sulfuric acid. The reagent stream solution (R1) comprises of acidic potassium permanganate (1.5×10^{-4} M), and Rhodamine B (8 mg L^{-1}) was prepared by making appropriate dilution of the $KMnO_4$ stock solution and Rhodamine B solution in 0.70 % (m/v) sodium hexametaphosphate diluents in 6.0 mM sulfuric acid solution. The mixed carrier solution (R2) of 0.70 % (m/v) sodium hexametaphosphate and formaldehyde (1.7 M) was prepared by making appropriate dilution a 32 mL of concentrate formaldehyde in 0.70 % (m/v) of sodium hexametaphosphate and 6.0 mM sulfuric acid solution in 250 mL volumetric flask. The heteropoly acid solution (R3) consisted of 8.0×10^{-4} M ammonium metavanadate, 7.0×10^{-3} M ammonium molybdate was prepared by making appropriate dilution of ammonium metavanadate solution and ammonium molybdate solution in 0.03 M sulfuric acid. The luminol solution (R4) was prepared by making appropriate dilution of luminal stock solution to the final concentration of 5.0×10^{-5} M in 0.10 M NaOH solution.

3.2.4 Design and fabrication of microfluidic device

The micro channel was designed by Adobe IIustrator 10 software and a designed-micro channel was illustrated in Figure 13 (A). CO_2 laser was used for the engraving and cutting of a micro channel in the polymethyl methacrylate (PMMA) followed by the pattern. The flow conduit comprises the carrier and reagent stream inlets, a spiral coil of a 500 µm-wide and 200 µm -deep of all 52.0 cm-long channel with 2.5 cm diameter. The microchip consisted of two halves of similar CL micro-conduit platforms sandwiched with polydimethyl-siloxane (PDMS) middle sheet prepared by mixing of 10:1 prepolymer and curing agent (Sylgard 184, Dow Corning, Midland, USA). The prepolymer mixture was stirred thoroughly and degassed in a vacuum for 15 min, then poured onto the glass slide template and cured at 70 °C for 1 h. After curing, the PDMS replica was peeled from the template and cut to respectively sheet size. The completed set up microfluidic device was declared as sandwich type as illustrated in Figure 13(B) with aluminium foil sheet was put in the middle. After that the device was sealed by tightening the PMMA sandwich sheets with 6 screws.

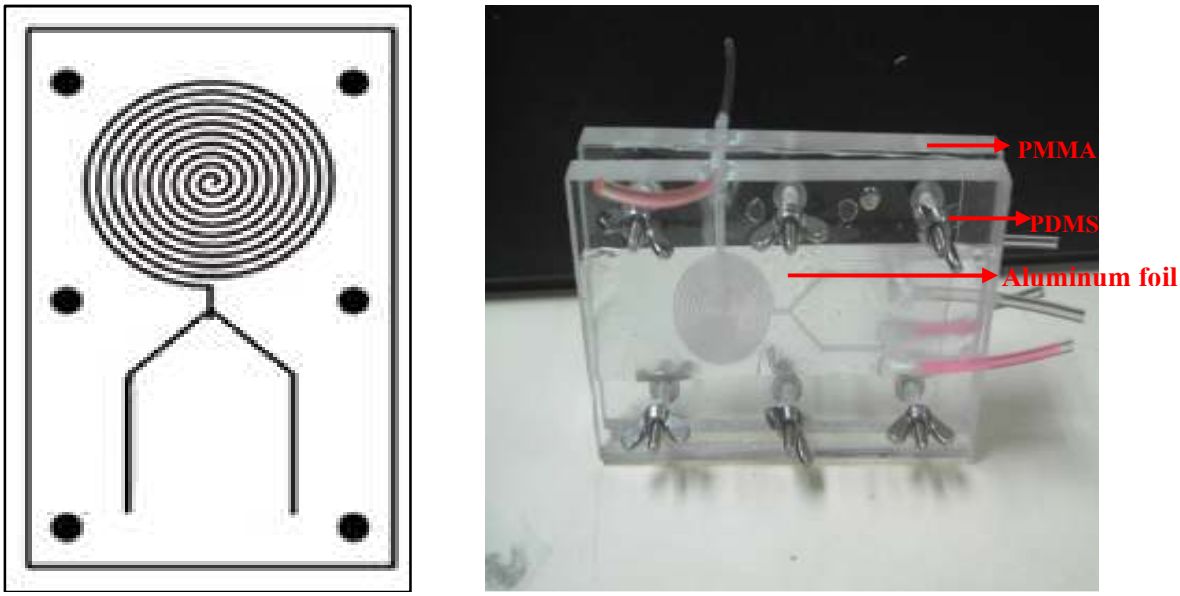

(A) (B)

Figure 13 Illustration of the laser-engraved flow lines of the microfluidic platform. (A); a sandwich type microfluidic device (B)

3.2.5 Instrument set-up

The μFI-CL system used in all experiment is depicted in Figure 14. The experimental setup consisted of five peristaltic pumps with rate selector (Minipuls 3, Gilson, France), a sample injection vale (V-450, Upchurch Scientific, USA) and PTFE connection tubing (0.5 mm i.d., Agilent, USA). The CL signals were monitored in custom built flow-through luminometer, where a microfluidic device was mounted flush against two sensitive photomultiplier tubes (PMT, 9828SB and 9924SB, ET-enterprise, UK), as illustrated in Figure 15. The operational potential for both PMTs was provided by two high voltage power supplies (Thorn- EMI model PM20, Electron tubes Ltd., UK) at the voltage of 0.85 and 0.90 kV, respectively. The output signal of the PMTs, proportional to the CL intensity, were monitored continuously and displayed by a personal computer via a digital multimeter USB/RS-232 (UT60G, Hong Kong) interface with the voltage divider (C637BFN2, Electron Tubes, UK). The UNI-T® UT60G AC/DC software was used for the determination of the peak maximum.

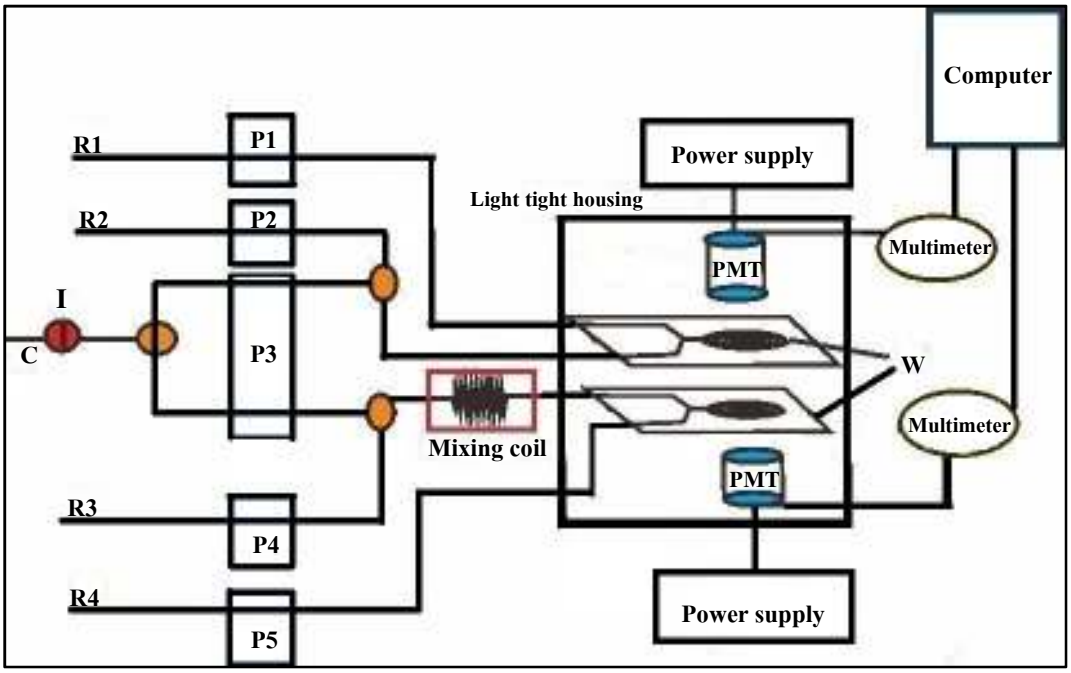

Figure 14 The manifold of μFI-CL system: R1= acidic potassium permanganate, R2= sodium hexametaphosphate/ formaldehyde, C=carrier stream(sulfuric acid),R3=ammonium metavanadate/ammonium molybdate, R4= luminol, W = waste, I = injection valve, PMT = photomultiplier tube and P1-P5 = peristaltic pump

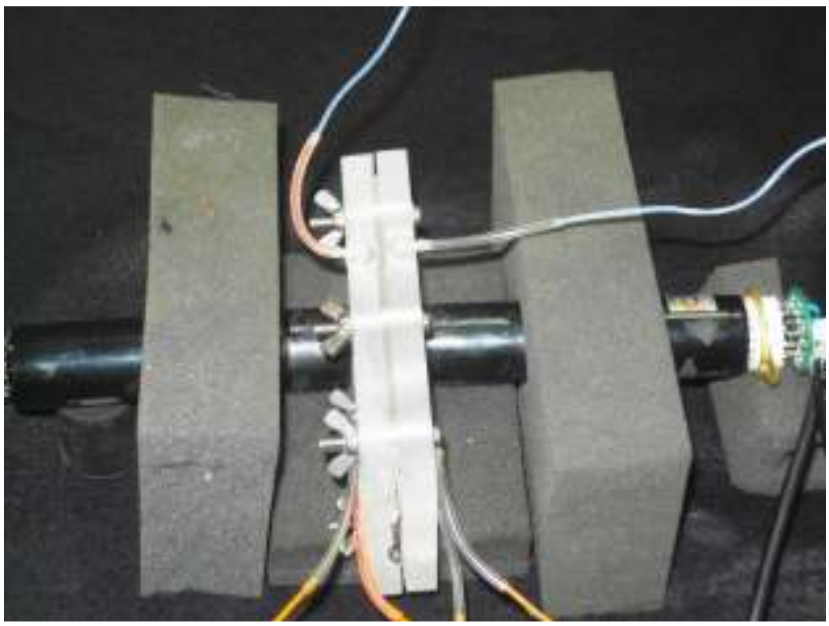

Figure 15 A microfluidic set-up for chemiluminescence detection of As(III) and As(V)

3.2.6 Preparation of samples

3.2.6.1 Preparation of sample containers

Polyethylene bottles available for water testing analysts, chemists and certain retail outlets are used in this work. The bottles are cleaned prior to sampling by firstly, rinsing with tap water, washing with washing –up liquid, washing with tap water and then immersing in 1:1 nitric acid for 24 hours. Secondly, they are rinsed with deionized water. Finally, they are left to dry out.

3.2.6.2 Sampling

Seven ground water samples (LP01-07) were collected from arsenic contaminated areas of Hang Chat district in Lampang province, Thailand, which is suffering from nearby mining and industrial waste landfill impacts. Water samples were collected in 1000 mL of clean PE containers, then the samples were treated by adding 2 mL of sulfuric acid and cooled at 4 $^{\circ}$°C until analysis. Samples were filtered through a 0.45 µm nylon filter to remove solid particles prior to analysis.

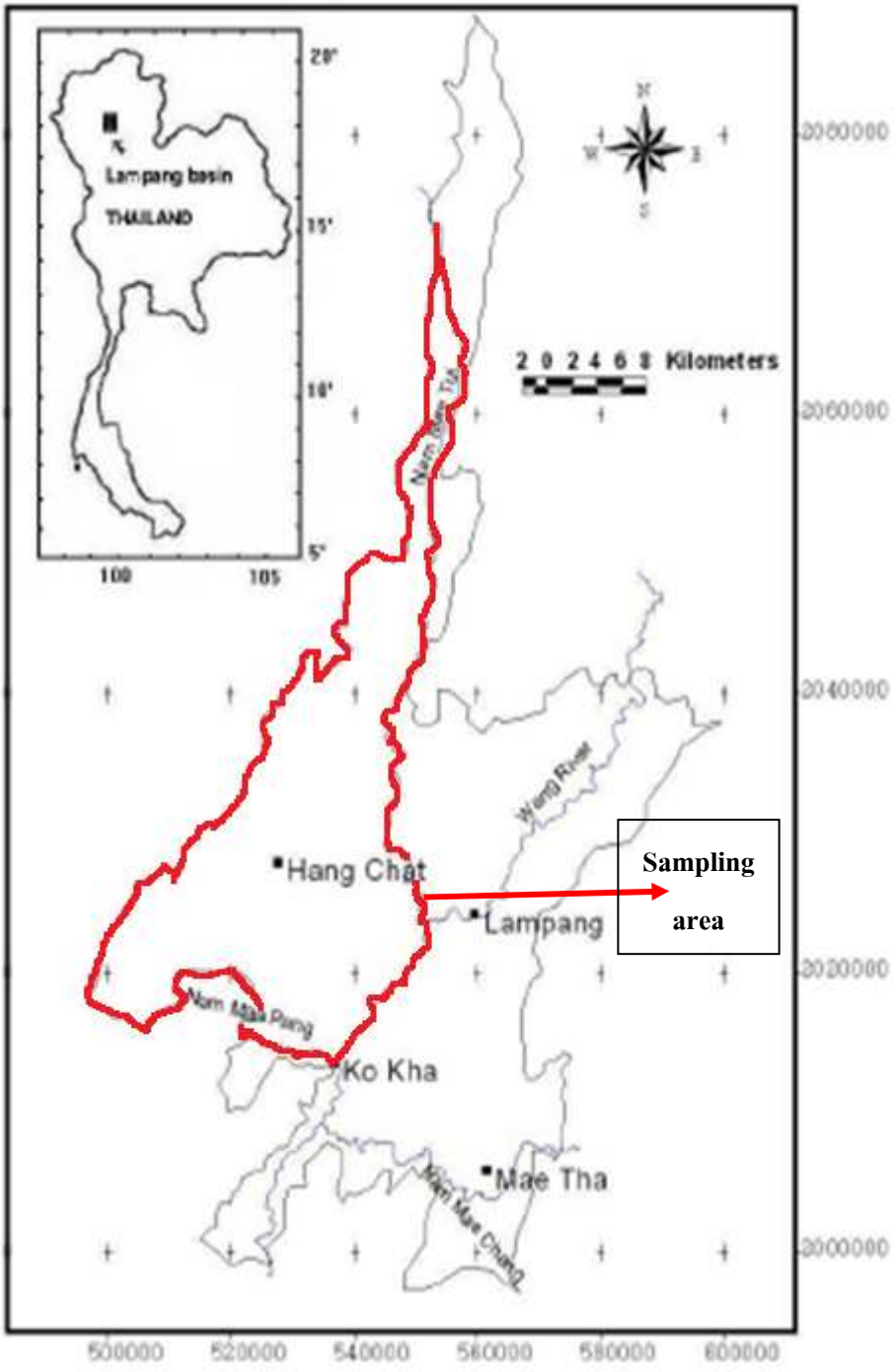

Figure 16 Sampling area at Hang Chat district in Lampang province, Thailand (Kwansiririkul et al., 2004)

(a) LP01

(b) LP02

(c) LP03

(d) LP04

(e) LP05

(f) LP06

(g) LP07

Figure 17 Sampling point at Hang Chat district in Lampang province, Thailand

3.2.7 Analytical procedure

A 150 µL of mixed standard or sample solution was injected into 6.0 mM sulfuric acid carrier solution (C), which was propelled by peristaltic pump P3. The carrier solution was then equally split and merged with the CL carrier solutions for each reaction on both sides of spiral-designed microfluidic platforms. Peristaltic pumps (P1 and P2) were employed to control the carrier streams of sodium hexametaphosphate/formaldehyde (R2) and reagent stream of acidic potassium permanganate (R1) at the equal flow rate of 5.50 mL min^{-1}, to symplify the flowing system. On the other hand, the carrier stream flow rate for luminol chemiluminescence detection, ammonium metavanadate/ammonium molybdate (R3), was set at 0.50 mL min^{-1} while the luminol reagent stream solution was set at the flow rate of 2.5 mL min^{-1}. The instrument set-ups were allocated for As(III) and As(V) determination, respectively.

Once the combination mixtures of each reaction were passed through the microfluidic flow conduits, the CL intensity was instantly detected by two sensitivity PMT tubes put flush against each side of microfluidic chip. The output of the PMTs which is proportional to the CL intensity was monitored simultaneously and continuously. The signals of the analytes were the maximum output corresponding to the peak maxima.

3.2.8 LC-ICP-MS Method

Experiments for the LC- ICP-MS method were performed with an Agilent 1100 series LC/diode array detector system including the following modules: Inductively coupled plasma–mass spectrometer (ICP-MS) Agilent 7500C series. The separation was carried out using an ODS column-CAPCELL Pack C18MG, 3.5 µm × 250 mm × 4.6 mm (Shiseido, Japan), thermostated at 25 ºC. The mobile phase was 0.05% methanol, 10 mM sodium 1-butane sulfonate, 4 mM malonic acid, 4 mM tetramethylammonium hydroxide in deionized water adjusted to pH 3.0 with nitric acid and set at a flow rate of 0.75 mL min^{-1}. The quadrupole mass analyzer was monitored as follows: detection ion m/z = 75.0 a.m.u. with sampling rate of 1 Hz.

3.3 Results and discussion

The previous reports by Taokaenchan et al. (Narin Taokaenchan, 2012) and Som-aum et al. (Som-Aum, 2008) were used for preliminary studies. The integration of a microfluidic device with two specific CL reactions was proposed in a single microfluidics chip which ran on a simple device made from small pieces of polymethylmethacrylate (PMMA) and polydimethylsiloxane (PDMS). The chemiluminescence detection of As(III) and As(V) based on the acidic permanganate (Ueda et al., 2001) and luminol (Attiq-Ur-Rehman et al., 2008) were employed for specific detections for each arsenic species.

3.3.1 Principle of chemiluminescence reaction for As(III) and As(V) determination

The CL reaction for As(V) was generated based on the oxidation of luminol with a vanadomolybdoarsenateheteropoly acid (AsVMo-HPA) complex in an alkaline solution as shown in the reaction formulas 1-3 (Som-Aum, 2008; Ueda et al., 2001). The reaction rate could be improved by elevating the reaction temperature (Attiq-Ur-Rehman et al., 2008).

$$Mo(VI) + As(V) + H^{+} \longrightarrow [AsMo_{10}O_{33}]^{9-} \quad (1)$$

$$[AsMo_{10}O_{33}]^{9-} + Mo(VI) + V(V) \longrightarrow [AsVMo_{11}O_{40}]^{4-} \quad (2)$$

$$\text{Luminol} + [AsVMo_{11}O_{40}]^{4-} + OH^{-} \longrightarrow \text{Aminophthalate} + N_2 + \text{other products} + h\nu \quad (3)$$

The As(III) species have been successfully determined with chemiluminescence detection by using acidic permanganate reaction. Adcock (Adcock et al., 2007) reviewed a possible CL mechanism of As(III) with acidic $KMnO_4$which may be attributed to the following reactions formulas(4-6) :

$$5\ H_3AsO_3 + 2MnO_4^- + 6\ H^+ \longrightarrow 5H_3AsO_4 + 2Mn^{2+*} + 3\ H_2O \quad (4)$$

In the presence of certain fluorophore, the energy resulting from the redox reaction can be an effective transfer to fluorophore dye which in turn generates the CL emission (Beauchemin et al., 1989).

$$Mn^{2+*} + \text{fluorophore} \longrightarrow Mn^{2+} + \text{fluorophore}^* \quad (5)$$

$$\text{fluorophore}^* \longrightarrow \text{fluorophore} + h\nu \quad (6)$$

3.3.2 Optimization of the micro fluidic parameters

To establish the optimum microfluidic conditions for the determination of As(III) and As(V), the effects of the key chemical and physical parameters on the CL signal were thoroughly investigated using an univariate approach. The μFI system's parameters optimized in this study were the: PMT applied voltage; concentration of reagent solution for determination of As(III) consisting of concentration of mixture $KMnO_4$ and Rhodamine B in reagent stream; concentration of mixture sodium hexameta phosphate and formaldehyde in reagent stream, respectively; the concentration of reagent solution for determination of As(V) consists of concentration of mixed ammonium metavanadate and ammonium molybdate reagent stream, concentration of luminol in the reagent stream, (iv) sample injection volume and (v) flow rates of each carrier and reagent streams for both CL detection system. A series of the experiments were conducted to establish the optimum analytical conditions for the CL oxidation of As(III) by acidic $KMnO_4$ and AsVMo-HPA by luminol. All measurements were performed in triplicate.

3.3.2.1 Effect of photomultiplier tube applied voltage

The effect of the photomultiplier tube (PMT) voltage was investigated in the range 700-1000 V for both PMTs. For these experiments, 100 µg L^{-1} of mixed standard solution of As(III) and As(V) were injected into the µFI-CL system. The potential of the power supplies were increased stepwise and the CL signals were measured after the injection of mixed arsenic solution at each potential step. The noise from the background current fluctuation was also measured at each potential step. As expected, The CL intensities were increased when the applied voltage was increased stepwise. However, the background noise was also increased. It was found that the signal-to-noise (S/N) ratio reached a maximum value at 850 V for As(III) and 950 V for As(V), respectively. The results are illustrated in Figure 18.

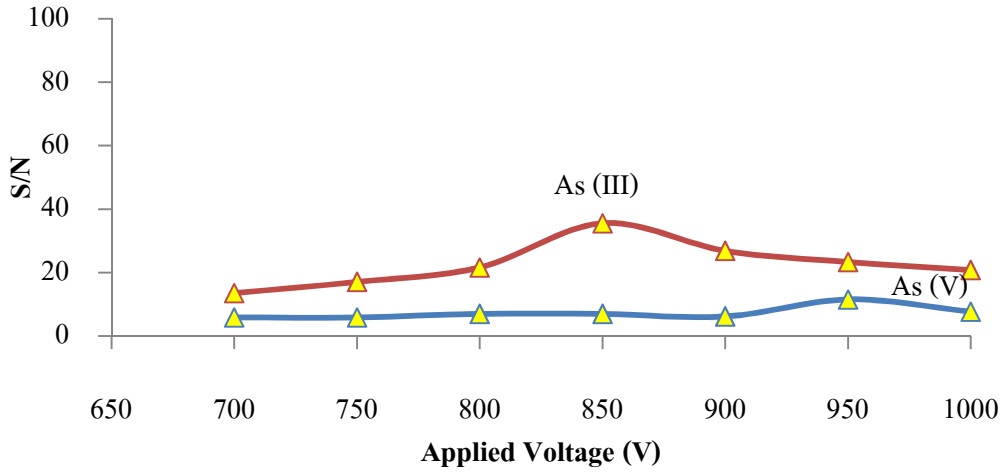

Figure 18 Effect of photomultiplier tube on the applied voltage

3.3.2.2 Effect of carrier and CL reagent concentrations on the CL intensity for As (III) determination

The CL reagent stream solution (R1) was composed of sodium hexameta phosphate, $KMnO_4$ and Rhodamine B in sulfuric acid media, while the carrier stream solution (R2) comprised of acidic sodium hexameta phosphate and Rhodamine B. The effect of sodium hexameta phosphate concentration on both streams was studied over the concentration range from 0.4-0.9% (m/v) when the concentration of sulfuric acid was fixed at 5×10^{-3} M. The CL intensity increases when the concentration of sodium hexameta phosphate increased. At the concentration of 0.7 % (m/v) sodium hexameta phosphate, the highest signal was observed; after this concentration the noise signal increase gradually made the S/N ratio decrease dramatically.

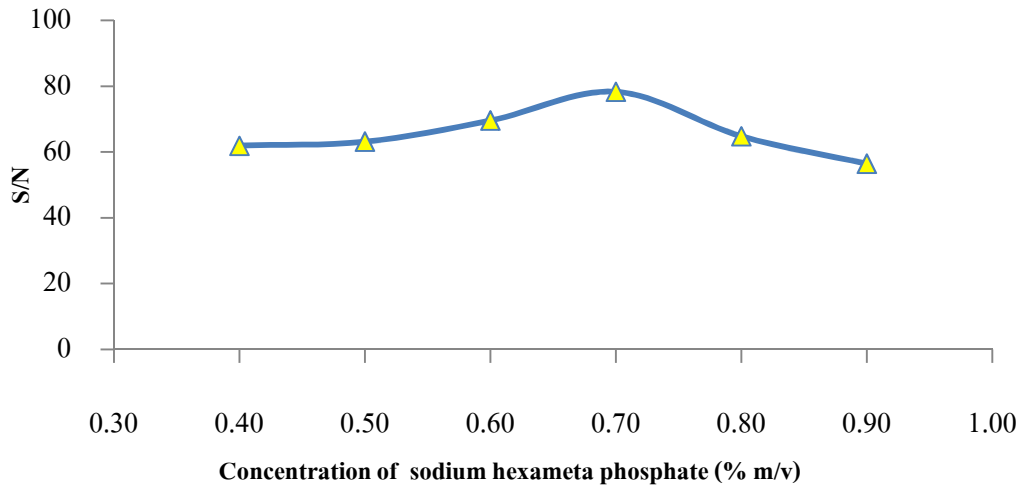

Figure 19 Effect of sodium hexameta phosphate on As(III) CL signal

The concentration of $KMnO_4$ was studied similarly to the previous parameter by varying the concentration from 0.05- 0.4 M, the result showed that the CL intensity reached the maximum when the concentration of $KMnO_4$ was at 0.15×10^{-3} M.

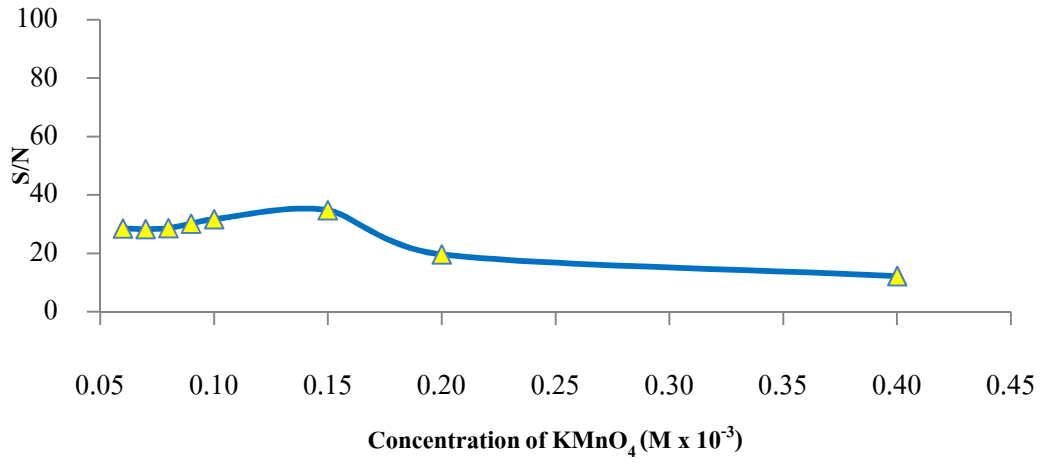

Figure 20 Effect of $KMnO_4$ on As(III) CL signal

Previous reports by Satienperakul et al. (Satienperakul et al., 2010) and Anastos et al. (Anastos et al., 2004) and reported that CL intensity from the reaction of acidic permanganate can be increased by adding formaldehyde and Rhodamine B. In this research, the addition of Rhodamine B (8 mg L^{-1}) into the $KMnO_4$ reagent solution resulted in the increase of CL intensity by two orders of magnitude. Beyond this concentration, the CL signal decreased gradually with increasing rhodamine B concentration. Besides, it was also noted that the addition of formaldehyde into sodium hexameta phosphate carrier solution significantly increased the CL intensity and reached maximum at the concentration of 1.7 M.

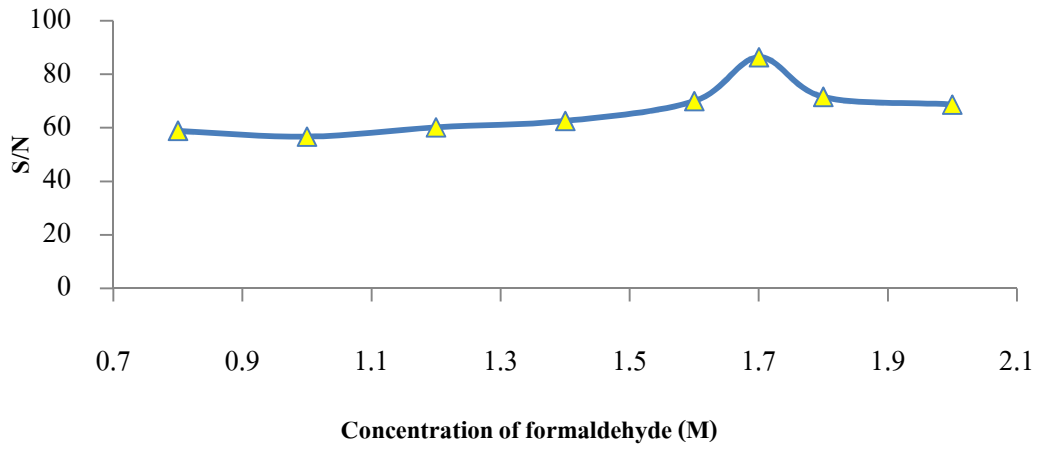

Figure 21 Effect of formaldehyde on As(III) CL signal

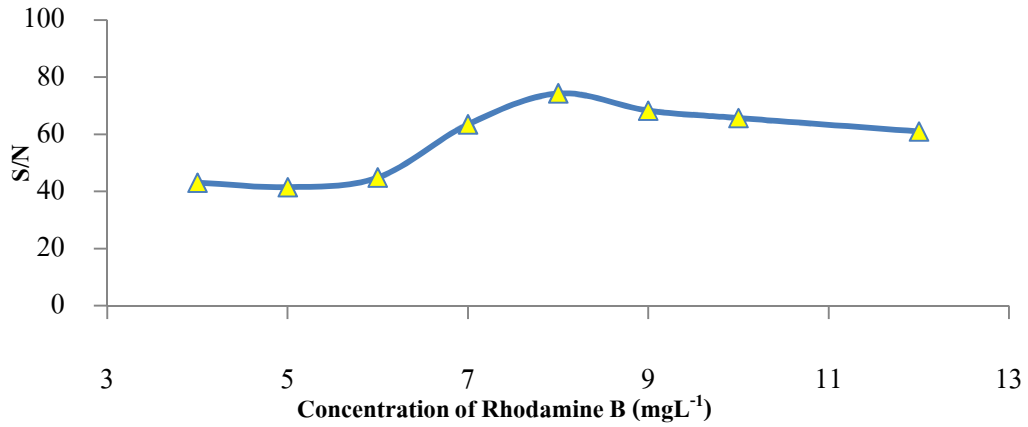

Figure 22 Effect of Rhodamine B on As(III) CL signal

3.3.2.3 Effect of carrier and CL reagent concentrations on the CL intensity for As (V) determination

The research study by Fujiwara et al. (Fujiwara et al., 1996) on the determination of the As(V) was based on the heteropoly acid reaction with luminol. The best heteropoly acid reagent was mixed with the ammonium metavanadate and ammonium molybdate in sulfuric acid. In this work, the investigation for the suitable condition for the complexation of vanadomolybdoarsenate heteropoly acid in reagent stream was studied by optimizing the concentration of a mixed reagent.

The concentration of ammonium metavanadate, ammonium molybdate and sulfuric acid in the reagent stream (R3) were studied in the ranges of 5.0-9.0×10^{-4} M, 5.0-9.0×10^{-3} M and 0.5-6.0×10^{-2} M, respectively. The increase in the concentration of ammonium metavanadate, ammonium molybdate and sulfuric acid resulted in the steep increase up to 8.0×10^{-4} M, 7.0×10^{-3} M and 3.0×10^{-2} M, respectively, above which the background response increased, causing an unstable baseline in CL intensity. Therefore the concentration of ammonium metavanadate, ammonium molybdate and sulfuric acid were chosen and used for vanadomolybdoarsenate heteropoly acid (AsVMo-HPA) complex formation in this study.

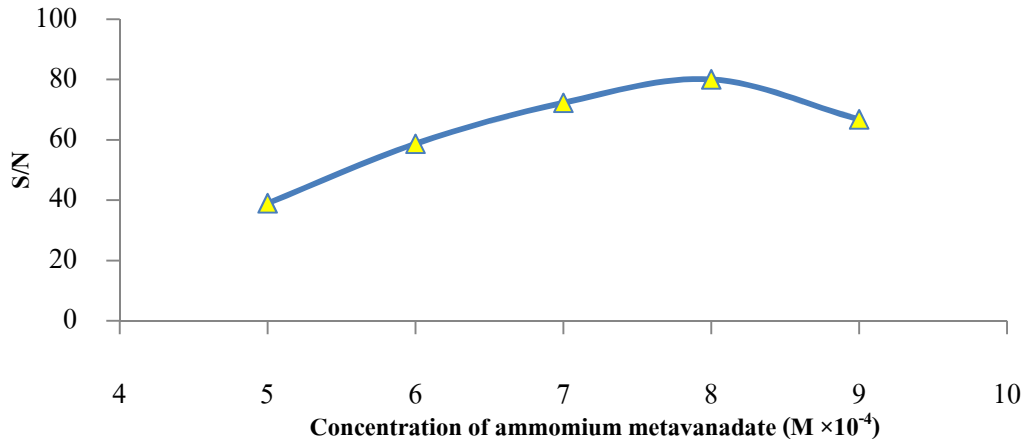

Figure 23 Effect of ammonium metavanadate on As(V) CL signal

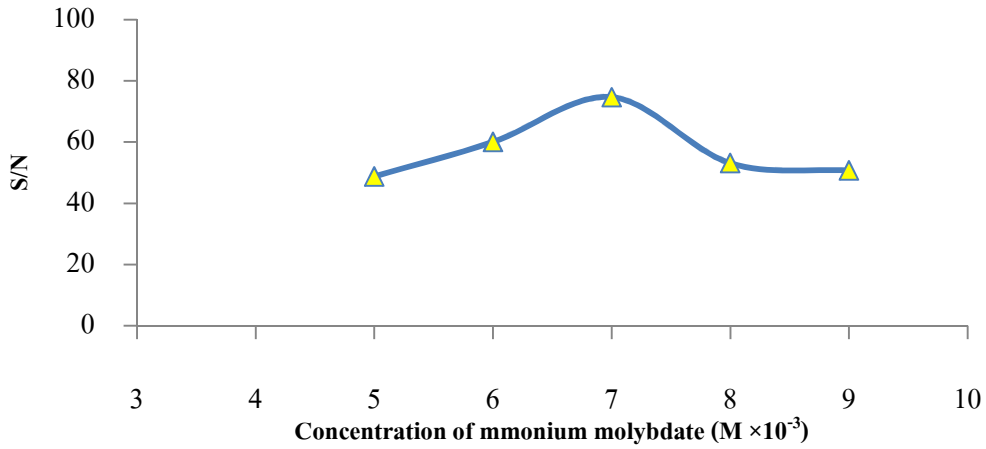

Figure 24 Effect of ammonium molybdate on As(V) CL signal

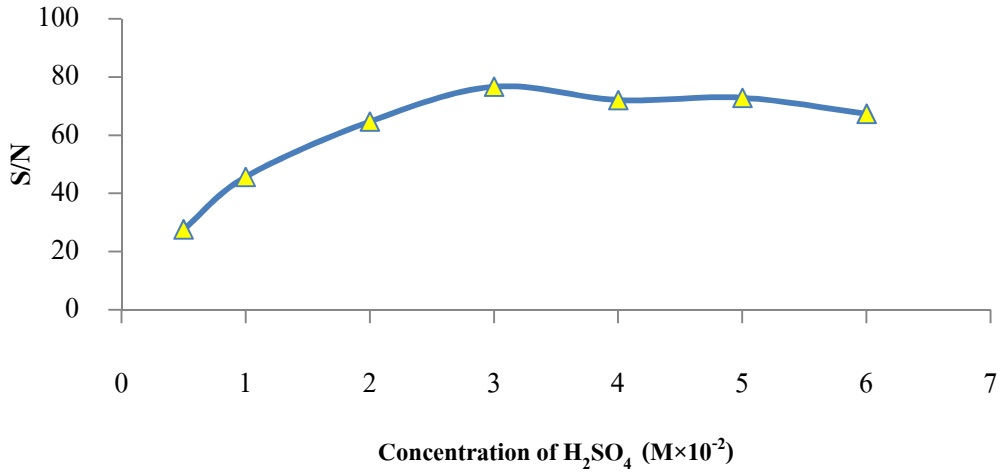

Figure 25 Effect of H_2SO_4 on As(V) CL signal

The CL intensity of the vanadomolybdoarsenate heteropoly acid (AsVMo-HPA) with luminol in NaOH media (R4) does not only affect on the CL intensity, but also the linearity of the method. The effect of luminol concentration on CL intensity was examined over the range 1.25×10^{-5}-30.0×10^{-5} M in alkaline media of 0.1 M NaOH. The CL intensity rapidly increased when the concentration of luminol was increased up to 5.0×10^{-5} M, above which the CL intensity decreased. Therefore, a concentration of luminol was chosen and used subsequently in this work.

The efficiency of luminol CL is highly dependent on the concentration of NaOH. The concentration of NaOH was varied from 0.0125-0.25 M. The optimal NaOH concentration was at 0.10 M, and therefore, a NaOH concentration of 0.10 M was selected and used subsequently.In the complexation of vanadomolybdoarsenate heteropoly acid we found that the CL intensity could arise due to the increasing of temperature, hence, these solutions (R3, R4) and the reaction coil were kept in the water bath at 80 °C during the operation.

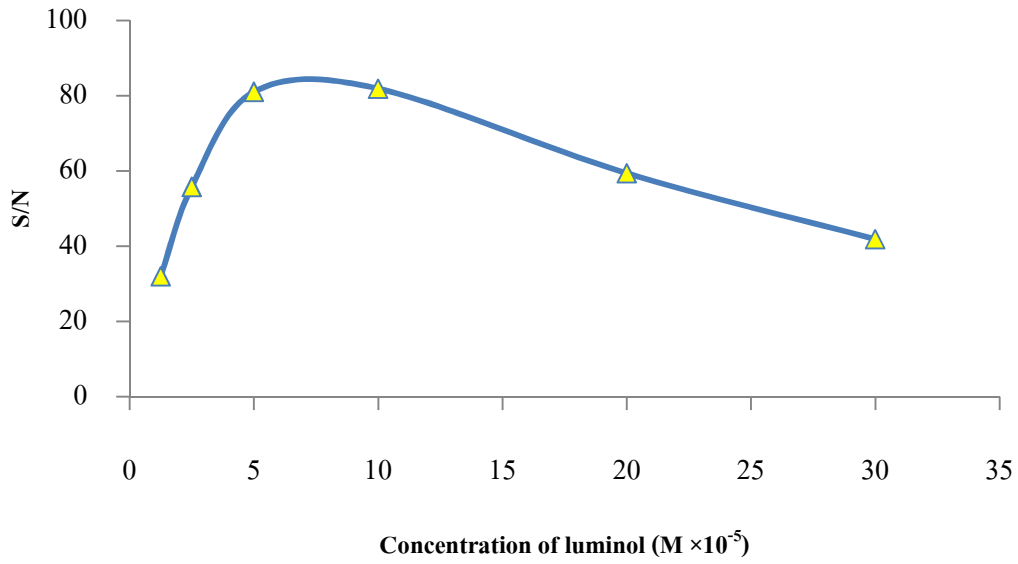

Figure 26 Effect of luminol on As(V) CL signal

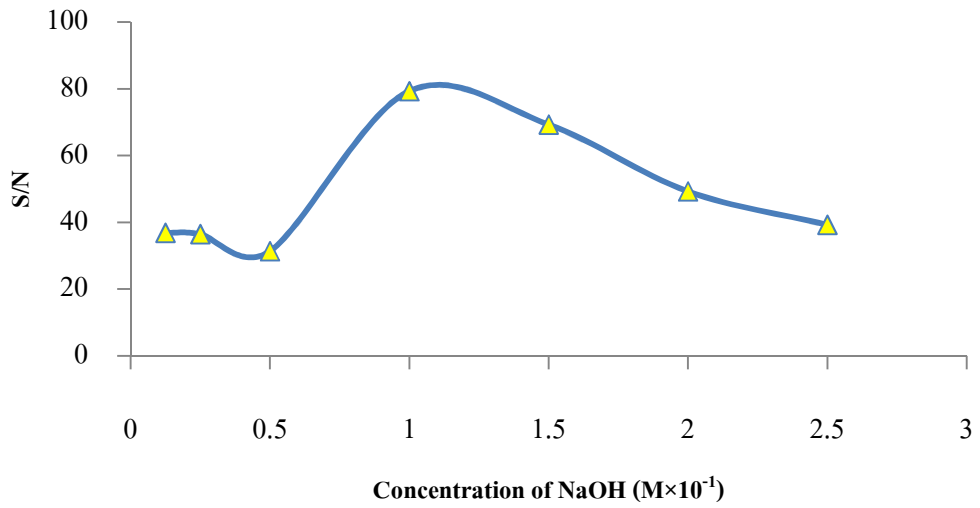

Figure 27 Effect of NaOH on As(V) CL signal

3.3.2.4 Effect of reagent and carrier stream flow rate (total)

Flow rate is an important parameter in CL detection as the same time taken to transfer the excited product into the flow cell is critical for maximum collection of the emitted light. The effect of the flow rates of the four channels was simultaneously over the range 0.5-5.0 mL min^{-1} in term of the sensitivity, sample throughput and reagent consumption. The CL intensity of mixed arsenic standard solution (100 µg L^{-1}) gave maximum intensity at total flow rate of 5.8 and 4.2 mL min^{-1} for the determination of As(III) in the upper half and As(V) in the bottom half, respectively.

3.3.2.5 Effect of injection volume

Similarly, the influence of the sample volume on the CL intensity of the flow system, over the range of 20-250 µL, was investigated by injecting the mixed arsenic standard solution at 100 µg L^{-1}. It was found that the CL intensity was increased when the volume of sample volume increased up to 150 µL, and become almost constant. Thus, a volume of 150 µL was selected for economy of the sample consumtion and speed of response for all remaining experiments.

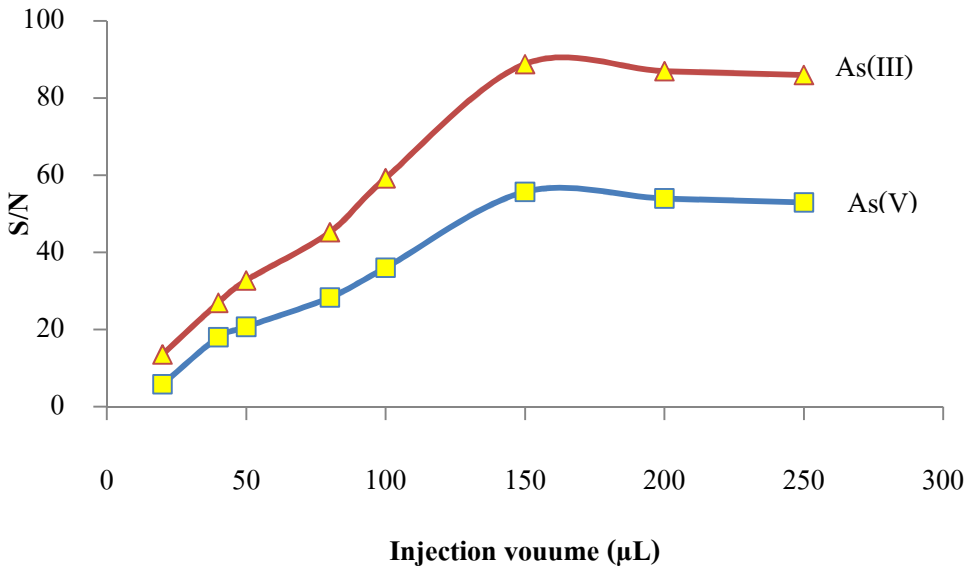

Figure 28 Effect of injection volume on As(III) and As(V) CL signal

3.3.2.6 Summary of the optimum conditions

The selected optimum conditions for As(III) and As(V) determinations were achieved by the so-called univariate method. The summary of their optimal values is shown in Table 8.

Table 8 Optimization of microfluidic system parameter

Parameters	Range studied	Optimal value	
		As(III)	As(V)
PMT applied voltage (V)	700-1000	850	950
H_2SO_4 concentration (M), C	$0.5\text{-}6.0\times10^{-2}$	3.0×10^{-2}	
Injection volume (μL)	20 – 250	150	
Total flow rate (mL)	0.5–6.0	5.8	4.2
$KMnO_4$ concentration (M), R1		0.15×10^{-3}	-
Rhodamine B concentration (mg L^{-1}), R1	4-12	8.0	-
Sodium hexametaphosphate concentration (% m/v), R2	0.4-0.9	0.7	-
Formaldehyde concentration (M), R2	0.05- 0.4	1.7	-
Ammonium metavanadate (M), R3	$5.0\text{-}9.0\times10^{-4}$	-	8.0×10^{-4}
Ammonium molybdate (M), R3	$5.0\text{-}9.0\times10^{-3}$	-	7.0×10^{-3}
Luminol (M), R4	$1.25\times10^{-5}\text{-}30.0\times10^{-5}$	-	5.0×10^{-5}
NaOH (M), R4	0.0125-0.25	-	0.10

3.3.3 Analytical figures of merit

3.3.3.1 Linearity of calibration graph

Under the optimal condition (Table 9), using the μFI-CL system as illustrated in Figure 14, the linear calibration curve, the limits of detection and the limits of quantification for the deterination of As(III) and As(V) were investigated. Figure 29 shows the calibration curves for As(III) and As(V), while Figure 30 illustrated the μFI-CL grams for As(III) and As(V), respectively. It was found that the calibration curve found to be linearity over range of 20-60 μg L^{-1}.

Table 9 The data of calibration curve for As(III) and As(V)

Concentration (μg L^{-1})	CL intensity (a.u.), n=3	
	As(III)	As(V)
20	27.5	5.6
30	33.6	6.6
40	38.1	7.3
50	43.6	8.3
60	50.2	9.3

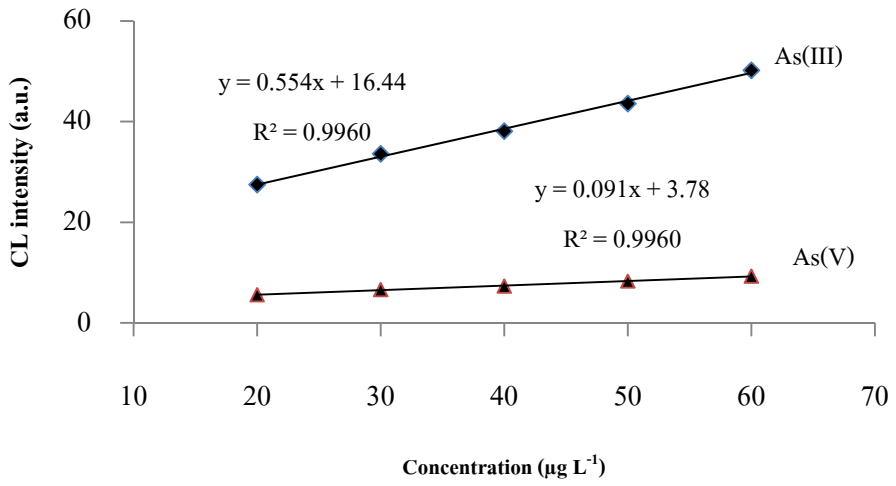

Figure 29 Calibration curves for As(III) and As(V)

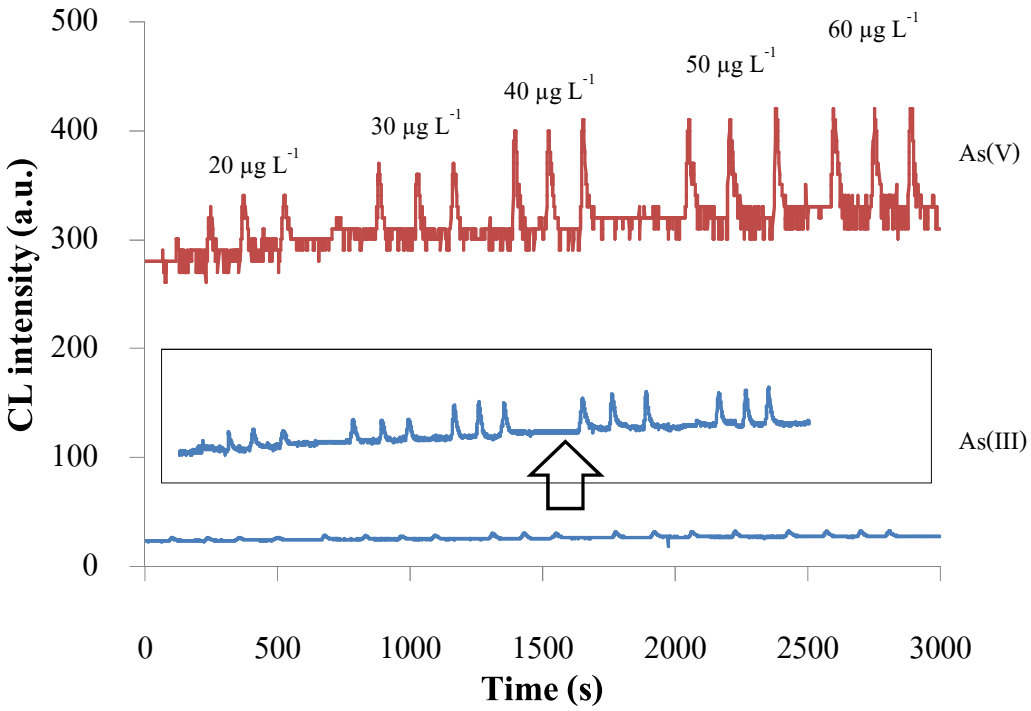

Figure 30 Illustrated the µFI-CL grams for As(III) and As(V)

3.3.3.2 The limits of detection and the limits of quantification

The limits of detection and the limits of quantification for the deterination of As(III) and As(V) were investigated. In this research , the limits of detection and the limits of quantification were calculated based on signal-to-noise ratio (S/N) of 3 and signal-to-noise ratio (S/N) of 10, respectively .

The limits of detection (signal-to-noise ratio of 3) of As(III) and As(V) were found to be 4 µg L^{-1} and the limits of quantification (signal-to-noise ratio of 10) were found to be 10 µg L^{-1}, respectively. The limits of detection provided from the proposed method it is lower than the miximum residue limit (MRL) level at 10 µg L^{-1} set by regulatory authorities in the USEPA.

3.3.3.3 Reproducibility and repeatability

The repeatability of the method was determined by repeating measurements of 40 µg L^{-1} As(III) and As(V) for 10 replicates. The reproducibility (intra-day) variations of the method were determined using triplicate injections of the standard As(III) and As(V) solutions at the concentraton of 40 µg L^{-1} and analysed on the same day. The reproducibility (inter-day) precision was studied by comparing the results of the assays performed on different days on the same injected standard As(III) and As(V) solutions in three replicates. The result was expressed in term of percentage relative standard deviation (% RSD). Results are shown in Table 10-12.

Table 10 Replicate measurements by using standard 40 µg L^{-1} of As(III) and As(V)

Experiment number	CL Intensity (a.u.)	
	As(III)	As(V)
1	38.5	7.3
2	38.0	7.1
3	38.1	7.0
4	38.0	7.5
5	38.3	7.1
6	37.8	7.3
7	38.0	7.5
8	38.3	7.1
9	37.5	7.0
10	38.2	7.2
Average	38.1	7.2
S.D	0.28	0.19
% RSD	0.74	2.57

Table 11 Reproducibility for intra-day variations

Times (hour)	CL intensity (a.u.), n=3	
	As(III)	As(V)
3	38.5	7.3
6	38.0	7.0
9	37.5	7.0
Average	38.0	7.1
S.D.	0.47	0.17
% RSD	1.23	2.43

Table 12 Reproducibility for inter-day variations

Times (day)	CL intensity (a.u.), n=3	
	As(III)	As(V)
1	38.5	7.3
2	37.5	7.0
3	37.8	7.0
Average	37.9	7.1
S.D.	0.49	0.20
% RSD	1.28	2.75

Table 13 shows the results of statistical analysis of the experimental data for As(III) and As(V) tested. It was found that the linearity of the calibration curve was over the range of 20-60 μg L^{-1}. The analytical characteristic for As(III) and As(V) and the precision of the proposed method was attained by analyzing 10 samples of 40 μg L^{-1}.

Table 13 Analytical figures of merit for determination of As(III) and As(V)

Analytical parameter	As(III)	As(V)
Regression equation	$CL_{intensity} = (0.554)C_{As(III)}(\mu g\ L^{-1}) + (16.44)$	$CL_{intensity} = (0.091)C_{As(V)}(\mu g\ L^{-1}) + (3.78)$
Linear range, $\mu g\ L^{-1}$	20-60	20-60
Correlation coefficient (r^2)	0.9960	0.9960
Limit of detection($S/N \geq 3$) ,$\mu g\ L^{-1}$	4	4
Limits of quantification ($S/N \geq 10$) , $\mu g\ L^{-1}$	10	10
Precision (% RSD), n=10	0.74	2.57
Intra-day precision (% RSD)	1.23	2.43
Inter-day precision (% RSD)	1.28	2.75

3.3.4 Interference studies

Interfering effects on common cations and anions such as Fe^{2+}, Zn^{2+}, Mg^{2+}, Mn^{2+}, Cu^{2+}, Fe^{3+}, F^-, Cl^-, NO_3^- , NO_2^-, SO_4^{2-} and PO_4^{3-} were investigated to study for interferences in the determination of 10 µg L^{-1}As(III) and As(V) using the proposed method. The tolerance limit was chosen as the amount of an error of ± 10 % in peak height. The maximum tolerance concentration for each coexisting anion and cation is illustrated in Table 14. F^-, Cl^-, NO_3^-, NO_2^-, SO_4^{2-} and Mg^{2+} showed no effect on the determination of high concentration levels of As (III) and As (V). Serious interferences came from Zn^{2+}, Mn^{2+}, Cu^{2+}, Fe^{2+}, $Fe^{3+}$and PO_4^{3-} where they react with $KMnO_4$ and luminol in the reagent stream even at the same concentration.

Table 14 Maximum tolerance of co-existing anion and cation for the determination of 10 µg L^{-1} As(III) and As(V)

Cations/Anion	Concentration ratios	% Error ,n=3	
		As(III)	As(V)
Fe^{2+}	1:0	-	-
	1:1	-4.00	0.54
	1:10	-4.00	0.00
	1:100	>100	>100
	1:1,000	>100	>100
	1:10,000	>100	>100
Zn^{2+}	1:0	-	-
	1:1	7.69	-2.24
	1:10	>-100	>-100
	1:100	>-100	>-100
	1:1,000	>-100	>-100
	1:10,000	>-100	>-100

Table 14 (continue)

Cations/Anion	Concentration ratios	% Error ,n=3	
		As(III)	As(V)
Mg^{2+}	1:0	-	-
	1:1	0.00	-2.24
	1:10	3.33	3.59
	1:100	6.67	5.83
	1:1,000	3.33	8.97
	1:10,000	20.00	19.28
Mn^{2+}	1:0	-	-
	1:1	-4.35	-2.24
	1:10	>100	>100
	1:100	>100	>100
	1:1,000	>100	>100
	1:10,000	>100	>100
Cu^{2+}	1:0	-	-
	1:1	-5.00	1.18
	1:10	>-100	>-100
	1:100	>-100	>-100
	1:1,000	>-100	>-100
	1:10,000	>-100	>-100
Fe^{3+}	1:0	-	-
	1:1	47.62	33.2
	1:10	>100	>100
	1:100	>100	>100
	1:1,000	>100	>100
	1:10,000	>100	>100

Table 14 (continue)

Cations/Anion	Concentration ratios	% Error ,n=3	
		As(III)	As(V)
F^-	1:0	-	-
	1:1	-4.00	-2.24
	1:10	-4.00	4.04
	1:100	0.00	5.83
	1:1,000	-4.00	5.83
	1:10,000	>100	>100
Cl^-	1:0	-	-
	1:1	0.00	-2.78
	1:10	6.67	0.00
	1:100	-6.67	-1.11
	1:1,000	0.00	-1.39
	1:10,000	6.67	-1.67
NO_3^-	1:0	-	-
	1:1	-7.69	0.00
	1:10	-3.85	5.96
	1:100	-3.85	8.26
	1:1,000	0.00	8.26
	1:10,000	0.00	8.72
NO_2^-	1:0	-	-
	1:1	-5.26	-2.24
	1:10	-5.26	4.04
	1:100	0.00	5.83
	1:1,000	>100	>-100
	1:10,000	>100	>-100

Table 14 (continue)

Cations/Anion	Concentration ratios	% Error ,n=3	
		As(III)	As(V)
SO_4^{2-}	1:0	-	-
	1:1	-7.14	5.08
	1:10	0.00	1.27
	1:100	7.14	5.51
	1:1,000	-7.14	1.69
	1:10,000	0.00	6.36
PO_4^{3-}	1:0	-	-
	1:1	0.00	-0.8
	1:10	>100	>100
	1:100	>100	>100
	1:1,000	>100	>100
	1:10,000	>100	>100

3.3.5 Application to the real samples

The developed μFI-CL method was applied to the determination of As(III) and As(V) in ground water samples. The water samples were collected from Hang Chat district, Lampang province, Thailand. The comparative results with those obtained from LC-ICP-MS method are illustrated in Table 15. The $t_{calculated}$ values for As (III) were 0.63 and 1.21 for As(V), respectively. There are no significant differences between the result values from both methods at 95 % confidence ($t_{critical}$2.45).

The accuracy of the proposed method was obtained by spiking three amounts of As(III) and As(V) standards sample solutions. The recovery was in the range 93-98 % as shown in Table 16

Table 15 Comparative results for the determination of As(III) and As(V) in ground water samples

Sample	Amount found (μg L^{-1})			
	μFI-CL[a]		LC-ICP-MS [b]	
LP01	ND	8.70±0.10	ND	6.80
LP02	ND	13.02±0.11	ND	14.86
LP03	125.81±0.71	22.01±0.42	124.01	19.49
LP04	57.07±0.60	11.04±0.07	57.63	11.07
LP05	ND	ND	ND	ND
LP06	ND	19.78±0.85	ND	18.59
LP07	ND	83.86±0.73	ND	83.00

[*] Standard deviation from three determinations.

[**] ND = not detected, ([a] LOD = 4 μg L^{-1}, [b] LOD = 1 μg L^{-1}).

Table 16 Recovery of the μFI-CL results by spiked samples

Level (n=3)	Added (μg L^{-1})		Found (μg L^{-1})		Recovery	
	As(III)	As(V)	As(III)	As(V)	As(III)	As(V)
1	35	35	32.79 ± 0.06	32.61 ± 0.57	93.68 ± 1.86	93.18 ± 1.62
2	45	45	43.46 ± 0.90	41.67 ± 0.57	96.56 ± 2.01	92.59 ± 0.06
3	55	55	52.03 ± 0.38	53.55 ± 1.13	94.59 ± 0.68	32.79 ± 0.06

3.3.6 Conclusions

A simultaneous microfluidic device coupling with dual-channel chemiluminescence detections, employing acidic potassium permanganate oxidation for As(III) and oxidation of luminol with a vanadomolybdoarsenateheteropoly acid (AsVMo-HPA) complex in an alkaline solution for As(V) has been successfully developed. The method is simple and rapid with low detection limit which could be established to imply with the requirement for a maximum residue limit of 4 μg L^{-1} of arsenic in surface water sample. The proposed procedure was applied to the determination of As(III) and As(V) in contaminated ground water samples from Lampang Province, Thailand. The concentration of As(III) and As(V) found in ground water samples approximately 1.0 – 126.0 μg L^{-1} , two of ground water samples were found total arsenic level not exceed 10 μg L^{-1}(MRL). Five of ground water samples were found total arsenic level more than 10 μg L^{-1}(MRL) and three of five ground water samples were found total arsenic level above 60 μg L^{-1} and toxic.

Moreover, the μFI-CL appears more attractive since it does not require sophisticated instruments, no external source, just a simple optical system only which makes these coupling easily to be adapted for being portable equipment and readily be a great potential to be an on-site detection equipment.

CHAPTER 4

Determination of Trace Cadmium Based on Minicolumn Preconcentration Coupled with Flow Injection Chemiluminescence Method

4.1 Introduction

Cadmium is one of the most toxic heavy metal elements, for animals and humans even at low concentration. Cd(II) is listed as the sixth most poisonous substance jeopardizing human's health. In mammals, cadmium is known to accumulate exclusively in the kidneys, where the major contamination sources of this element are anthropogenic: industry wastewaters, mining operation.

The increasing on environmental awareness has resulted in ever heightening pollution controls. It has become necessary to monitor cadmium content in a variety of samples. Considering it, health organizations have established permissible limits for cadmium in drinking water. The World Health Organization (WHO) established at 3 μg L^{-1}(Zhang et al., 2011), while the limit established by Environmental Protection Agency (EPA) is at 5 μg L^{-1}(United States Environmemtal Protection Agency, 2009).

The determination of trace amount of cadmium has received considerable attention in the battle against environmental pollution. In the determination of cadmium, various methodsincluding ICP-MS (Al-Swaidan, 1994; Hutton et al., 2004; Orecchio et al., 2014; Yilmaz et al., 2013), ion chromatography (Blazewicz et al., 2010; Cardellicchio et al., 1993; Paull et al., 2000; Tanikkul et al., 2004), anodic stripping analysis (Panigati et al., 2002; Prabakar et al., 2011; Rutyna and Korolczuk, 2014; Yi et al., 2012; Zhu et al., 2007) and electrothermal atomic absorption spectrometry (Campillo et al., 1999; Damin et al., 2007; Jurado et al., 2007; S. Li et al., 2009) have been used. Many of these methods either are time consuming or require complicated and expensive instrumentation. Therefore, methods that could determine low concentration of cadmium rapidly and conveniently in real sample were researched.

The preconcentration method using metal-complex and adsorb on sorbent prior to analysis have increasingly replaced the traditional liquid-liquid extraction methods which generally use great amount of organic solvents to obtain high enrichment factor and require laboratories process and improve the sensitivity of detection. Ammonium pyrrolidinedithiocarbamate (APDC) has been used recently in various preconcentration and separation techniques. Usually metal-APDC complex are measured by flame atomic absorption spectrometry (FAAS) (An-Na and Yun-Fei, 2011), graphite furnace atomic absorption spectrometry (GFAAS) (Tokman and Akman, 2004) and electrothermal atomic absorption spectrometry (ETAAS) (Xu et al., 2000) after the elution with organic solvent.

Chemiluminescence (CL) is an attractive detection method for analytical determination because of the very low detection limit, rapidity and wide linear working range that can be achieved while using relatively simple instrumentation. However, the advantages of the CL method also faced a challenge of selectivity and most CL system could not be used to determine the analytes directly. For example, a variety of metal ions such as Co^{2+}, Cu^{2+}, Ni^{2+} and Mn^{2+} are sensitivity to the luminol-hydrogen peroxide reaction (B. Li et al., 2006).

In this present work, polystyrene bead was applied as a material for adsorb Cd-APDC complex in mini-column, after eluted Cd-APDC complex with methanol and then detected by flow injection chemiluminescence (FI-CL) with luminol-hydrogen peroxide system. The proposed method is simple, rapid, cost-effective and sensitive. It was used to determine trace Cd(II) in soil samples from contaminated agriculture areas.

4.2 Research methodology

4.2.1 Reagent and solution

All chemicals used as list in Table 17 were of analytical reagent (AR) grade. Purified water, using a compact ultrapure water system (18.2 MΩ, Millipore, France) was used for all solution preparations.

Table 17 Chemical reagent and their manufacturers for determination cadmium

	Reagent	Grade	Manufactures	Country
1.	Ammonium pyrrolidinedithiocarbamate (APDC)	AR	Fluka	UK
2.	Cadmium chloride ($CdCl_2$ .2.5 H_2O)	HPLC	Sigma-Aldrich	USA
3.	Ethylenediamine tetraacetic acid, EDTA ($C_{10}H_{14}N_2Na_2O_6$)	AR	QRec	New Zealand
4.	Luminol ($C_8H_7N_3O_2$)	HPLC	Sigma-Aldrich	USA
5.	Hydrogen peroxide (H_2O_2), 30 %	AR	Merck	Germany
6.	Methanol (CH_3OH)	HPLC	Merck	Germany
7.	Nitric acid (HNO_3)	AR	Merck	Germany
8.	Sodium carbonate (Na_2CO_3)	AR	Ajax	Australia
9.	Sodium bicarbonate ($NaHCO_3$)	AR	BDH	UK
10.	Polystyrene bead	-	-	-

4.2.2 Standard preparation

Cadmium stock solution (1,000 mg L^{-1}) was prepared by dissolving 0.2031 g of $CdCl_2$ $2.5H_2O$ in 100 mL of 2 % nitric acid. The cadmium stock solutions were kept in a sealed container in a refrigerator at 4 °C when not in use. Standard solutions of cadmium (2-60 µg L^{-1}) were made up by making appropriate dilution of cadmium stock solution in ultrapure water pH 1.7 (adjust with nitric acid).

4.2.3 Reagent preparation

The stock solution of luminol (5.0×10^{-2}M) was prepared by dissolving 0.4430 g of luminol in 50 mL of 0.1 M NaOH solution. Hydrogen peroxide solution (0.4 M) was prepared by pipetting of 4.09 mL H_2O_2 and diluted to 100 mL with deionized water. EDTA solution (0.1 M) was prepared by dissolving 3.7224 g of EDTA in 100 mL deionized water. Ammonium pyrrolidinedithiocarbamate (APDC) solution (1 % w/v) was prepared by dissolving 1.0 g of APDC in 100 mL of deionized water. Sodium carbonate solution (0.2 M) was prepared by dissolving 5.3000 g of Na_2CO_3 in 250 mL of deionized water. Sodium bicarbonate solution (0.2 M) was prepared by dissolving 1.68 g of $NaHCO_3$ in 100 mL of deionized water. Carbonate buffer (0.02 M) was prepared by making appropriate dilution of 0.2 M of Na_2CO_3 and 0.2 M $NaHCO_3$ in deionized water.

The carrier stream solution (C) was a 80 % (v/v) of methanol. The reagent stream solution (R1) comprises of luminol (2.0×10^{-3} M), and EDTA (8.0×10^{-3} M) was prepared by making appropriate dilution of the luminal stock solution and EDTA solution in 0.02 M carbonate buffer solution. The H_2O_2solution (R2) was prepared by making appropriate dilution of H_2O_2 0.4 M solutions to the final concentration of 4.0×10^{-3} M in 0.02 M carbonate buffer solution.

4.2.4 Instrument set-up

The FI-CL system used in all experiment is depicted in Figure 31. The experimental setup consisted of two peristaltic pumps with rate selector (Minipuls 3, Gilson, France), a sample injection vale (V-450, Upchurch Scientific, USA) and PTFE connection tubing (0.5 mm i.d., Agilent, USA). The CL signals were monitored in custom built flow-through luminometer, where a flat spiral glass mixing coil as illustrated in Figure 32 was mounted flush against a sensitive photomultiplier tubes (PMT, 9828SB, ET-enterprise, UK). The operational potential for the PMT was provided by a high voltage power supply (Thorn- EMI model PM20, Electron tubes Ltd., UK) at the voltage of 950 V. The output signal of the PMT, proportional to the CL intensity, was monitored continuously and displayed by a personal computer via a digital multimeter USB/RS-232 (UT60G, Hong Kong) interface with the voltage divider (C637BFN2, Electron Tubes, UK). The UNI-T® UT60G AC/DC software was used for the determination of the peak maximum.

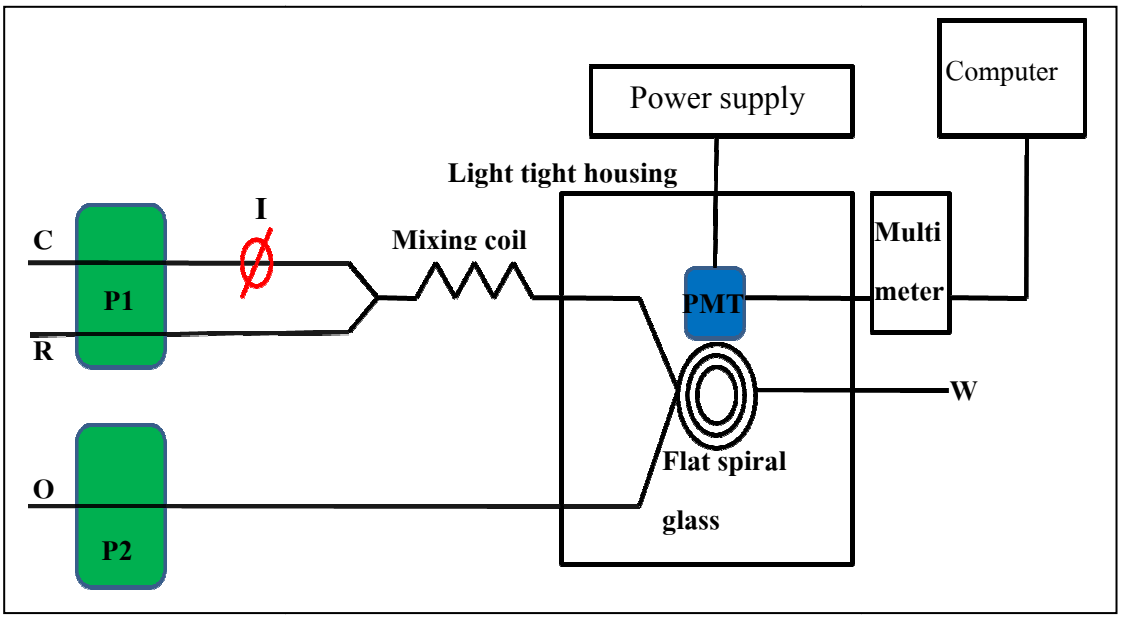

Figure 31 The manifold of FI-CL: C= 80 % methanol, R=luminol 2.0×10^{-3} M and EDTA 8.0 x 10^{-3} M in 0.02 M carbonate buffer solution, ,O = H_2O_2 4.0×10^{-3} M in 0.02 M carbonate buffer solution

Figure 32 A flat spiral glass mixing coil for determination of Cd (II) by FI-CL

4.2.5 Analytical procedure

4.2.5.1 Preconcentration

The preconcentrarion column was prepared by packing a small glass tube (50mm in length x 8.0 mm i.d.) with the 0.2 g polystyrene bead as illustrated in Figure 33a. The ends of the column were fitted with commercial absorbing cotton to keep the adsorbent material inside the column.

A flow manifold for preconcentration step (Figures 33b), it consists of a peristaltic pump with rate selector (Minipuls 3, Gilson, France), the polystyrene bead was cleaned by passing 3 mL of 1.5 M nitric acid and 5 mL of deionized water in to into the column, respectively. The 50 mL of standard cadmium and sample were mixed with 0.002 % APDC and then passed through the column with a flow rate of 2.5 mL min^{-1}. The cadmium complex was then eluted with 1 mL of methanol for analysis.

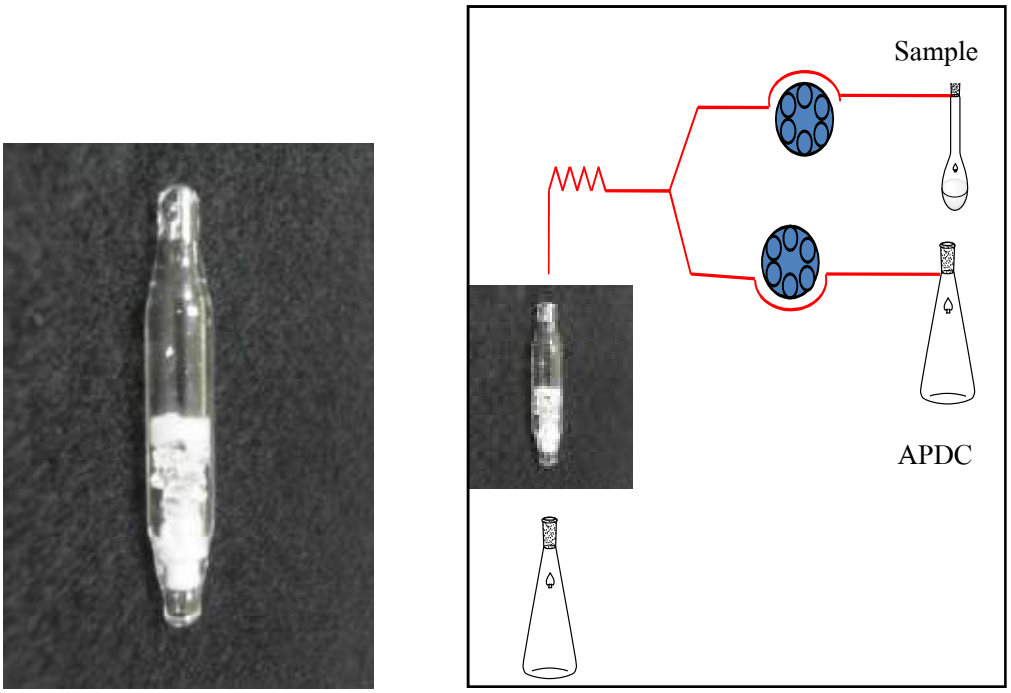

(a) **(b)**

Figure 33 The preconcentration steps of Cd(II) complex: a) a mini column for preconcentration of Cd(II) complex, b) diagram for an off line preconcentration

4.2.5.2 Cadmium determination

A 200 μL of standard or sample solution was injected into 80 % (v/v) methanol carrier solution (C), which was propelled by peristaltic pump (P1) at flow rate of 1.5 mL min^{-1}. The carrier solution was then merged with the reagent stream solution (R) comprises of luminol (2.0×10^{-3} M), and EDTA (8.0×10^{-3} M) in carbonate buffer at the flow rate of 2.50 mL $min^{-1}$by peristaltic pump (P2). On the other hand, the H_2O_2 oxidizing solution (O) was flow by peristaltic pump (P1) at flow rate 1.5 mL min^{-1}, then mixed and merged with the mixed liminol solution and were passed through the a flat spiral glass conduits, the CL intensity was instantly detected by a sensitivity PMT tubes put flush against of a flat spiral glassflow through cell. The output of the PMT which is proportional to the CL intensity was monitored simultaneously and continuously. The signals of the analytes were the maximum output corresponding to the peak maxima.

4.2.6 Preparation of soil samples

4.2.6.1 Sampling

Eleven soil samples were collected from cadmium contaminated area at Padang, Mea Sort district, Tak province, Thailand, which is suffering from nearby mining and industrial waste landfill impacts. Soil samples were collected in PP plastic bag.

4.2.6.2 Preparation of sample

A soil samples were dried at room temperature and ground pass through 65 mesh sieved. Approximately 1.0 g of dried soil samples were weighed into a plastic bottle contanning 20 mL of 1 M ammonium acetate buffer, then was mechanically shaken for 2 hr and filtered through Whatman filter paper No.3. The filtrate solution was adjusted to 25 mL with 1 M ammonium acetate buffer. The 10 mL of filtrate solution was digested with 2 mL of nitric acid for 1 hr and diluted and adjusted to 25 mL with DI water.

4.3 Results and discussion

4.3.1 Optimization of FI-CL systems

Many reported have been used luminol CL reaction in are alkalinity medium for determination Co (II) (Giokas et al., 2007; B. Li et al., 2006; Yeh et al., 2005) and Cd(II) (Changqing et al., 1999), So we used Zhu et al. report for preliminary studies.

To establish the optimum flow injection conditions for the determination of Cd(II), the effects of the key chemical and physical parameters on the CL signal were thoroughly investigated using an univariate approach. The FI system's parameters optimized in this study were the: PMT applied voltage; concentration of reagent solution for determination of Cd(II) consisting of concentration of methanol solution in carrier stream solution; concentration of mixed luminol and EDTA in reagent stream solution; concentraton of carbonate buffer in reagent stream; concentration of H_2O_2 in oxidizing stream solution; sample injection volume and flow rates of each carrier, reagent and oxidizing streams for FI-CL system. All measurements were performed in triplicate.

4.3.1.1 Effect of photomultiplier tube applied voltage

The effect of the photomultiplier tube (PMT) voltage was investigated in the range 700-1000 V for the PMT. For these experiments, 0.5 mg L^{-1} of standard solution of Cd(II) injected into FI-CL system. The potential of the power supplies were increased stepwise and the CL signals were measured after the injection of cadmium solution at each potential step. The noise from the background current fluctuation was also measured at each potential step. As expected, The CL intensities were increased when the applied voltage was increased stepwise. However, the background noise was also increased. It was found that the signal-to-noise (S/N) ratio reached a maximum value at 950 V for Cd(II). The results are illustrated in Figure 34.

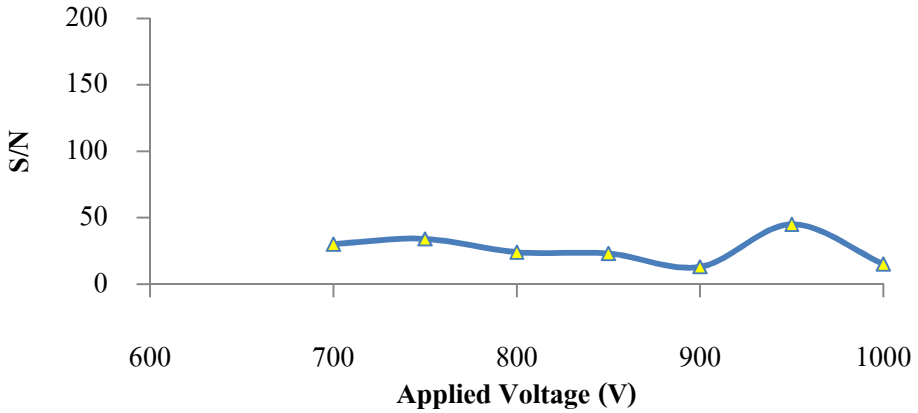

Figure 34 Effect of photomultiplier tube applied voltage

4.3.1.2 Effect of carrier stream concentrations on the CL intensity for Cd(II) determination

The carrier solution (C) was a methanol solution in deionized water, the effect of methanol concentration was studied over the concentration range from 0-100 % (v/v). At the concentration of methanol 0-20 % (v/v) negative signal was observed, however, when the concentration of methanol was increased over 40 % (v/v), the positive signal was obtained. At the concentration of 80 % (m/v) methanol, the highest signal was observed; after this concentration the noise signal increased gradually made the S/N ratio decreased dramatically.

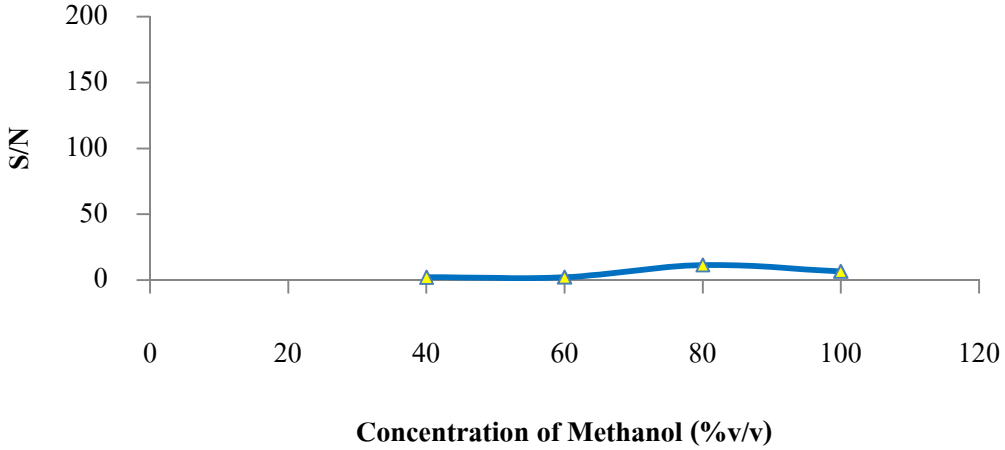

Figure 35 Effect of methanol concentration in the carrier stream (R) on FI-CL signal

4.3.1.3 Effect of the reagent concentrations on the CL intensity for Cd(II) determination

The CL reagent stream solution (R) was composed of luminol and EDTA in carbonate buffer, while the oxidizing stream solution (O) is a H_2O_2 solution in carbonate buffer. To simplify the CL detection system, the effect of carbonate buffer concentration on both streams was studied over the concentration range from 0.01-0.1 M. The CL intensity increased when the concentration of carbonate buffer increased. At the concentration of 0.02 M of carbonate buffer, the highest signal was observed; after this concentration, the noise signal increased gradually made the S/N ratio decreased dramatically.

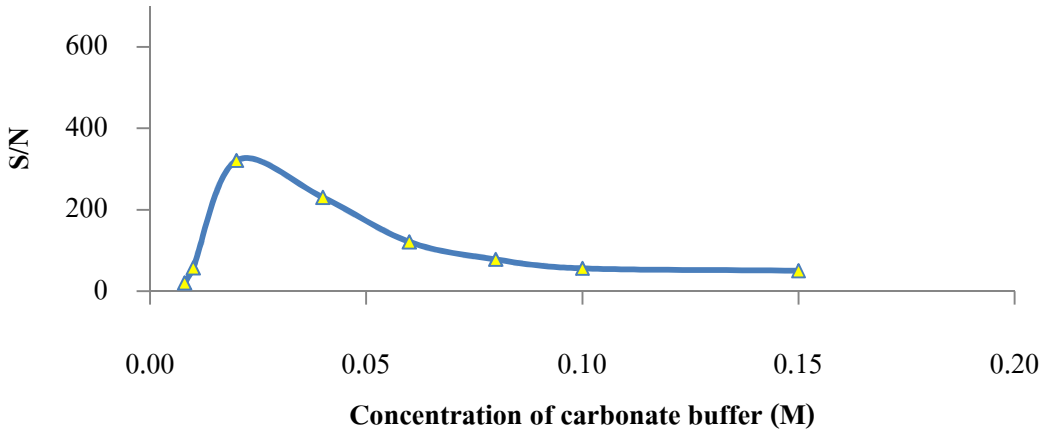

Figure 36 Effect of carbonate buffer on the FI-CL signal

The concentration of luminol was studied similarly to the previous parameter by varying the concentration from 5.0×10^{-4}–2.0×10^{-2}M, the result showed that the CL intensity reached maximum when the concentration of luminol was at 2.0×10^{-3} M.

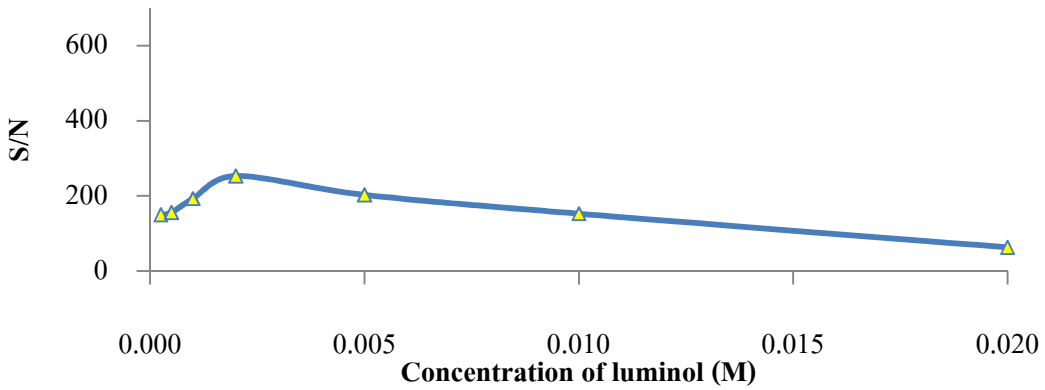

Figure 37 Effect of luminol on the FI-CL signal

The research study by Yeh and coworkers (Yeh et al., 2005) and Li and coworkers (Li et al., 2006) on the determination of the Cd(II) was based on the H_2O_2 reaction with luminol. In this research, the investigation for the suitable condition of H_2O_2 concentration reagent stream (O) was studied by optimizing the concentration of H_2O_2.

The concentration of H_2O_2 in the 0.02 M of carbonate buffer was studied in range of 1.0×10^{-3}-3.0×10^{-2} M. The increase in the concentration of H_2O_2, the optimal H_2O_2 concentration was at 4.0×10^{-3} M and was selected and used in subsequential investigation.

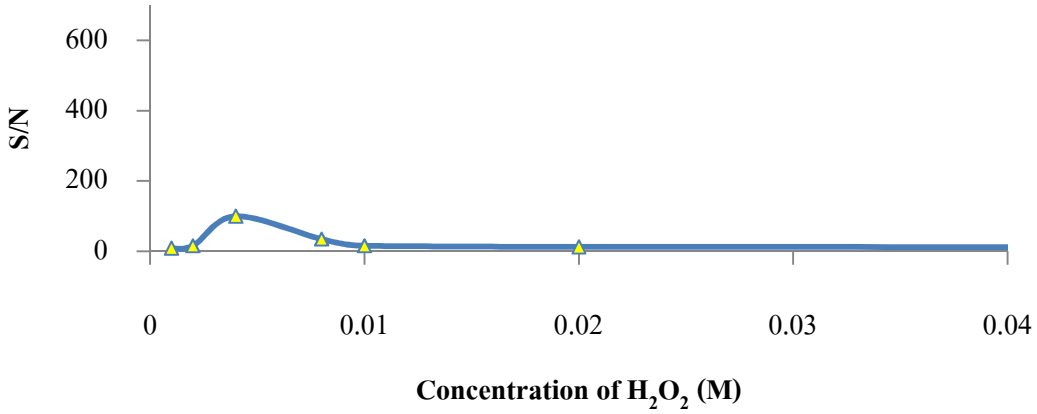

Figure 38 Effect of H_2O_2 on the FI- CL signal

The reports by Giokas and coworkers (Giokas et al., 2007), the CL intensity from the reaction of alkalinity luminol can be increased by adding EDTA. In this research, the addition of EDTA into the luminal reagent solution in the range of 1.0×10^{-3}-0.02 M resulted in the increase of CL intensity. At $8.0\times10^{-3}$of EDTA the maximum signal-to-noise ratio was observed as depicted in Figure 39.

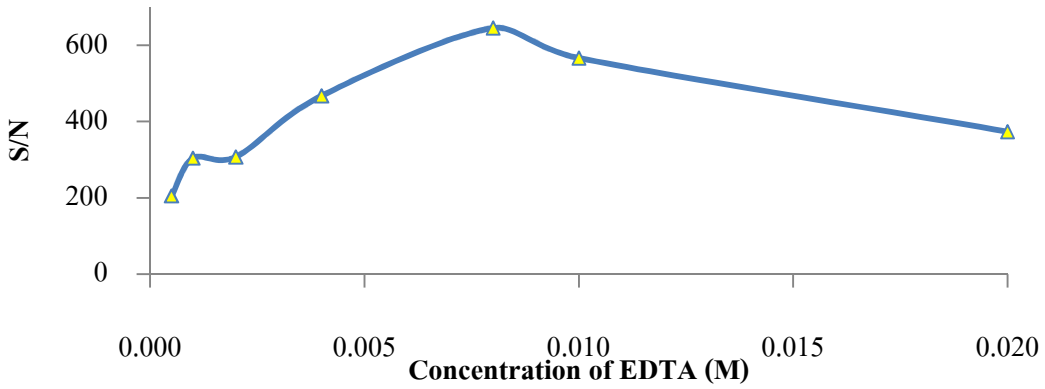

Figure 39 Effect of EDTA on the FI-CL signal

4.3.1.4 Effect of reagent and carrier stream flow rate (total flow rate)

Flow rate is an important parameter in CL detection to transfer the excited product into the flow cell at the critical timing for maximum collection of the emitted light. The effect of the flow rates of the three channels at the equal flow rate was simultaneously investigated over the range of 0.5-7.0 mL min^{-1} in term of the sensitivity, sample throughput and reagent consumption. The CL intensity of cadmium standard solution (0.5 mg L^{-1}) gave maximum intensity at the total flow rate of 6.5 mL min^{-1} for the determination of cadmium.

4.3.1.5 Effect of injection volume

Similarly, the influence of the sample injection volume on the CL intensity of the FI-CL system was investigated, over the range of 40-250 µL, by injecting the cadmium standard solution at 0.5 mg L^{-1}. It was found that the CL intensity was increased when the volume of sample volume increased up to 200 µL, beyond this point CL intensity become almost constant. Thus, a volume of 250 µL was selected for economy of the sample comsumtion and speed of the response for all remaining experiments. The summary of their optimal values is shown in Table 18.

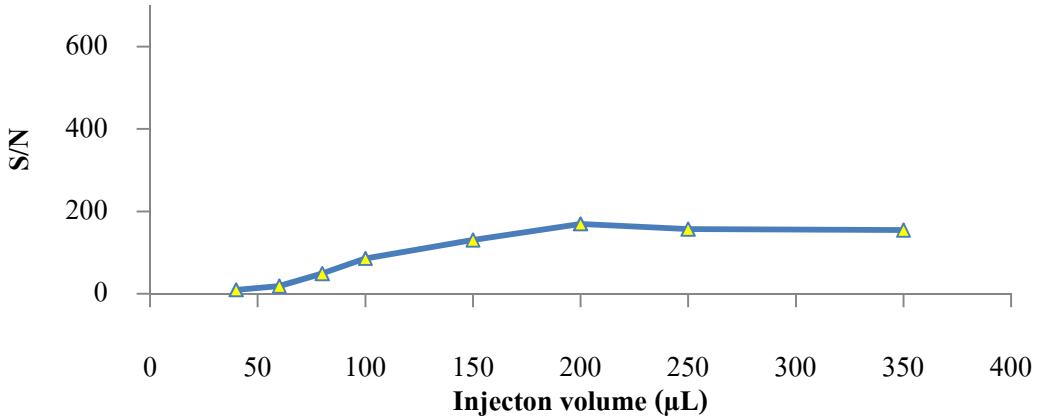

Figure 40 Effect of sample injection volume on the FI-CL signal

4.3.1.6 Summary of the optimum conditions

The selected optimum conditions for cadmium determinatios was achieved by the univriation method. The summary of their optimal values are shown in Table 18.

Table 18 Optimization FI CL parameter

Parameters	Range studied	Optimal values
PMT applied voltage (V)	700-1000	950
Methanol concentration (%v/v), C1	0-100	80
Carbonate buffer concentration (M)	0.01-0.1	0.02
Luninol concentration (M), R1	$5.0 \times 10^{-4} - 2.0 \times 10^{-2}$	2.0×10^{-3}
EDTA (M), R1	$5.0 \times 10^{-4} - 2.0 \times 10^{-2}$	8.0×10^{-3}
H_2O_2 (M), R2	1.0×10^{-3}-3.0×10^{-2}	4.0×10^{-3}
Injection volume (µL)	20 – 250	200
Total flow rate (mL)	0.5–7.0	6.5

4.3.1.7 Analytical figures of merit

4.3.1.7.1 Linearity of the calibration graph

Under the optimal condition (Table 18), using the FI-CL system as illustrated in Figure 31, the linear calibration curve, the limit of detection and the limit of quantification for the deterination of Cd(II) was investigated. Figure 41 shows the calibration curves for Cd(II), while Figure 42 illustrated the FI-CL grams for Cd(II). It was found that the calibration curve found to be linearity over range of 30-80 µg L^{-1}.

Table 19 The data of calibration curve for Cd(II)

Concentration (µg L^{-1})	CL intensity (a.u.), n=3
30	176
40	229
50	291
60	342
70	396
80	437

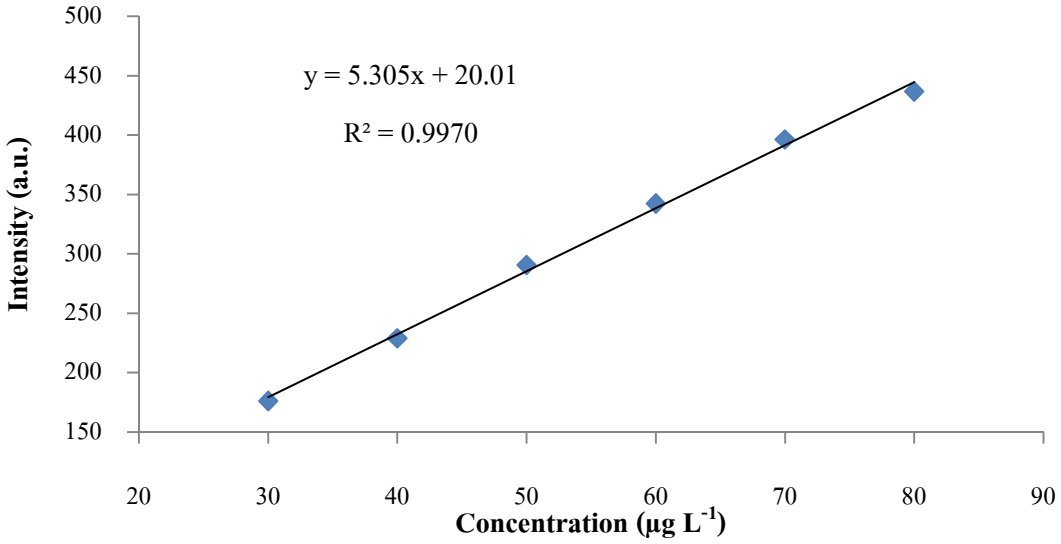

Figure 41 Calibration curve for Cd(II)) by FI-CL

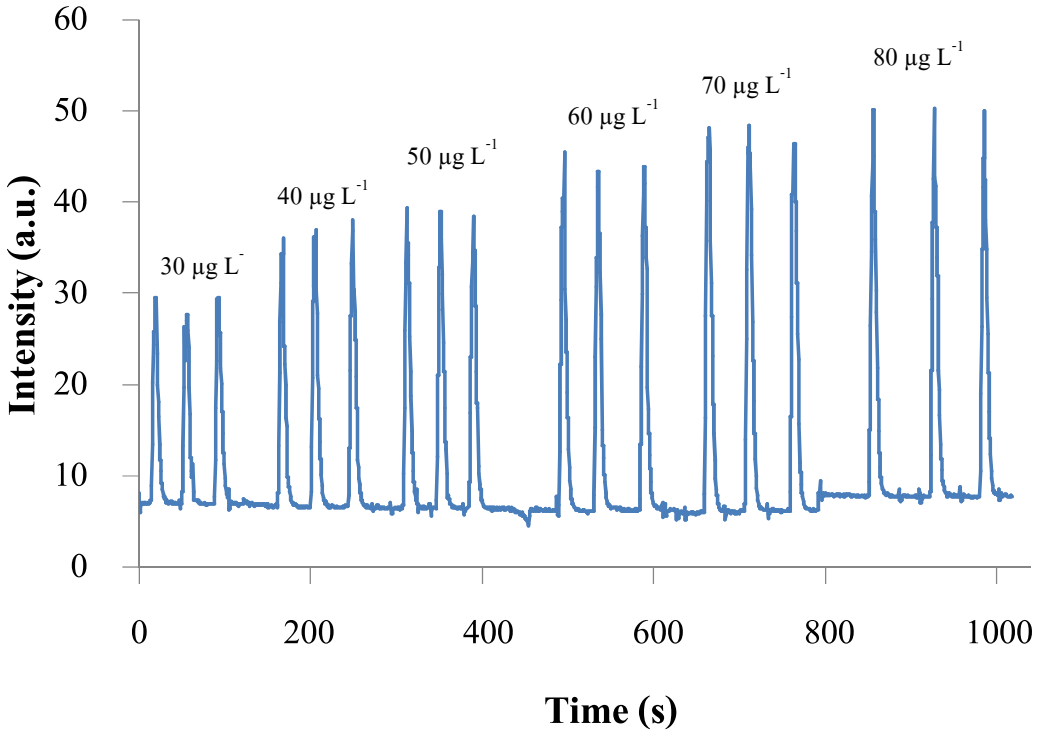

Figure 42 Illustrated the FI-CL grams for Cd(II) determination

4.3.1.7.2 The limit of detection and the limit of quantification

The limit of detection and the limit of quantification for the determination of cadmium(II) were investigated. In this chapter, the limit of detection and the limit of quantification were calculated based on signal-to-noise ratio (S/N) of 3 and signal-to-noise ratio (S/N) of 10, respectively . The limits of detection (signal-to-noise ratio of 3) and the limits of quantification (signal-to-noise ratio of 10) of cadmium(II) were found to be 10 μg L^{-1} and 30 μg L^{-1}, respectively.

4.3.1.7.3 Reproducibility and repeatability

The repeatability of the procedure was determined by repeating measurements of 60 μg L^{-} Cd(II) for 10 replicates. The reproduceibility (intra-day) variations of the method were determined using triplicate injections of standard Cd(II) solution at concentraton of 60 μg L^{-1} and analysed on the same day. The reproduceibility (inter-day) precision was studied by comparing the results of assays performed on different days on the same injected standard Cd(II) solution in three replicates. The result was expressed in term of percentage relative standard deviation (% RSD). Results were ars shown in Table 20-22.

Table 20 Replicate measurements by using standard 60 μg L^{-1} of Cd(II)

Experiment number	CL Intensity (a.u.)
1	330
2	342
3	330
4	342
5	325
6	334
7	330
8	325
9	342
10	330
Average	333
SD	6.73
% RSD	2.02

Table 21 Reproducibility for intra-day variations

Times (hour)	CL intensity (a.u.), n=3
1	342
3	334
6	325
9	325
average	331.5
SD	8.19
% RSD	2.47

Table 22 Reproducibility for inter-day variations

Times (day)	CL intensity (a.u.), n=3
3	342
6	330
9	325
average	332
SD	8.74
% RSD	2.63

Table 23 shows the results of statistical analysis of the experimental data for Cd(II) tested. The regression equaition was calculated from the calibration curve, along with the slopes and intercepts are given. It was found that the calibration curve was linearity over range the of 30-80 μg L^{-1}. The analytical characteristic for Cd(II) and the precision of the proposed method was attained by analyzing 10 samples of 60 μg L^{-1}.

Table 23 Analytical figures of merit for determination of Cd(II)

Analytical parameter	Cd (II)
Regression equation	$CL_{intensity} = (5.305)C_{Cd(II)}(\mu g\ L^{-1}) + 20.01$
Linear range, $\mu g\ L^{-1}$	30-80
Correlation coefficient (r^2)	0.9970
Limit of detection (S/N$\geq$3), $\mu g\ L^{-1}$	10
Limits of quantification (S/N$\geq$10), $\mu g\ L^{-1}$	30
Precision (% RSD)	2.02
Intra-day precision (% RSD)	2.47
Inter-day precision (% RSD)	2.63

4.3.2 Optimization of minicolumn preconcentration systems

The improvement in sensitivity and selectivity for determination Cd(II) can be achieved by application of sorption preconcentration by complex with ammonium pyrrolidine dithiocarbamate (APDC) and adsorb on a non-polar sorbent such as human hair (An-Na and Yun-Fei, 2011) or C_{18} sorbent (Colbert et al., 1998).

The preliminary study on precencentration procedure using polystyrene beads and the C_{18} sorbent system developed by Colbert and coworkers (Colbert et al., 1998) and An-Na and coworkers (An-Na and Yun-Fei, 2011) initiated some idea for an off-line preconcentration. In this chapter, polystyrene bead and C_{18} sorbent are chosen and used to investigate the sorption of Cd-APDC complex. The sorption of Cd-APDC complex on polystyrene and C_{18} beads was investigated and quantitatively compared as present in Table 24

Table 24 Chemiluminescence intensity related to different type of sorbent

Adsorbent type	Weight (g)	Volume of solution load (mL)	Concentration of Cd(II), µg L^{-1}	CL intensity (a.u.)
C_{18}	0.1	50	10	5.5
			20	5.4
			30	5.3
polystyrene	0.1	50	10	45
			20	65
			30	85

The results from Table 23, indicated that CL intensity can be increased when polystyrene was used as a sorbent in mini column preconcentration, hence the polystyrene beads are suitable to use as a sorbent in our system. The effects of the key parameters on the CL signal were thoroughly investigated using an univariate approach. The preconcentration system parameters optimized in this studied were the: weight of polystyrene, volume of sample loading and concentration of APDC. All measurements were performed in triplicate.

4.3.2.1 Effect of volume of sample loading

Initially, 3.0 mL of 1.5 M nitric acid and 5.0 mL of DI water were load through a polystyrene bead (0.3 g), after that standard Cd(II) solution concentration at 20 µg $L^{-1}$was pumped and mixed with 0.02 % (m/v) APDC-at the same flow rate 2.5 mL min^{-1} through the polystyrene bead mini-column. Finally, the elution of APDC-Cd complex with 1.0 mL methanol was performed and injected the eluent to the optimized FI-CL system for the determination of Cd(II).

The effect of sample volume loading was investigated in the range of 5-100 mL. The CL intensity increases when the volume of sample load increases. At volume50 mL, the highest signal was observed; after this concentration the noise signal increased dramatically made the S/N ratio decreased significantly.

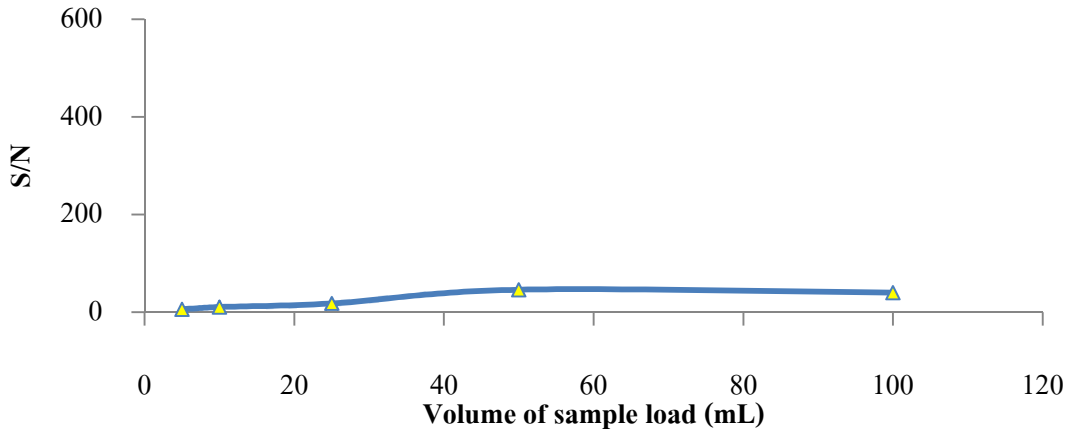

Figure 43 Effect of sample volume loading on FI-CL signal

4.3.2.2 Effect of weight of polystyrene sorbent

The effect of weight of polystyrene as a mini column sorbent was investigated in the range of 0.05 – 0.4 g. The CL intensity rapidly increased when the weight of polystyrene was increased up to 0.20 g, above which the CL intensity decreased. Therefore, a 0.2 g of polystyrene was chosen and used subsequently in this work.

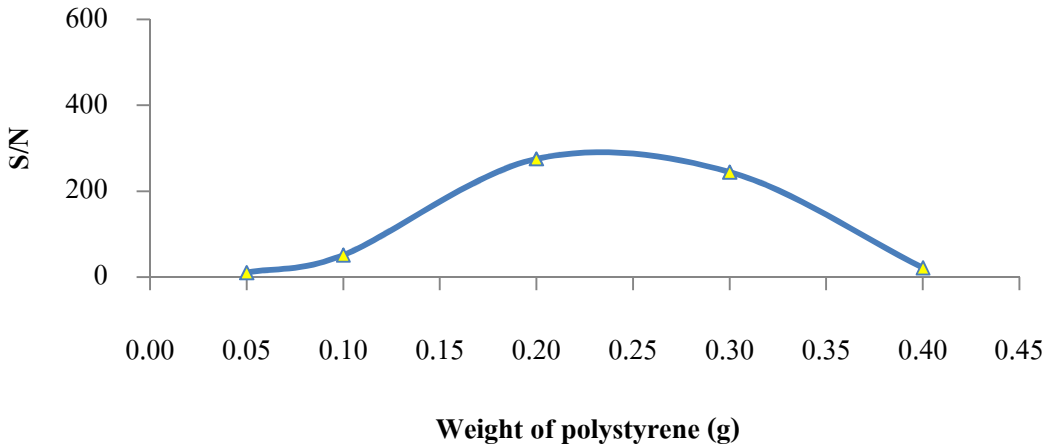

Figure 44 Effect of weight of polystyrene on FI-CL signal

4.3.2.3 Effect of concentration APDC

The concentration of ammonium pyrrolidinedithiocarbamate (APDC) was studied in range of 4.0×10^{-4}-4.0×10^{-2}% (m/v). The increase in the concentration of APDC resulted in the steep increase up to 2.0×10^{-4}% (m/v), above which the intensity dramatically decreased.

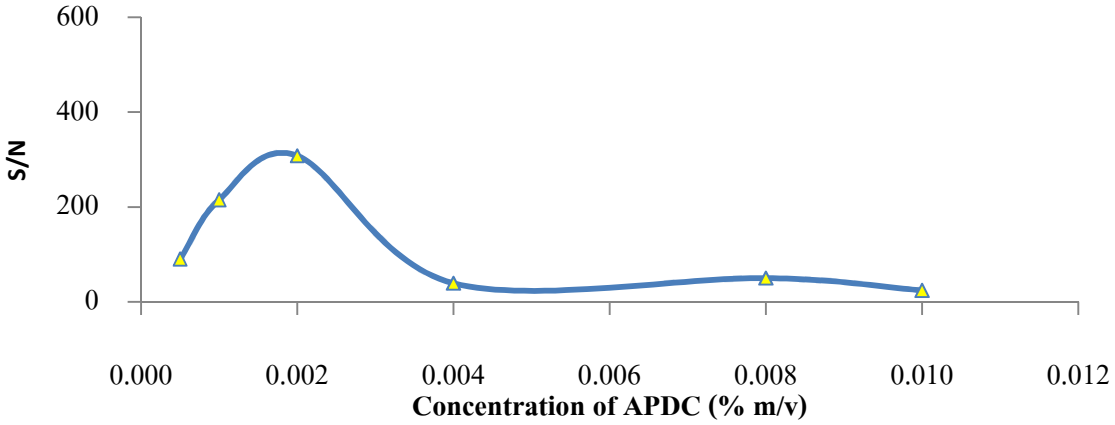

Figure 45 Effect of concentration of APDC on FI-CL signal

4.3.2.4 Summary of the optimum conditions

The selected optimum conditions for cadmium determinatios was achieved by the so-called univariate method. The summary of their optimal values is shown in Table 25.

Table 25 Optimization preconcentration parameters

Parameters	Range studied	Optimal value
Weight of polystyrene (g)	0.05-0.40	0.20
Sample volume (mL)	10-100	50
APDC concentration (%m/v), C1	4.010^{-4}-4.0×10^{-2}	2.0×10^{-3}

4.3.2.5 Analytical figures of merit

4.3.2.5.1 Linearity of calibration graph

Under the optimal condition, using a mini column preconcentration procedure for the determination of trace Cd(II) with FI-CL system as illustrated in Figure 31, the linear calibration curve, the limits of detection and the limits of quantification for the deterination of Cd (II) was investigated. Figure 46 shows calibration curves for cadmium(II), while Figure 47 illustraed the FI-CL grams for cadmium(II). It was found that the calibration curve found to be linearity over the range 2-6 µg L^{-1}.

Table 26 The data of calibration curve for Cd(II) using mini column preconcentration

Concentration (µg L^{-1})	CL intensity (a.u.), n=3
2	3236
3	3600
4	4180
5	4567
6	5180

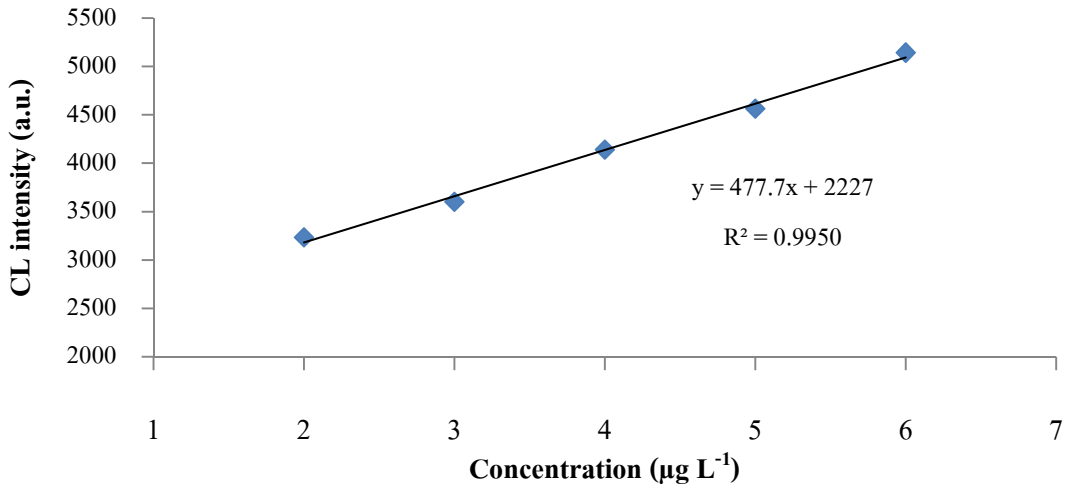

Figure 46 Calibration curve for Cd(II) using mini column preconcentration

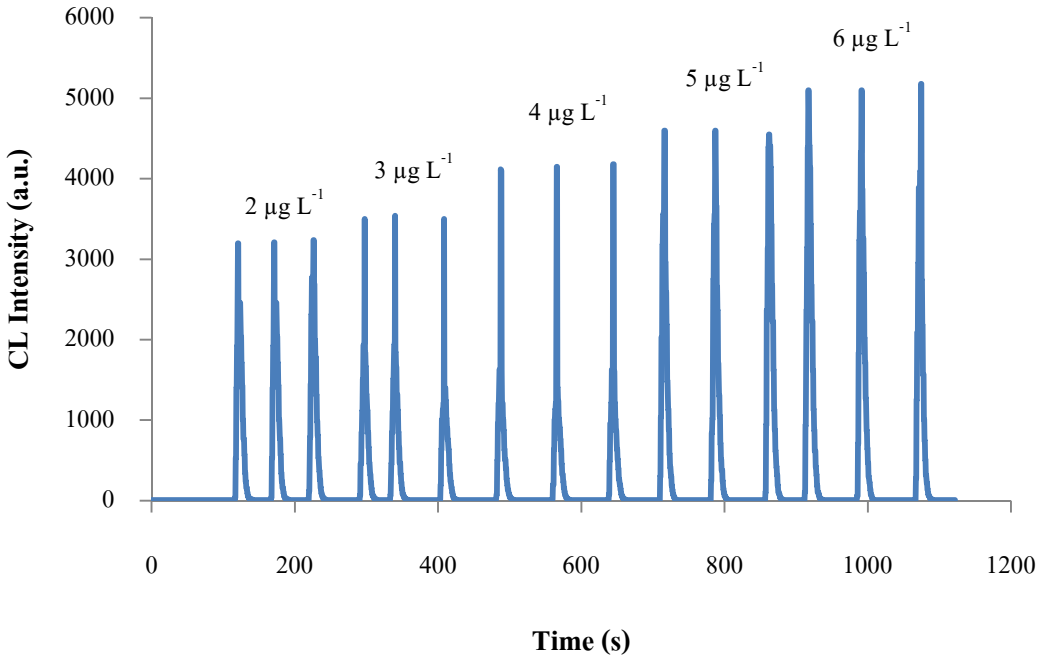

Figure 47 Illustrated the FI-CL grams for Cd(II) using mini column preconcentration

4.3.2.5.2 The limits of detection and the limits of quantification

The limits of detection and the limits of quantification for the determination of Cd(II) was investigated.In this session,the limits of detection and the limits of quantification were calculated based on $3SD_{blank}$ /slope and 10 SD_{blank} /slope, respectively .

The limits of detection of cadmium(II) was found to be 0.6 µg L^{-1} and the limits of quantification was found to be 2.0 µg L^{-1}, respectively.

4.3.2.5.3 Reproducibility and repeatability

The repeatability of the procedure was determined by repeating measurements of 4 µg L^{-1}cadmuim (II) for 10 replicates. The reproducibility (intra-day) variations of the method were determined using triplicate injections of standard Cd(II) solution at concentraton of 4 µg L^{-1} and analysed on the same day. The reproducibility (inter-day) precision was studied by comparing the results of the assays performed on different days on the same

injected standard Cd(II) solution in three replicates. The result was expressed in term of percentage relative standard deviation (% RSD). Results are shown in Table 27-29.

Table 27 Replicate measurements by using standard Cd(II) of 4 μg L^{-1}

Experiment number	CL Intensity (a.u.)
1	4100
2	4150
3	4180
4	4160
5	4145
6	4175
7	4170
8	4125
9	4120
10	4180
Average	4150.5
SD	27.83
% RSD	0.67

Table 28 Reproducibility for intra-day variations

Times (hour)	CL intensity (a.u.), n=3
1	4180
3	4145
6	4130
9	4110
average	4141.25
SD	29.55
% RSD	0.71

Table 29 Reproducibility for inter-day variations

Times (day)	CL intensity (a.u.), n=3
3	4180
6	4150
9	4100
average	4143.33
SD	40.41
% RSD	0.98

The Table 30 shows the results of statistical analysis of the experimental data for Cd(II) tested. The regression equaition was calculated from the calibration curve, along with the slopes and intercepts are given. It was found that the calibration curve found to be linearity over range 2-6 μg L^{-1}. The analytical characteristic for Cd(II) and the precision of the proposed method was attained by analyzing 10 samples of 4 μg L^{-1}.

Table 30 Analytical figures of merit for determination of Cd(II)

Analytical parameter	Cd (II)
Regression equation	$CL_{intensity} = (477.7)C_{Cd(II)}(\mu g\ L^{-1}) + 2227$
Linear range, μg L^{-1}	2-6
Correlation coefficient (r^2)	0.9950
Limit of detection, μg L^{-1}	0.60
Limits of quantification , μg L^{-1}	2.00
Precision (% RSD)	0.67
Inter-day precision (% RSD)	0.71
Intra-day precision (% RSD)	0.98

4.3.3 Application to real samples

The developed FI-CL method was applied to the determination of exchangeable Cd(II) in soil samples. Eleven soil samples were collected from Tak province, Thailand. The comparative results with those obtained from the ICP-MS method are illustrated in Table 31. There are no significant differences between the result values from both methods at 95 % confidence ($t_{critical}$2.78). The accuracy of the proposed method was obtained by spiking three amounts of Cd(II) standards sample solutions. The recovery was in the range 96-103 % as shown in Table 32.

Table 31 Comparative results for the determination of exchangeable Cd(II) in soil samples

Feed sample	Amount found (mg kg-1)± SD		t-value
	FI-CL	ICP-MS	
Soil01	729.86±4.12	725.71±0.72	1.69
Soil02	248.20±0.80	247.65±0.04	1.15
Soil03	436.18±1.53	437.33±0.35	1.19
Soil04	267.25±2.48	264.13±0.32	2.10
Soil05	199.80±1.24	198.22±2.66	0.82
Soil06	322.44±0.47	322.25±0.34	0.39
Soil07	621.48±1.10	622.97±0.46	1.89
Soil08	157.79±0.82	158.23±0.74	0.65
Soil09	102.06±1.25	102.49±0.22	0.56
Soil10	670.69±1.63	671.59±0.36	0.88
Soil11	117.82±1.63	116.07±0.37	1.72

Standard deviation from three determinations for the proposed method and the reference method.

$t_{calculated}$ values are given by superscript letters and are less than $t_{critical}$2.78 at 95% confidence.

Table 32 Recovery of the FI-CL results by spiked water samples

Level (n=3)	Added (μg L^{-1})	Found(μg L^{-1})	Recovery
	Cd(II)	Cd(II)	
1	3	2.89 ±0.02	96.33±0.53
2	4	4.09 ±0.01	102.25±0.15
3	5	4.89±0.01	97.81±0.15

4.3.4 Conclusions

A simple flow injection chemiluminescence procedure was proposed for determination of cadmium in environmental samples couple with an off-line preconcentration step. A mini column, packed with polystyrene bead as an adsorption material, was used for preconcentration of Cd(II) ions based on the complex formation with the ammonium pyrolidinedithiocarbamate (APDC). The Cd-PDC complex adsorbed on polystyrene beads was eluted by methanol and susequently determined by the flow injection chemiluminescence system. The chemiluminescence reaction based on Cd(II) catalyzed the luminol-H_2O_2 CL reaction in the present of alkaline media was employed for sensitive determination. Under the optimum condition linear calibration graph was obtained over the concentration range 2-6 μg L^{-1}. The method is simple and rapid with low detection limit which could be established to imply with the requirement for a maximum residue limit of 37 mg kg^{-1} of cadmium in soil sample. The proposed procedure was applied to the determination of Cd(II) in contaminated soil samples from Tak Province, Thailand. The concentration of exchangeable Cd(II) found in soil samples was found in the range of 102– 729 mg kg^{-1}, and over MRL level (37 mg kg^{-1}) 20 folds. The results indicate the Cd(II) in soil are exchangeable phase, Cd(II) can exchange and come out to environment by rain or the plant can absorb, it is very toxic.

Moreover, the FI-CL appears more attractive since it does not require sophisticated instruments, no external source, just a simple optical system only which makes these coupling easily to be adapted for being portable equipment and readily be a great potential to be an on-site detection equipment.

CHAPTER 5

Enhanced Electrogenerated Chemiluminescence of Tris(2,2′-bipyridyl)ruthenium(II) System by L-cysteine-capped CdTe Quantum Dots and Its Application for the Determination of Nitrofuran Antibiotics

5.1 Introduction

Nitrofurans (NFs) are antibiotic drugs, which have been widely used in the dairy, livestock, poultry and aquaculture production industries in past decades. The nitrofuran derivatives in which there exists the greatest possibility of contamination are furaltadone (FTD), furazolidone (FZD), nitrofurazone (NFZ) and nitrofurantoin (NFT). Due to concerns about their carcinogenicity and mutagenicity, these antibiotics have been banned in the EU (Regulation (EC) No 1442/1995) and many countries overseas. Therefore the use of nitrofurans for livestock has also been prohibited in countries such as Australia, USA, Philippines, Thailand and Brazil (Vass et al., 2008). Unfortunately, nirofuran antibiotics are still available and in use in a number of third world countries including Thailand. Several analytical methods have been described for the determination of nitrofuran residues in food and animal tissues, such as liquid chromatography (LC), in combination with different detection techniques, for example photodiode array(DAD) (Chumanee et al., 2009), fluorescence (Sheng et al., 2013) and mass spectrometry (MS) (Barbosa et al., 2007). These methods are time-consuming and require expensive instrumentation, hence, there is now an urgent need for a rapid, low cost, high-capacity and sensitive method to screen NF residue-contaminated feed, stored grain and agricultural products in order to control the quality of exported foods to the EU.

In addition to the desire to monitor the contaminate compounds in real time, there is a tremendous input of energy and resources towards developing sensors for almost everything of interest to humans, especially as they are brought about by concerns with health and pollution. In recent years, chemical sensors and biosensors play an essential role in the fields of environmental (Prakash et al., 2013), medical diagnostics (Yu et al., 2014) and pharmaceutical analysis (Khorshid and Issa, 2014). Many analytical methods and techniques have improved chemical sensors and biosensors in sensitivity and miniaturization. There is also a need to

determine analytes at increasingly lower levels to lower the detection limits, and to improve the accuracy and precision at those limits.

In addition to photo chemiluminescence (CL), electrochemiluminescence and electrogenerated chemiluminescence (ECL) have also recently been developed for chemical sensors based on an optical reaction and electrochemical potential control. In ECL, electrochemically-generated intermediates undergo a highly exergonic reaction to produce an electronically excited state that then emits light upon relaxation to a lower-level state. ECL excitation can be caused by energetic electron transfer (redox) reactions of electrogenerated species. Such luminescence excitation is a form of chemiluminescence where one or all reactants are produced electrochemically at the electrodes. The advantages of ECL include the simple optical system, no external light source, low cost and miniaturization, high sensitivity and selectivity. Thus ECL has grown significantly in importance in analytical chemistry as an attractive method of detection because it can combine the advantages of luminescence and electrochemical techniques as well as provide added selectivity and superior sensitivity due to the low background.

Typical ECL reagents, such as luminal and tris(2, 2′-bipyridyl)ruthenium (II)($Ru(bpy)_3^{2+}$) have been used extensively in various fields (Chu et al., 2012; Haslag and Richter, 2012). The detection of many species (or coreactants) has been demonstrated by virtue of their ability to generate light during reactions with the oxidized form of the complex. Furthermore, the investigation into potential enhancers has focused on fluorescence compounds, surfactants and aromatic compounds to increase the emission intensity from $Ru(bpy)_3^{2+}$ reactions (Gerardi et al., 1999) and luminol reaction (Fletcher et al., 2001).

In recent decades, many researcherspaid much attention to CL enhancement using metal nanomaterials (Zhang et al., 2005). Furthermore, in the past few years, they began to be aware of the potential application of quantum dots (QDs) in the ECL field since QDs can significantly improve the sensitivity and the stability of the chemiluminescence light, mainly resulting from the high surface area and special structure of these nano materials. QDs are now complementary and may be superior to the existing ECL reagents, and have great potential for developing novel ECL sensors. In many cases, when they are coated with organic molecules and macromolecules, they can improve aqueous solubility and opportunities for bio conjugation

properties, enhance the inherent sensitivity and expand new applications of CL detection (Guo et al., 2013). These coatings can be classified broadly as ligand-based or polymer-based, and neutral or charged. Ligand coatings are comprised of small molecules that coordinate directly to the inorganic surface of the QDs. The most common ligands have been monodentate (e.g.mercaptopropionic acid, MPA) or amino groups (e.g. L-cysteine) (Mntungwa et al., 2013). These ligands are compact, charged, and colloidal stability is maintained via electrostatic repulsion. The L-cysteine-capped CdTe-QDs have been found to have a strong effect on the fluorescent properties in addition to acting a stabilizer (Li et al., 2010) and in some cases, the formation and annihilation rates of CdTe-QDs significantly influenced the CL emission (Chen et al., 2014).

To the best of our knowledge, only a few chemiluminescence-based methods have been reported for the determination of nitrofurans including FTD, FZD and NFT in agricultural samples, where they are usually administered to animals by means of medicated feed or drinking water. The Argentina legislation established levels of nitrofurans in animal feed at maximum limits of 400 μg kg^{-1}, and 2 μg L^{-1} in water, for the compounds nitrofurazone, furaltadone, furazolidone and nitrofurantoin (Viñas et al., 2007). So far, only three reports proposing the determination of NFs in various samples were proposed in flow base chemiluminescence methods. Thongsrisomboon and coworker (Thongsrisomboon et al., 2010) reported a flow injection CL method for the determination of furazolidone, nitrofurantoin and nitrofurazone in animal feed based on its chemiluminescence induced by potassium permanganate in a sulfuric acid medium with detection limits (S/N = 3) of 0.25 mg L^{-1}, and a sample throughput of 120 h^{-1}. Du and coworker (Du et al., 2007) reported the flow based method for the determination of nitrofurazonein human plasma and urine samples with the H_2O_2-N-bromosuccinimide (NBS) reaction in an alkaline medium Li and coworker (X. Li et al., 2009) presented the post-chemiluminescence (CL) reaction of luminol–H_2O_2 for use in CL-based detection with liquid chromatography by combining with flow injection manifolds for the determination of furazolidone in animal feed.

In this chapter, the first account of the investigation of the ECL-based sensor for the determination of selected nitrofurans in animal feed samples, including furaltadone, furazolidone and nitrofuratoin, was proposed by means of an ECL coreactant. A carbon screen-printed electrode coupled with a tris(2, 2′-bipyridyl)ruthenium (II) complex was used to create oxidative-reduction ECL. Adding cadmium telluride quantum dots (CdTe-QDs) (Kang et al., 2012; Yin et al., 2013) create sunstable products from intermediate radicals in the $Ru(bpy)_3^{2+}$CL reaction process, where nitrofurans cause an indirect inhibitory effect on $Ru(bpy)_3^{2+}$ compounds (Chen et al., 2014). The ECL CdTe-QDs system shows high sensitivity, good stability, and reproducibility, indicating CdTe-QDs could be a new and promising material for opening new avenues in ECL application.

5.2 Research methodology

5.2.1 Reagent and solution

All chemicals used as list in Table 19 were of analytical reagent (AR) grade. Purified water, using a compact ultrapure water system (18.2 MΩ, Millipore, France) was used for all solution preparation.

Table 33 Chemical reagent and their manufactures for determination of nitrufurans

	Reagent	Grade	Manufactures	Country
1.	Ammonium chloride (NH_4Cl)	AR	Sigma-Aldrich	USA
2.	2,2’ bipyridyl ($C_{10}H_8N_2$)	AR	Sigma-Aldrich	USA
3.	Cadmium chloride ($CdCl_2$)	HPLC	Sigma-Aldrich	USA
4.	Calcium chloride (CaCl)	AR	Sigma-Aldrich	USA
5.	Chloramphenicol ($C_{11}H_{12}C_{12}N_2O_5$)	HPLC	Sigma-Aldrich	USA
6.	Chloteracycline ($C_{22}H_{23}ClN_2O_8$)	HPLC	Sigma-Aldrich	USA
7.	Cloxaciline ($C_{19}H_{18}ClN_3O_5S$)	HPLC	Fluka	UK
8.	L-cysteine ($C_3H_7NO_2S$)	AR	Sigma-Aldrich	USA
9.	*N,N* dimethylformamide (C_3H_7NO)	AR	Fisher	UK
10.	Furaltadone ($C_{13}H_{16}N_4O_6$)	HPLC	Sigma-Aldrich	USA
11.	Furazolidone ($C_8H_7N_3O_5$)	HPLC	Sigma-Aldrich	USA
12.	Magnesium sulfate ($MgSO_4$)	AR	Sigma-Aldrich	USA

Table 33 (continue)

Reagent	Grade	Manufactures	Country
13. 3-mercaptopropionic acid (MPA) ($C_3H_6O_2S$)	AR	Sigma-Aldrich	USA
14. Nitrofuratoin ($C_8H_6N_4O_5$)	HPLC	Sigma-Adrich	USA
15. Neomycin ($C_{23}H_{46}N_6O_3$)	HPLC	Sigma-Aldrich	USA
16. Oxytetracycline ($C_{22}H_{24}N_2O_9$)	HPLC	Fluka	UK
17. Penicillin G ($C_{16}H_{18}N_2O_4S$)	HPLC	Fluka	UK
18. Phosphinic acid (H_3PO_4)	AR	Sigma-Aldrich	USA
19. Potassium nitrate (KNO_3)	AR	Fluka	UK
20. Ruthenium (III) chloride ($RuCl_3$)	AR	Fluka	UK
21. Sodium borohydride ($NaBH_4$)	AR	Sigma-Aldrich	USA
22. Sodium chloride (NaCl)	AR	Labscan	Ireland
23. Sodium phosphate dibasic (Na_2HPO_4)	AR	CARLO ERBA	Italy
24. Sodium sulfate (Na_2SO_4)	AR	Sigma-Aldrich	USA
25. Tellurium powder	AR	Sigma-Aldrich	USA
26. Tetracycline ($C_{22}H_{24}N_2O_8$)	HPLC	Fluka	UK

5.2.2 Standard preparation

Nitrofurans including furaltadone (FTD), furazolidone (FZD) and nitrofuratoin (NFT) were purchased from Sigma-Aldrich (USA). The stock standard solutions of FTD, FZD and NFT at concentrations of 50 mM were prepared by dissolving the required amount of reagents in *N,N* dimethylformamide (Fisher Scientific, UK). The resulting solutions were stored refrigerated at 4 °C and protected from light, due to the instability of very dilute nitrofurans under UV radiation. Each of the standard solutions for the calibration curve were diluted with 0.11 M phosphate buffer at pH 7.50.

5.2.3 Synthesis of L-cysteine and MPA-capped CdTe nanoparticles

The synthesis of water-soluble CdTe QDs was modified by Mntungwa and coworker (Mntungwa et al., 2013). Briefly, tellurium powder (0.041 g, 0.32 mmol) was mixed with deionized water (10.0 mL) in a three-necked round bottom flask as illustrated in Figure 48. 10.0 mL aqueous solution of sodium borohydride (0.031 g, 0.79 mmol) was carefully added to this mixture and the flask was immediately purged with nitrogen gas to create an inert atmosphere. After 2 h, 20.0 mL of an aqueous solution of $CdCl_2$ (0.059 g, 0.32 mmol), and 20.0 mL of L-cysteine solution (1.1883 g, 6.40 mmol) with a molar ratio of 1:20 (Cd^{2+}:cysteine ester) were added simultaneously to the pink telluride ion solution. The pH of the solution was raised to 7 using HCl (0.10 M) and NH_3 (0.10 M) solutions after which the solution was then heated at 100 °C for 3 h. After completion of the reaction, excess methanol was added resulting in the reversible flocculation of the nano particles. The flocculate was separated from the supernatant by centrifugation. The resultant particles were dissolved in ethanol to give a solution of nano crystallines for characterization. The reaction procedure described above was also followed for the MPA-capped CdTe nanoparticles with MPA (0.0132 g, 6.40 mmol) replacing the L-cysteine.

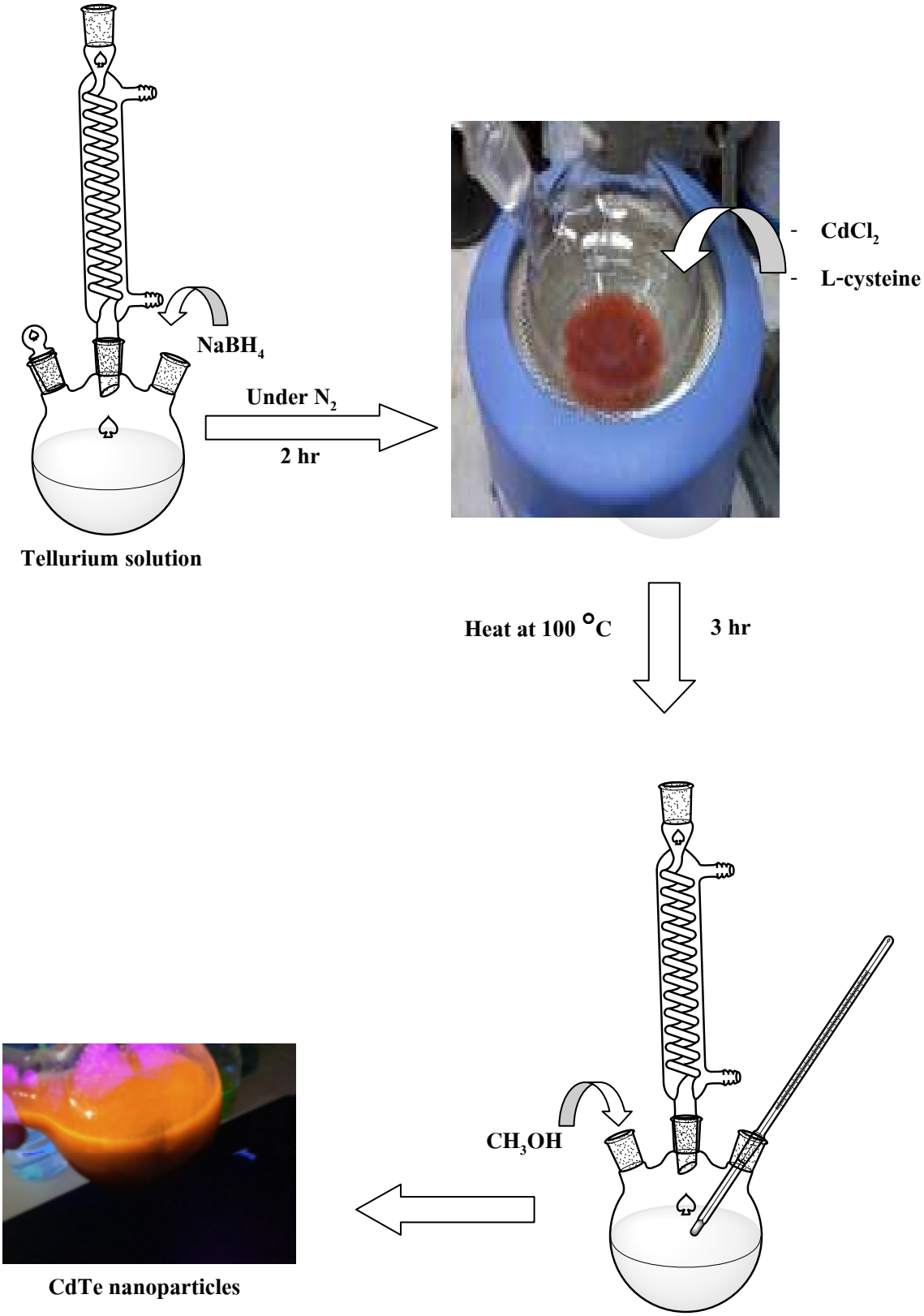

Figure 48 The process for synthesis a water-soluble CdTe-QDs

5.2.4 Synthesis of tris(2, 2′-bipyridyl)ruthenium (II)($Ru(bpy)_3^{2+}$)

Tris(2, 2′-bipyridyl)ruthenium (II)($Ru(bpy)_3^{2+}$) synthesis was a modification of that reported by Broomhead and coworker (Broomhead et al., 2007). Briefly, dried $RuCl_3$ (2.43 g, equivalent to 0.01 mol ruthenium) and 2,2-bipyridine (6.3 g, equivalent to 0.03 mol)were dissolved and mixed with deionized water (250 mL) in a three-necked round bottom flask fit with a reflux condenser. 15.0 mL of fresh sodium phosphate solution was prepared by slowly adding sodium hydroxide pellets to hypophosphorous acid until the mixture appeared cloudy and then adding hypophosphorous acid until the mixture appeared clear again. The mixture solution was heated at 120 °C and refluxed at this temperature for 1 hr. The solution was allowed to cool after an hour, after which it was filtered. Potassium chloride (18.0 g, 0.24 mmol) was added to the filtrate and heated to reduce the volume until than 200 mL. The precipitate was separated and collected by vacuum filtration (washing with 20 mL ice cold water and 40 mL ice-chilled acetone). The resultant crystals were dried and stored in desiccators.

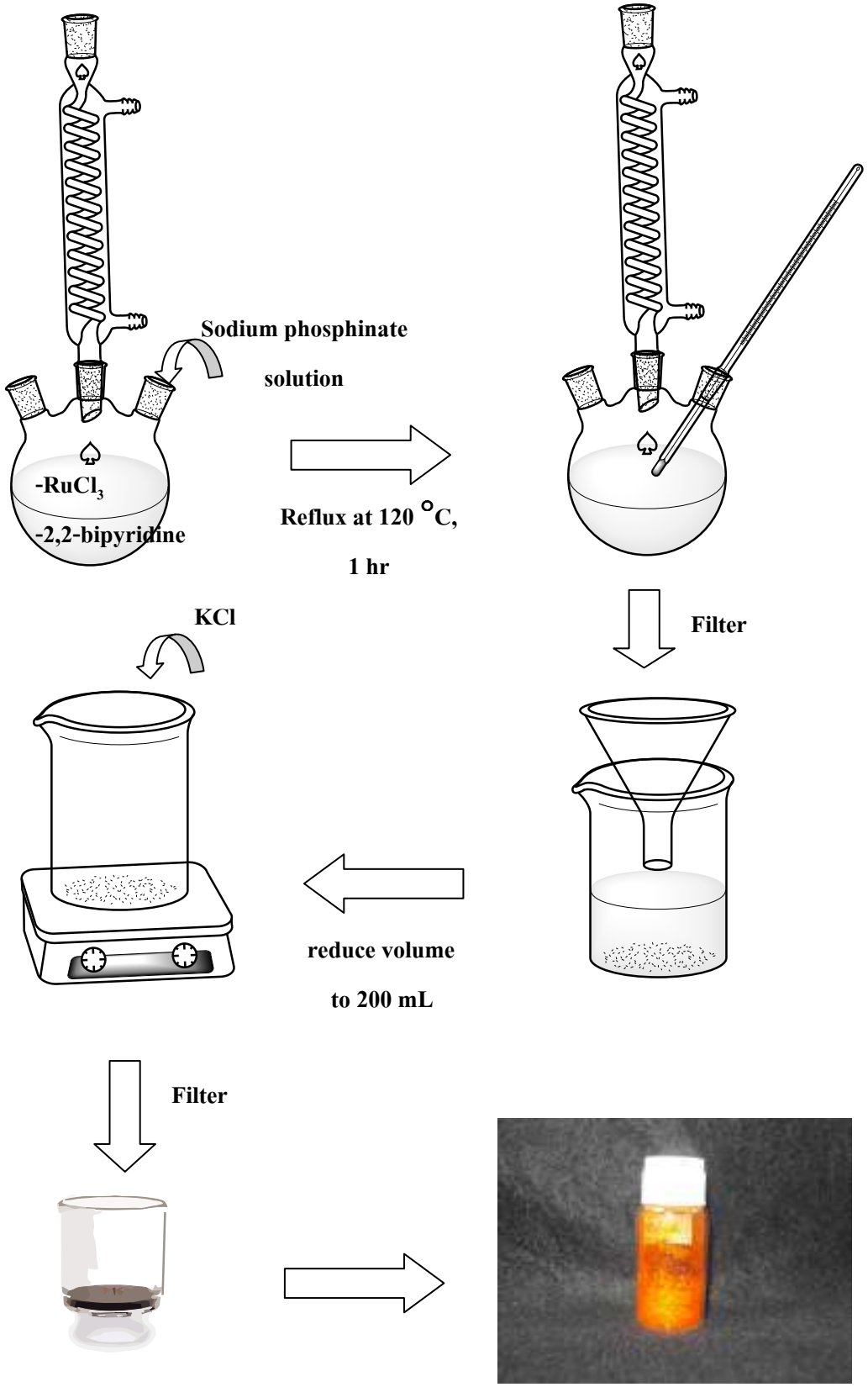

Figure 49 The process for synthesis a tris(2, 2′-bipyridyl)ruthenium (II) ($Ru(bpy)_3^{2+}$)

5.2.5 Apparatus

The size and morphology of the CdTe-QDs were characterized by a JOEL 2100 transmission electron microscope (TEM) (JEOL Ltd., Japan) operated at 200 keV. Bright field TEM (BF-TEM) images and spot energy dispersive X-ray spectroscopy (EDS) were used for morphology and chemical composition identification. The CdTe-QDs were dispersed in ethanol using ultrasonic vibration for about 5 min. The mixture were dropped onto 200 mesh copper grids coated with continuous carbon films and allowed to dry at room temperature before investigation. Fluorescence (FL) spectra were recorded by a luminescence spectrometer-LS50B (PerkinElmer Corporation, America) equipped with a 7.3 Watt xenon discharge lamp as a light source.

The ECL measurement set-up is illustrated in Figure 50. The electrochemical and ECL measurements were observed using a cyclic voltammetry (CV) technique on the Autolab PGSTAT101 (Autolab, Switzerland). A conventional three-electrode configuration was employed, together with a carbon screen-printed electrode (Dropsens, Spain) as the working electrode. A5-mL quartz cuvette (Hellma, Germanny) was used as the ECL cell, and was placed directly in front of the face of photomultiplier tube. The ECL signal was monitored in a light-tight Faraday cage, which consisted of a quartz cuvette flush against the red sensitive photomultiplier tubes (PMT, Thorn-EMI 9828SB, Electron Tubes Ltd., UK) in a sealed metal box (Autolab, Switzerland). The operational potential for the PMT was provided by a high voltage power supply (Thorn- EMI model PM20, Electron tubes Ltd., UK) at a constant voltage of 850V. The output of the PMT, proportional to the ECL intensity, was monitored continuously and displayed on a personal computer via a digital multimeter USB/RS-232 (UT60F, Hong Kong) interfaced with the voltage divider (C637BFN2, Electron Tubes, UK). UNI-T® UT60F AC/DC software was used to determine the maximum peak.

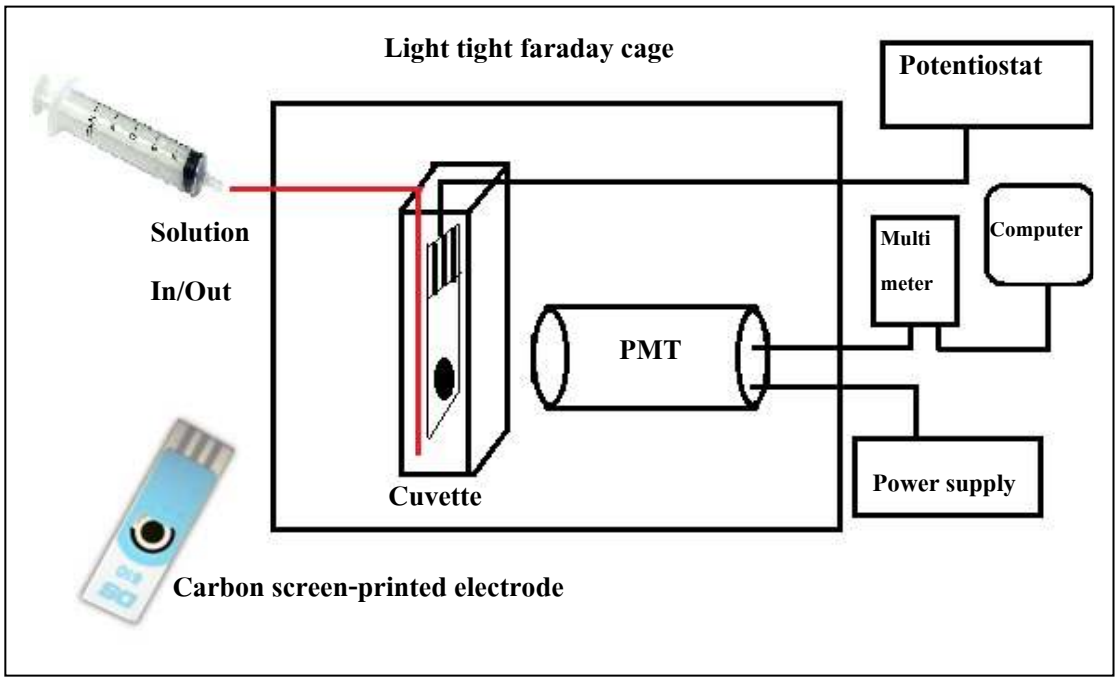

Figure 50 Schematic diagram of the ECL set-up

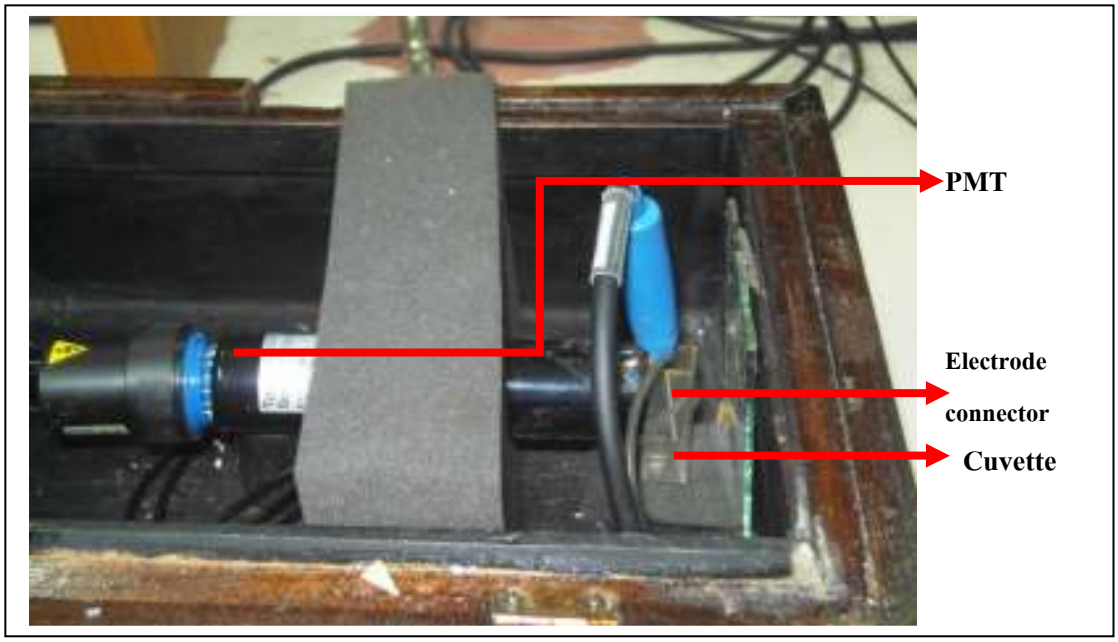

Figure 51 The ECL mesurnement set up for determination of nitrofurans

5.2.6 Animal feed sample preparation (Barbosa et al., 2007)

A 5.0 g thoroughly minced feed was weighed into a 250 mL polypropylene copolymer centrifuge flask. Then, 20 mL of ammonium acetate 79 mmol L^{-1} solutions (pH 4.6) were added and the pH was adjusted to 8 with diluted ammonium hydroxide solution. The mixture was allowed to stand for 15 min, 30 mL of ethyl acetate was added before stirring for 20 min in a rotary shaker and centrifuged for 10 min at 3000 rpm. The organic layer was collected and evaporated to dryness in a rotary vacuum evaporator at 35 ^{o}C and 240 mbar. The resulting extract is reconstituted in 2 mL of a mixture of acetone and methanol 80:20 (v/v).

The extraction solution were cleaned up using a solid phase extraction (SPE) - Sep-Pak® NH_2 cartridge previously conditioned with 5 mL of a mixture of acetone and methanol 80:20 (v/v). The reconstituted extract was put onto the cartridge and, then, the nitrofurans were eluted with 5 mL of the previous mixture. The eluate was evaporated to dryness and the residue was reconstituted with 5 mL of 0.11 M PBS before injected to a ECL measurement system.

5.2.7 ECL procedures

Five milliliters of the mixed solution of $Ru(bpy)_3^{2+}$, CdTe-QDs and either the NFs standard or a sample in 0.11 M phosphate buffer was introduced into the ECL cell via a plastic syringe connected with Tygon tubing. The ECL reaction was then initiated by scanning or stepping the potential of the carbon screen-printed electrode to a value greater than the oxidative potential of the $Ru(bpy)_3^{2+}$ complex (1.10 V) using cyclic voltammetry. The ECL emission was measured by PMT and the ECL intensity was converted to the peak signal via a digital multimeter. The applied potential was controlled in the range of 0.4-1.6 V with a scan rate of 0.05Vs^{-1}. The amount of NFs was estimated based on the quenched ECL intensityΔI, where $\Delta I = I_0 - I_s$, and I_0 was the background ECL intensity of $Ru(bpy)_3^{2+}$/CdTe-QDs system in the absence of NFs; and I_s was the intensity in the presence of a standard or unknown sample with NFs.

5.3 Results and discussion

5.3.1 Characterization of the CdTe-QDs

Two ligands, cysteine and mercaptopropionic has been synthesized illustrated in Figure 52, which has -s-group as a capping group to functionalize the CdTe nanoparticles. Cysteine has been reported as a capping group to have better efficiency than MPA (Idowu et al., 2008), so in this work CdTe-cysteine nanoparticles were selected for further investigated.

(a) **(b)**

Figure 52 The CdTe nanoparticles : (a) Cysteine- CdTe nanoparticles and (b) Mercaptopropionic-CdTe nanoparticles

Figure 53(a) shows BF-TEM image of CdTe-QDs capped with cysteine. The particles are quasi-spherical, with an average size about 5-10 nm and narrow size distribution. Figure 53(b) presents the selected area electron diffraction pattern of these particles. It corresponds to the polycrystalline of the cubic phase of CdTe (JCPDS card no. 15-0770), which is in an agreement with Li et al. (Y.-S. Li et al., 2010)

The chemical composition obtained from TEM-EDS give the Cd- and Te-rich phase as illustrate in Figure 53(c), while the sulfur and copper contents given from the cysteine capped and the copper grid, respectively. The fluorescence emission spectra of cysteine-capped CdTe-QDs with a maximum PL emission at 564 nm are shown in Figure 54.

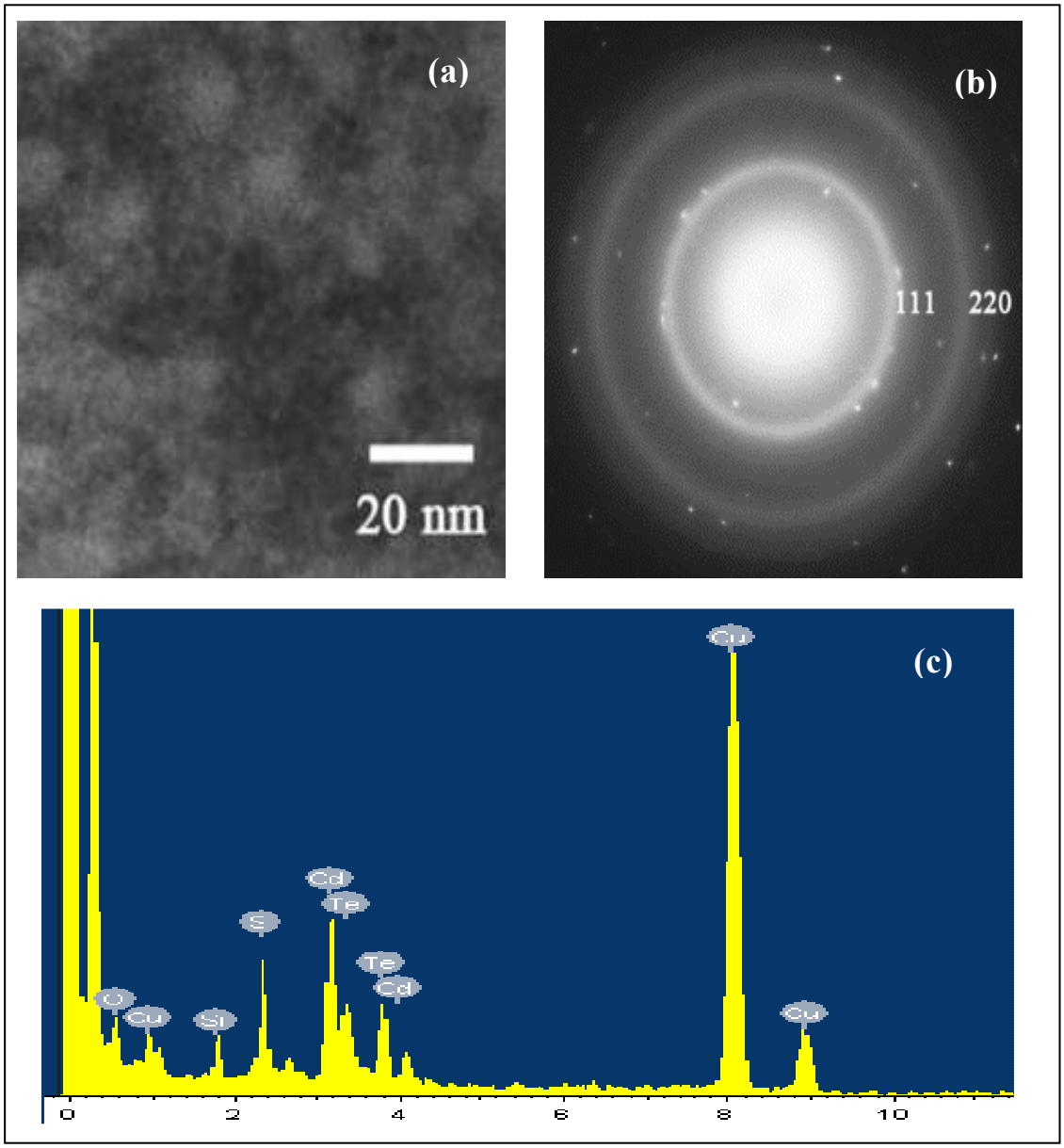

Figure 53 The properties of CdTe nanoparticles synthesized capped with cysteine:(a) BF-TEM image (bright particles), (b) the SADP corresponded to the cubic phase of CdTe (JCPDS card no. 15-0770), (c) EDS spectrum of the particles

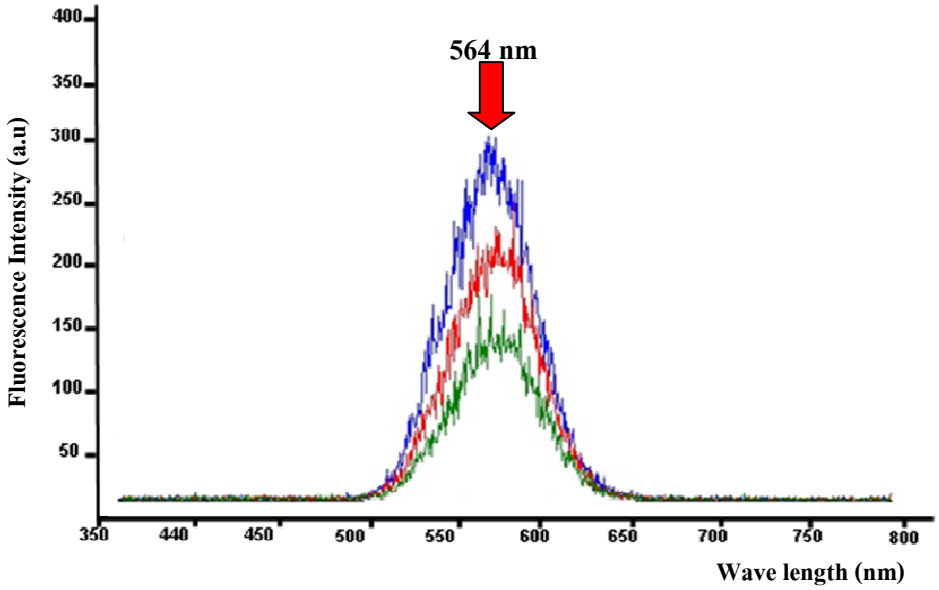

Figure 54 The emission spectra of cysteine-capped CdTe-QDs at various concentrations (excited at 275 nm)

5.3.2 Instrument set-up and preliminary investigation

In order to test the electrochemiluminescence response of nitrofurans with $Ru(bpy)_3^{2+}$, the preliminary investigation was performed with 5 mM $Ru(bpy)_3^{2+}$ in 0.1 M phosphate buffer solution (PBS), pH 7.4. Figure 55(a) shows the ECL response of 0.1 mM FTD in 0.1 M PBS. When the voltage was applied at the carbon SPE by cycling the potential through the range of 0.4-1.6 V by CV with a scan rate of 0.05 Vs^{-1}, no ECL signal was observed. As depicted in Figure 55(b), a weak ECL response was presented on cysteine-capped CdTe-QDs system at the concentration of 1 mM in 0.1 M PBS. When the FTD concentration of 500, 1000 and 1500 µM were added to the solution of $Ru(bpy)_3^{2+}$, a significant increasing in the ECL intensity was observed (Figures 55(d-f)). It might be because the FTD functions as a coreactantand generate ECL signal, though it is not sensitive enough for determine NFs in contaminated feed samples. However, in Figures 55(c) and 55(g) the ECL response shows that the ECL intensity of $Ru(bpy)_3^{2+}$ in 0.1 M PBS is enhanced with a 26-fold increase using cysteine-capped CdTe-QDs. The strong increase in ECL response resulted from the excited QDs.(Y.-S. Li et al., 2010) explained that the capped ligand and the size of CdTe-QDs have a profound effect on the CL intensity of the QD system. The wavelength of the fluorescent emission peak ranged from

480-650 nm, which corresponds to emitted wavelength of $Ru(bpy)_3^{2+}$ chemiluminescence at a 560 nm (Paris and Brandt 1959).

In addition, when various concentrations of FTD, as a NF representative, were added to the $Ru(bpy)_3^{2+}$/cysteine-capped CdTe-QDs system (Figures55(h-j)), an indirect inhibitory effect on the $Ru(bpy)_3^{2+}$ ECL signal was observed that was concentration dependent. This result may indicate that FTD is able to inhibit the ECL of $Ru(bpy)_3^{2+}$/cysteine-capped CdTe-QDs effectively and sensitively enough for the determination of nitrofurans.

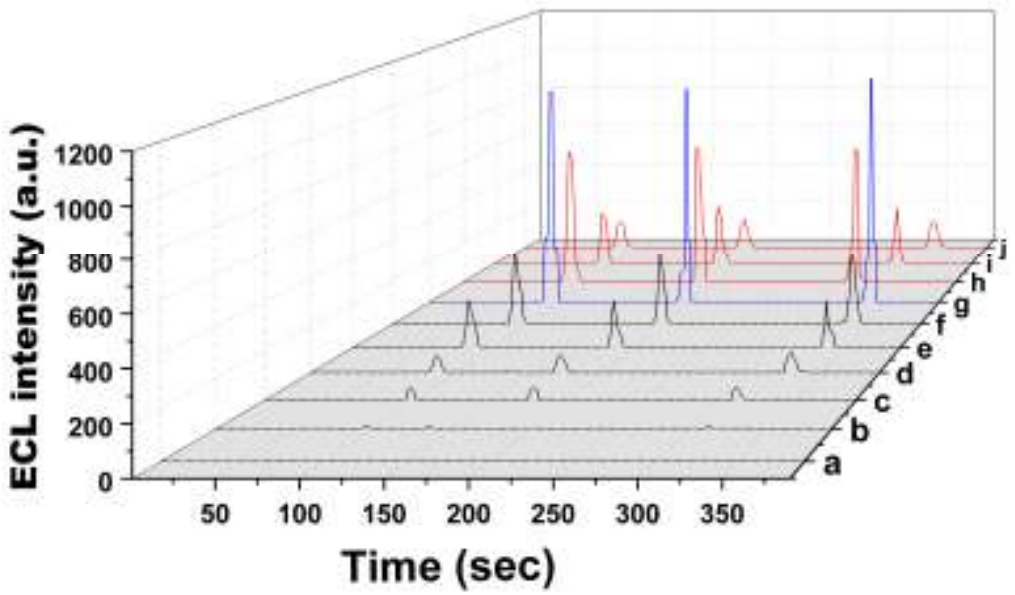

Figure 55 The ECL signal of the electrochemiluminescence reaction:

(a) FTD concentration at 100 µM; (b) L-cysteine CdTe-QDs concentration at 1 mM; (c) 5 mM of $Ru(bpy)_2^{3+}$; (d-f) 5 mM of $Ru(bpy)_2^{3+}$ with 500, 1000 and 1500µM FTD, respectively; (g) 5 mM of $Ru(bpy)_2^{3+}$/L-cysteine CdTe-QDs without FTD; (h-j) 5 mM of $Ru(bpy)_2^{3+}$/ L-cysteine CdTe-QDs with 50, 100 and 200 µM of FTD, respectively.

From the preliminary investigation, a possible mechanism to explain the ECL inhibition behavior observed in this system may arise from the competition of cysteine-capped CdTe-QDs and NFs on resonance energy transfer, which strongly enhance the ECL emission in solution. When the $Ru(bpy)_3^{2+}$ ions was oxidized during the anodic sweep by CV. The close contact between excited $Ru(bpy)_3^{3+}$ ions and CdTe-QDs made energy transfer possible to strong excite the luminescence of QDs. The control experiments were performed in the presence and the absence of CdTe-QDs. It was observed that very weak ECL signals could be observed in the presence of only NFs, compared with that in the presence of CdTe-QDs itself and both CdTe-QDs and NFs. Thus, we proposed that the competition of L-cysteine capped CdTe-QDs and NFs created imperfections resonance energy transfer, and eventually led to the ECL quenching. This is the key factor for the ECL inhibition of the $Ru(bpy)_3^{2+}$/cysteine-capped CdTe-QDs system. The following Figure 56 clearly illustrates the mechanism of the completitive enhanced ECL. Since no one has ever attempted to detect nitrosfuran with $Ru(bpy)_3^{2+}$/QDs ECL to our knowledge, it could implies that QDs have great potential for development of novel ECL sensors for nitrofurans screening for the first time.

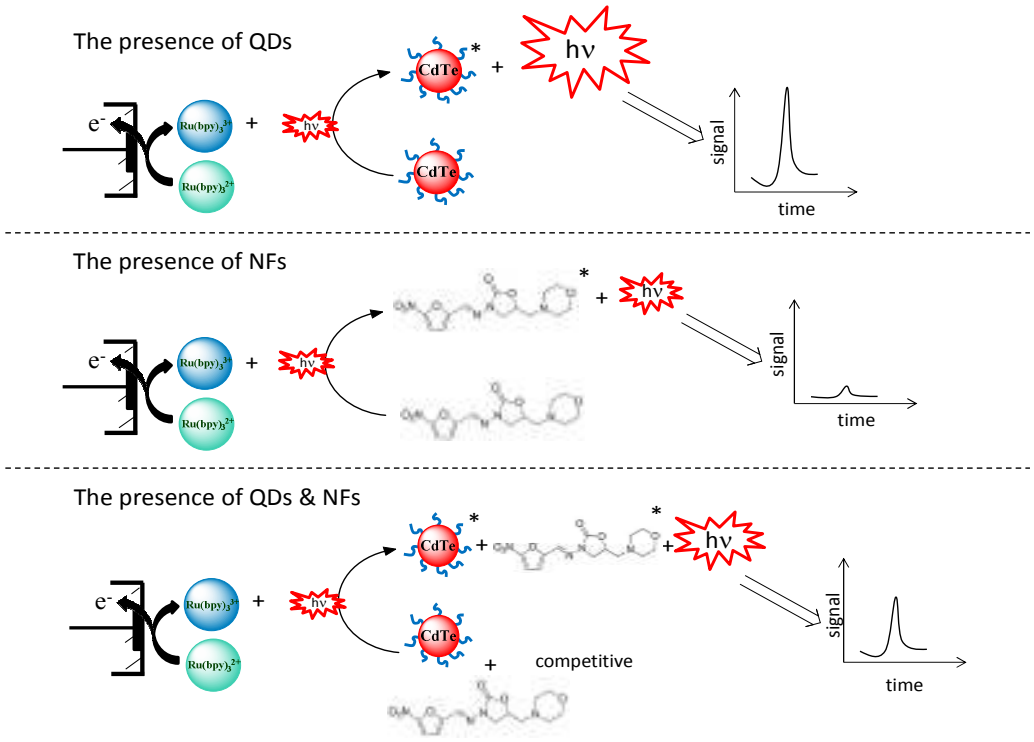

Figure 56 The mechanism of energy transfer to enhance the $Ru(bpy)_3^{2+}$/QDs ECL

5.3.3 Optimization of experimental conditions

To establish the optimum ECL conditions for the determination of nitrofurans, the effects of the key chemical and physical parameters on the ECL signal were investigated using an univariate approach and simplex optimization. The quenched ECL intensity was correlated with a number of factors, including the scan mode of the applied potential by CV, the applied voltage of the photomultiplier tube, the type of buffer solution used and its pH, and the concentrations of the $Ru(bpy)_3^{2+}$ complex and L-cysteine-capped CdTe-QDs. In order to obtain the highest sensitivity of this ECL system, all of these factors were thoroughly investigated.

5.3.3.1 Selection of CV scan rate

The cyclic voltammetry double potential step method was used to examine the ECL behavior of $Ru(bpy)_3^{2+}$ in 0.1 M PBS system on a carbon screen-printed electrode with the applied potential over the range of 0.4-1.6 V. A satisfactory and stable ECL signal was obtained when using CV mode for the measurements. The effect of scan rate on the ECL signal was subsequently studied. Figure 57 shows the ECL signal-to-noise response for the $Ru(bpy)_3^{2+}$ complex in 0.1M PBS at various scan rates applied from 0.02 Vs^{-1} to 0.5 Vs^{-1}. It was found that the maximum S/N ratio was obtained at 0.05 Vs^{-1}. Faster scan rates gave gradually decreasing ECL signals while the slower scan rate did not result in lower detection limits but slowed down the ECL analysis time. A scan rate of 0.05 Vs^{-1} was used in the following experiments, as it gave the maximum ECL signal value and a reasonably rapid analysis.

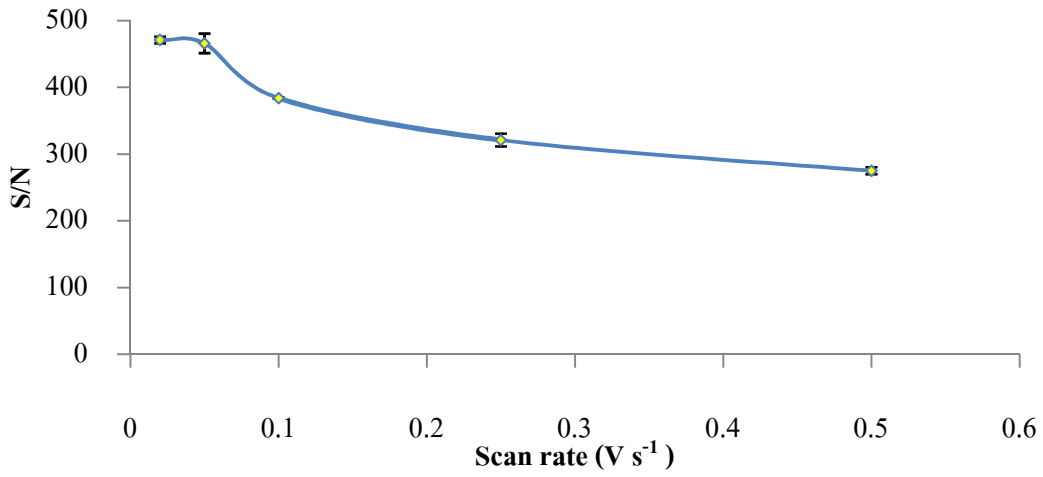

Figure 57 The effect of scan rate on ECL intensity

5.3.3.2 Effect of photomultiplier tube applied voltage

The effect of the photomultiplier tube (PMT) applied voltage was investigated in the range of 700-1,000 V to obtain the maximum signal-to-noise ratio. For these experiments, the potential of the power supply was increased stepwise: the ECL signal was measured after the cyclic potential was applied to the $Ru(bpy)_3^{2+}$ complex solution at each potential step. The noise from the background current was also measured at each potential step. As expected, the ECL signal increased when the power supply was increased stepwise. It was found that the signal-to-noise ratio reached a maximum value at 850 V. Furthermore, a high signal noise was observed for the applied voltage exceeding 1050 V. The PMT applied voltage of 850 V was used for all subsequent studies.

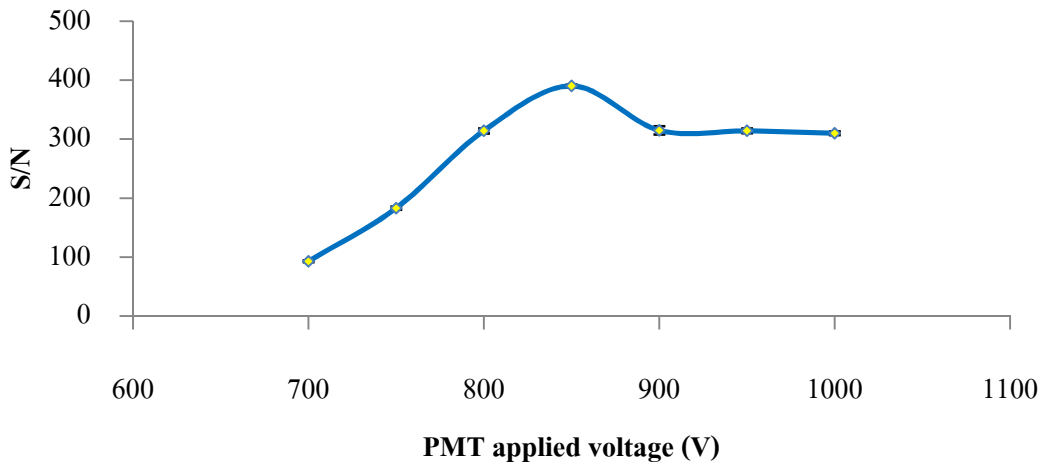

Figure 58 The effect of the photomultiplier on ECL intensity

5.3.3.3 Effect of the type of buffer solutions

For these experiments, 0.5 mM FTD standard solution was added to a 0.5 mM $Ru(bpy)_3^{2+}$ solution for the investigation of the ECL behavior of $Ru(bpy)_3^{2+}$/ FTD in different buffer media, including, 0.1 M acetate buffer solution, 0.1 M phosphate buffer solution, 0.1 M borate buffer solution, 0.1 M ammonium buffer solution, and 0.1 M carbonate buffer solution. The experimental results showed that a maximum ECL signal-to-noise ratio was obtained with the phosphate buffer solution.

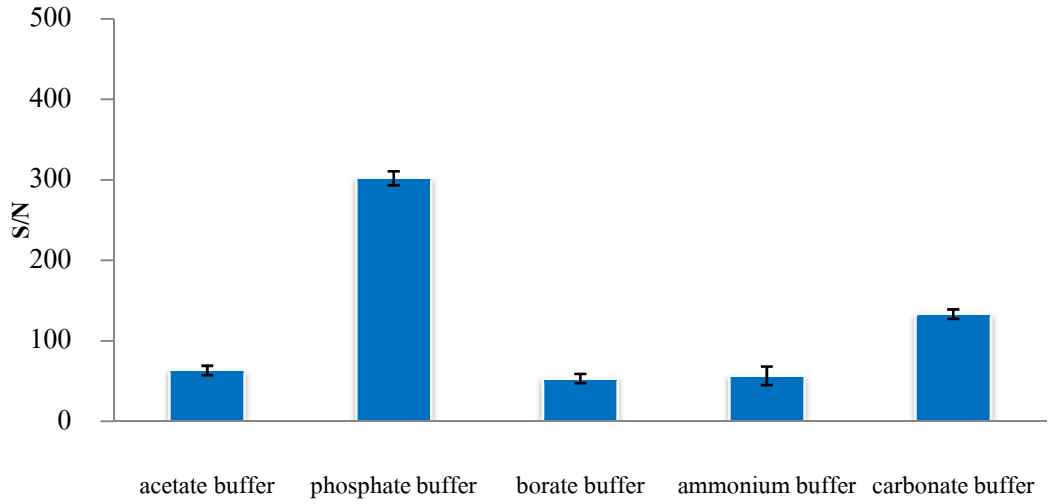

Figure 59 Effect of buffer on ECL intensity

In addition, the ECL signal was dependent on the pH value of the phosphate buffer solution. The ECL signal increased with increasing pH (from pH 5.7 to pH 8.0). When the pH of PBS was over 7.5, the ECL signal plateaued. Therefore, the 0.1 M phosphate buffer solution at pH 7.5 was selected for further investigations.

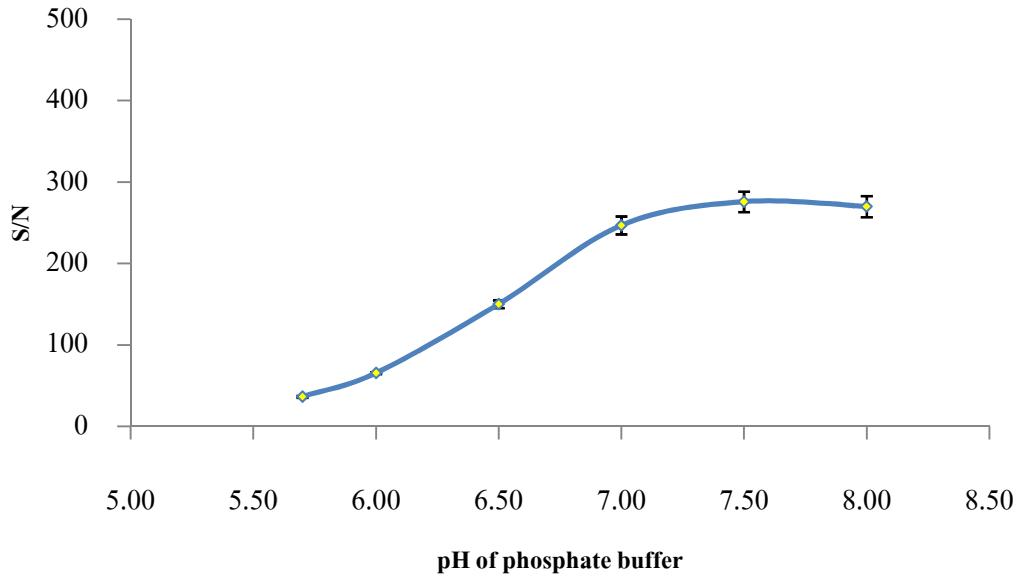

Figure 60 Effect of pH of phosphate buffer on ECL intensity

5.3.3.4 Effect of the concentration of $Ru(bpy)_3^{2+}$ and L-cysteine-capped CdTe-QDs

The effect of the concentrations of $Ru(bpy)_3^{2+}$ and L-cysteine-capped CdTe-QDs on the ECL signal was studied. First, the concentration of $Ru(bpy)_3^{2+}$ was examined over the range of 0.1-5.0 mM using the previously determined optimum conditions. The results show that the ECL signal increased steeply with the concentration of $Ru(bpy)_3^{2+}$up to 5.0 mM. The signal-to-noise ratio decreased due to the increase in background response when the concentration of $Ru(bpy)_3^{2+}$ exceeded 5.0 mM. Consequently, the concentration of $Ru(bpy)_3^{2+}$ at 5.0 mM was selected in the following experiments.

The effect of the CdTe-QD concentration on the ECL signal was found with the quantity of CdTe-QD in the $Ru(bpy)_3^{2+}$/FTD system in the concentration range of 0.16-1.61 mM, it was found that the ECL peak height increased with the concentration of CdTe-QDs until it reaches a maximum at 1.61 mM. Beyond this point, the ECL intensity continued to gradually decrease. Thus, the concentration of 1.61 mM CdTe-QD was chosen as the optimum concentration.

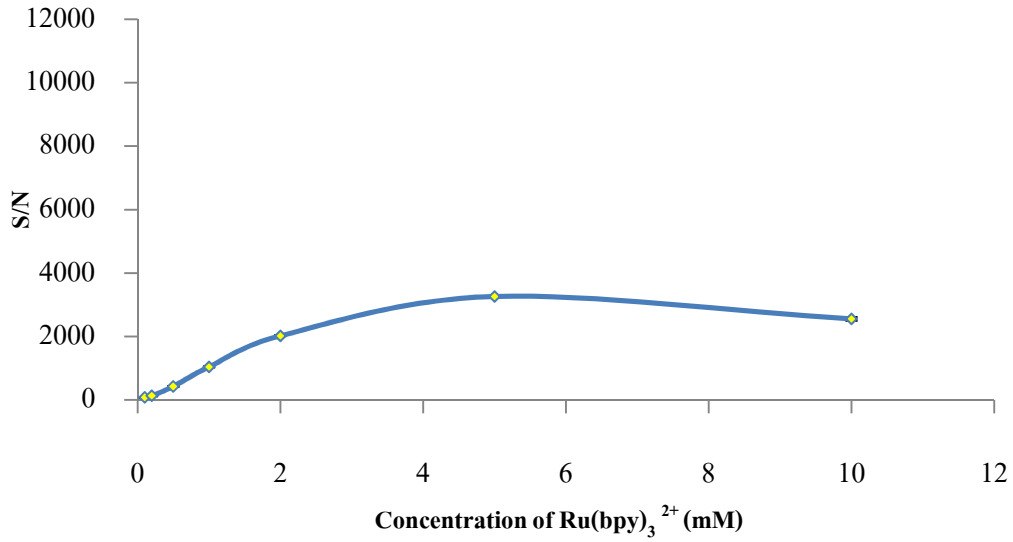

Figure 61 The effect of the concentration of $Ru(bpy)_3^{2+}$ on ECL intensity

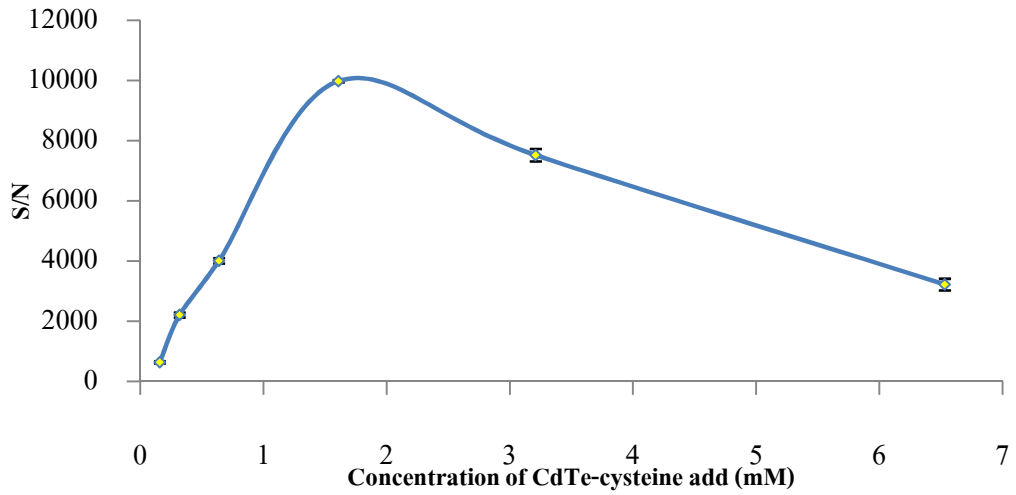

Figure 62 The effect of the concentration of L-cysteine-capped CdTe-QDs on ECL intensity

5.3.3.5 Simplex optimization

To ensure the ECL parameters obtained from the univariate approach were providing the highest sensitivity and reproducibility, the systematic optimization was investigated using Multisimplex software (2.1 trial version). Table 34 shows the range over which each parameter was investigated, the initial step size and its optimal value. The phosphate buffer solution was chosen as the ideal component of the electrolyte in the ECL cell and was used for all experiments. The initial conditions used to start the simplex algorithm were phosphate buffer pH 7.5 at the concentration of 100 mM, $Ru(bpy)_2^{3+}$ at the concentration of 5 mM and L-cysteine CdTe-QDs at the concentration 1.61 mM. After 13 experiments see Figure 63, the simplex algorithm no longer predicted improved outcomes. The details of each investigated parameter, including its optimal value compared with univariate approach, are also given in Table 34.

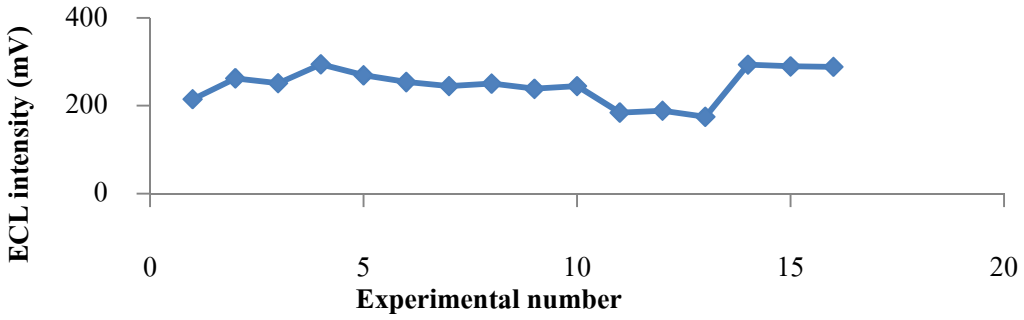

Figure 63 The relationship between the experimental number and ECL intensity

Table 34 System parameters optimized in this study

Parameter	Univariate optimization		Simplex optimization		
	Range studied	Optimal value	Range studied	Initial step size*	Optimal value
PMT applied voltage (V)	700-1000	850	-	-	-
Type of buffer	acetate buffer, phosphate buffer, borate buffer, ammonium buffer and carbonate buffer	phosphate buffer	-	-	-
pH of phosphate buffer	5.7-8.0	7.5	-	-	-
Phosphate buffer concentration (mM)	10-250	100	90-135	20	110
$Ru(bpy)_2^{3+}$ concentration (mM)	0.1- 10.0	5.0	4.75-5.25	0.5	5.25
L-cysteine CdTe-QDs concentration (mM)	0.16-6.43	1.61	1.45-2.15	0.10	1.77

*The step size varied during the optimization procedure

5.3.3.6 Analytical figures of merit

5.3.3.6.1 Linearity of the calibration graph

Under the optimal conditions, chemiluminescence intensity (ΔI) is found to have a linear relationship with the concentration of three types of nitrofurans: furaltadone (FTD), furazolidone (FZD) and nitrofuratoin (NFT), over a concentration range of 10-100 μM.

$$\Delta I = I_0 - I_s \quad (1)$$

Where I_0 is the background ECL intensity of the $Ru(bpy)_3^{2+}$/CdTe-QDs system in the absence of NFs and I_s is the intensity in the presence of a standard NFs.

It was found that the calibration curve found to be linearity over the range of 10-100 μM. Figure 64 shows calibration curves furaltadone (FTD), furazolidone (FZD) and nitrofuratoin (NFT), while Figure 65 illustrated the ECL grams for furaltadone (FTD), furazolidone (FZD) and nitrofuratoin (NFT), respectively.

Table 35 The data of the calibration curve for furaltadone (FTD), furazolidone (FZD) and nitrofuratoin (NFT)

Concentration (μM)	**$\Delta I = I_0 - I_s$**		
	FTD	**FZD**	**NFT**
10	128.0	145	60
20	138.0	156	92
40	158.0	187	123
60	178.0	206	163
80	198.0	240	203
100	218.0	265	235

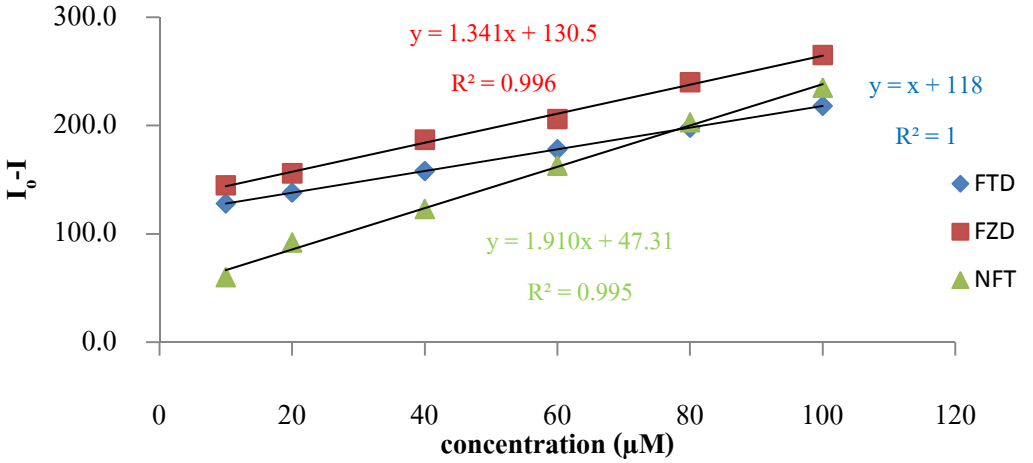

Figure 64 Calibration curves for furaltadone (-◆- FTD), furazolidone (-■-FZD) and nitrofuratoin (-▲-NFT)

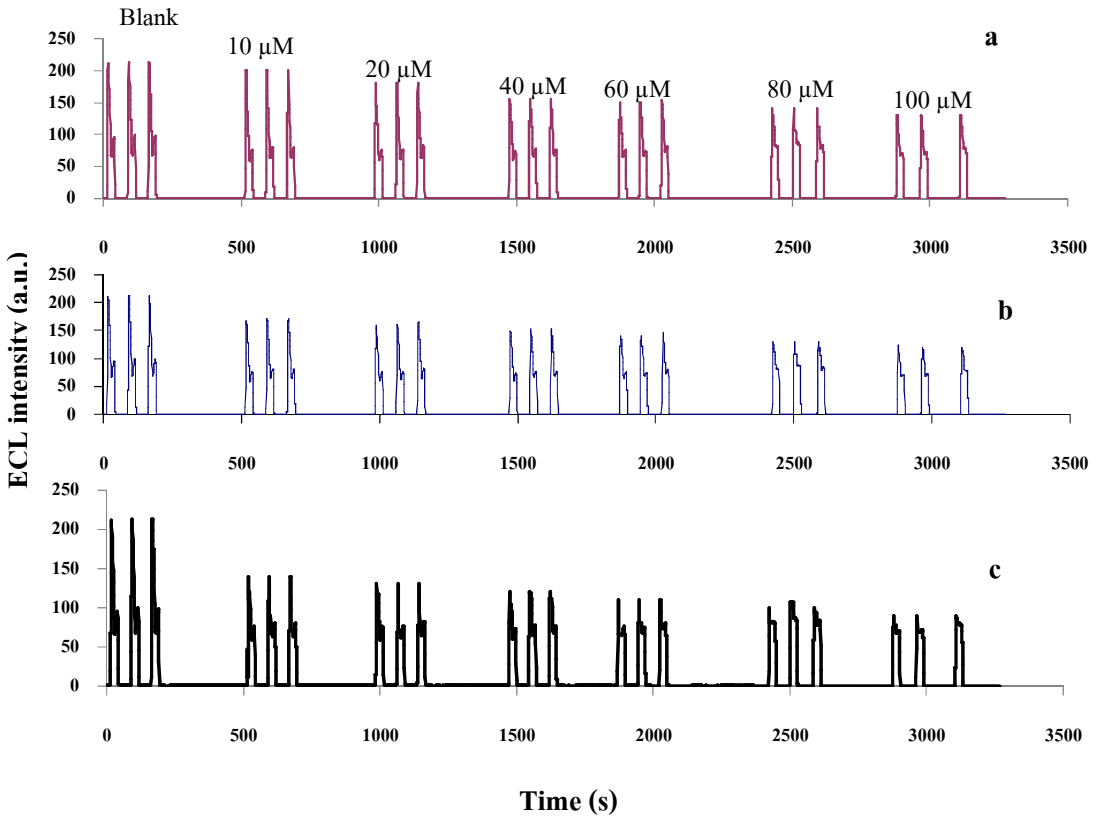

Figure 65 Illustrated the ECL grams of NFs: (a) furaltadone (FTD), (b) furazolidone (FZD) and (c) nitrofuratoin (NFT)

5.3.3.6.2 The limits of detection

In this work, the detection limits of furaltadone (FTD), furazolidone (FZD) and nitrofuratoin (NFT) were calculated according to 3 σ/s criteria where s is the slope of the calibration curve and σ is the standard deviation of the y-residue ($s_{y/x}$).

The detection limits were found to be 0.40, 0.73 and 0.60 μM for furaltadone (FTD), furazolidone (FZD) and nitrofuratoin (NFT), respectively.

5.3.3.6.3 Reproducibility and repeatability

The repeatability of the procedure was determined by repeating the measurements of 60 μM furaltadone (FTD), furazolidone (FZD) and nitrofuratoin (NFT) for 15 replicates. The reproducibility (intra-day) variations of the method were determined using triplicate injections of standard furaltadone (FTD), furazolidone (FZD) and nitrofuratoin (NFT) solutions at the concentraton of 60 μM and analysed on the same day. The reproducibility (inter-day) precision was studied by comparing the results of the assays performed on different days on the same injected standard furaltadone (FTD), furazolidone (FZD) and nitrofuratoin (NFT) solutions in three replicates. The result was expressed in term of the percentage relative standard deviation (% RSD). Results are shown in Table 36-38.

Table 36 Replicate measurements by using standard 60 μM of furaltadone (FTD), furazolidone (FZD) and nitrofuratoin (NFT)

Experiment number	ECL Intensity (a.u.)		
	FTD	**FZD**	**NFT**
1	12120	9010	7340
2	12250	9340	7260
3	12240	8780	7260
4	12190	8830	7300
5	12180	8560	7360
6	12240	8430	6980
7	12170	8400	7010
8	12220	8950	6840
9	12240	9530	7280
10	12260	9340	7500
11	12190	8840	7300
12	12070	9340	7270
13	12130	8890	6920
14	12030	8560	6830
15	12060	8400	6860
Average	12173	8880	7154
S.D	74.78	374.30	221.51
% RSD	0.61	4.22	3.10

Table 37 Reproducibility for intra-day variations

Times (hour)	ECL intensity (a.u.), n=3		
	FTD	**FTD**	**FTD**
1	12173	8880	7154
3	11170	8803	6710
6	11100	8750	6610
9	11180	7903	6410
Average	11405	8584	6721
S.D.	512	457	314
% RSD	4.50	5.33	4.68

Table 38 Reproducibility for inter-day variations

Times (day)	ECL intensity (a.u.), n=3		
	FTD	**FTD**	**FTD**
1	12173	8880	7154
2	12110	9460	7940
3	11010	8460	7480
Average	11764	8933	7524
S.D.	654	502	394
% RSD	5.56	5.62	5.25

The Table 39 show the results of statistical analysis of the experimental data for furaltadone (FTD), furazolidone (FZD) and nitrofuratoin (NFT) tested. It was found that the calibration curve found to be linearity over the range 10-100 μM. The analytical characteristic for furaltadone (FTD), furazolidone (FZD) and nitrofuratoin (NFT) and the precision of the proposed method was attained by analyzing 15 samples of 60 μM.

Table 39 Analytical performances characteristics of the proposed ECL method

Analytical parameter	FTD	FZD	NFT
Regression equation [a]	ΔI =1.000C+118	ΔI =1.341C+130.5	ΔI =1.910C+47.31
Linear range, μM	10-100	10-100	10-100
Correlation coefficient (r^2)	0.998	0.995	0.995
Detection limit[b] , μM	0.40	0.73	0.60
Precision[C] (% RSD)	0.61	4.22	3.10
Inter-day precision (% RSD)	4.50	5.33	4.68
Intra-day precision (% RSD)	5.56	5.62	5.25

a.$\Delta I = I_0 - I_s$, where $I_0$is the background ECL intensity of the $Ru(bpy)_3^{2+}$/CdTe-QDs system in the absence of NFs; and I_s is the intensity in the presence of a standard or unknown sample with NFs, and C is the concentration of each nitrofuran (μM).

b. Detection limits calculated based on $3\sigma/s$

c. Precision at each 60 μM of standards NFs (n=15).

5.3.3.7 Effect of potential interferences

In order to assess the proposed method for the analysis of NFs in animal feed, the interference effects of coexisting substances, such as common cations, anions and other antibiotics expected to be present in the animal feed samples, were also examined. The solutions used for this purpose contain 60 μM NFs along with interfering species. The upper limit for an interfering species was calculated to be when the relative error for the determination of a standard NF solution was less than 10%. The tolerable concentration ratios for ionic interfering species were determined to be as follows: 1000-fold for Na^+, K^+,Mg^{2+} NO_3^-, Cl^-; $SO_4^{2-}$and PO_4^{3-};100-fold for Ca^{2+}; 10-fold for NH_4^+.

In addition, the interference of other potential contaminants (antibiotics and drugs) was also tested using the same method described above. The tolerable concentration ratios were determined to be as follows: 1000-fold for penicillin; 100-fold for neomycin and cloxaciline; 10-fold for oxytetracycline, tetracycline and chlortetracycline; 1-fold for chloramphenical. Results show that this method is not as selective as the chromatographic methods reported since the determination of nitrofuransis greatly affected when certain tetracycline derivatives and chloramphenicol are present in up to 10-times weight ratio to nitrofurans. However, it is a simpler preliminary screening method with potential for in situ determination, while contaminating antibiotics can be removed from samples during the SPE extraction process.

Table 40 Maximum tolerance of co-existing anion and cation for the determination of 60 μM NFs

Cation/Anion	Concentration ratios	% Error, n=3
Na^+	1:0	-
	1:1	3.38
	1:10	-8.33
	1:100	-9.45
	1:1,000	-53.73
	1:10,000	-91.07

Table 40 (continue)

Cation/Anion	Concentration ratios	% Error, n=3
K^+	1:0	-
	1:1	8.03
	1:10	5.82
	1:100	4.53
	1:1,000	-9.59
	1:10,000	-63.54
NH_4^+	1:0	-
	1:1	-9.12
	1:10	-21.14
	1:100	-17.68
	1:1,000	-47.37
	1:10,000	-89.18
Mg^{2+}	1:0	-
	1:1	2.45
	1:10	-1.73
	1:100	-2.97
	1:1,000	-33.57
	1:10,000	-81.61
Ca^{2+}	1:0	-
	1:1	2.69
	1:10	-9.82
	1:100	-23.82
	1:1,000	>-100
	1:10,000	>-100

Table 40 (continue)

Cation/Anion	Concentration ratios	% Error, n=3
Cl^-	1:0	-
	1:1	3.38
	1:10	-8.33
	1:100	-9.45
	1:1,000	-53.73
	1:10,000	-91.07
NO_3^-	1:0	-
	1:1	8.03
	1:10	5.82
	1:100	4.53
	1:1,000	-9.59
	1:10,000	-63.54
SO_4^{2-}	1:0	-
	1:1	2.45
	1:10	-1.73
	1:100	-2.97
	1:1,000	-33.57
	1:10,000	-81.61
PO_4^{3-}	1:0	-
	1:1	-2.28
	1:10	-4.95
	1:100	0.63
	1:1,000	30.30
	1:10,000	30.21

Table 41 Maximum tolerance of co-existing potential contaminants (antibiotics and drugs) for the determination of 60 μM NFs

Antibiotics/drugs	**Concentration ratios**	**% Error, n=3**
Chloramphenical	1:0	-
	1:1	-17.74
	1:10	-36.44
	1:100	-87.67
	1:1,000	>-100
	1:10,000	>-100
Chlortetracycline	1:0	-
	1:1	-3.55
	1:10	-7.99
	1:100	-99.31
	1:1,000	>-100
	1:10,000	>-100
Cloxaciline	1:0	-
	1:1	-4.96
	1:10	-2.83
	1:100	>100
	1:1,000	>100
	1:10,000	>100
Neomycin	1:0	-
	1:1	2.15
	1:10	0.27
	1:100	-48.65
	1:1,000	>-100
	1:10,000	>-100

Table41 (continue)

Antibiotics/drugs	Concentration ratios	% Error, n=3
Oxytetracycline	1:0	-
	1:1	-9.20
	1:10	-25.52
	1:100	-99.29
	1:1,000	>-100
	1:10,000	>-100
Penicillin	1:0	-
	1:1	-2.64
	1:10	-2.39
	1:100	1.64
	1:1,000	>100
	1:10,000	>100
Tetracycline	1:0	-
	1:1	-5.63
	1:10	-13.62
	1:100	-99.54
	1:1,000	>-100
	1:10,000	>-100

5.3.4 Analytical applications

The developed method was then applied to determine NFs in poultry and porcine feed samples, obtained from shops where commercial feed was sold in Chiang Mai market. The feed samples were cleaned up using a solid phase extraction (SPE) cartridge prior to analysis by the proposed ECL method according to Barbosa et al. (2007). The SPE method was similar to that described previously (Thongsrisomboon et al., 2010); however the evaporated residue was reconstituted with 5 mL of 0.11 M PBS instead of H_2SO_4 carrier solution. The results of the NFs measurements were comparative to the HPLC procedure with photodiode-array detection (Barbosa et al., 2007), used as a reference method as can be seen in Table 42. The results show that only furaltadone residues are present in the collected animal feeds. The results were found to be statistically indistinguishable from those obtained by the ECL method at a 95% confidence level.

Three different concentrations of each NFs (25-85 μM) were spiked into the animal feeds to create synthetic samples. The average percentage recoveries of the spiked furaltadone drug measured by the proposed method were in the range of 93.33-96.86 %. With the performance of the proposed method (LODs of 0.40-0.73 μM), it can be seen that this method has enough sensitivity to meet regulatory requirements and can be applied to the control of nitrofuran residues in a wide range of animal feeds.

Table 42 Comparative determination of furaltadone residues in animal feed by the proposed ECL method and the reference HPLC method

Feed sample	**Amount found (mg kg^{-1})± SD**		
	ECL method[a]	**HPLC method[b]**	**t-value**
Feed A	1.49 ±0.04	1.45 ±0.02	1.74
Feed B	1.54 ±0.05	1.50 ±0.10	0.59
Synthetics Feed1	1.85 ±0.02	1.81 ±0.02	2.50
Synthetics Feed2	1.90 ±0.05	1.88 ±0.03	0.43
Synthetics Feed3	1.97 ±0.06	1.95 ±0.04	0.48

Standard deviation from three determinations each, for the proposed method and the reference method.

a. LOD of ECL method = 0.06 mg kg^{-1} (0.40μM).

b. LOD of HPLC method = 0.047 mg kg^{-1}.

$t_{calculated}$ values are less than $t_{critical}$ 2.78 at 95% confidence.

Table 43 The average percentage recoveries of NFs

Feed sample	Add (μM)	% Recoveries		
		FTD	FZD	NFT
Synthetics Feed	25	93.33 ± 2.31	90.91 ± 3.03	90.93 ± 1.23
	55	95.76 ± 2.78	96.43 ± 1.38	97.51 ± 1.12
	85	96.86 ± 2.96	96.15 ± 0.89	99.03 ± 2.17

5.3.5 Conclusion

L-cystein-capped CdTe-QDs were utilized to enhance the ECL intensity of a $Ru(bpy)_3^{2+}$ system and the ECL from the $Ru(bpy)_3^{2+}$/L-cysteine-capped CdTe-QDs system was significantly inhibited by the presence of nitrofurans. The proposed ECL method was successfully developed for the determination of total quantity of NFs residues. The results show that only furaltadone residues are present in the collected animal feeds. The concentration furaltadone found in porcine feed samples approximately 9.18-12.15 μM (1.49 – 1.97 mg kg^{-1}).

The method is simple, sensitive and accurate, and was demonstrated to measure NFs in animal feed samples with satisfactory results. The proposed ECL method could be used as a rapid screening method that can improve the effectiveness of residual control in industrial laboratories, although contamination in exported food products should be confirmed by a suitable instrumental method.

CHAPTER 6

Summary and Recommendation for Further Work

Flow injection chemiluminescence (FI-CL) and electrogenerated chemiluminescence (ECL) analysis are rapidly growing according to the number of scientific papers published every year. One of the main interests is its application to environmental studies, where the fast response of FI-CL and ECL makes the analytical information available in near real time, especially useful for the on-line monitoring of rapid transformations of target analytes. FI-CL and ECL are also cost-effective method and can be miniaturized with high analytical throughput. It also considerably decreases the amount of waste generated and hence the cost of waste disposal.

This thesis covers the application of chemiluminescence detection to develop two unrelated flow based methods for the determination of arsenic and cadmium in environmental samples and the ECL chemical sensor for nitrofurans. The first study was investigated the contamination of arsenic in seven ground water samples of Hang Chat district in Lampang province, Thailand, which is suffering from nearby mining and industrial waste landfill impacts. While the second attempt was the observation on the ranges of cadmium concentrations in the soil of Mae Sot district, Tak province where zinc mine is nearby located. The final part of this thesis reports the development of electrogenerated chemiluminescence sensor for the determination of nitrofuran antibiotics.

In addition, when the FI-CL and ECL detection methods are used with particular and sensitive procedures, the unique combination of selectivity, sensitivity detector can provide a powerful analytical method with simple and inexpensive analytical instruments that compare favorably to the complex and expensive analytical instruments/techniques currently used for some environmental analyses. The major conclusions from this thesis are summarized below.

6.1 Summary of achievements in this thesis

In the first part of this study, the simultaneous determination of As(III) and As(V) in aqueous solution based on the acidic permanganate and luminol chemiluminescence detection systemshave been applied to a split microfluidicsflow injection with dual-channel manifolds at rapid sampling rate. The μFI-CL system consisted of two halves of micro-conduit platforms, which ran on a simple device made from small pieces of the laser engraved polymethylmethacrylate (PMMA) and polydimethylsiloxane (PDMS). The specific CL reaction for As(III) was produced by the oxidation of acidic potassium permanganate in the presence of sodium hexametaphosphate media, while the CL reaction for As(V) was generated based on the oxidation of luminol with a vanadomolybdoarsenate heteropoly acid (AsVMo-HPA) complex in an alkaline solution. The μFI-CL method involved the injection of the mixed standard solution into an acid carrier stream where it was then splitted and merged with the reagent solutions of each reaction systems on a spiral-designed microfluidic platform. The solution mixtures were passed through each spiral flow channel, where the CL intensity of both resulting reaction mixtures were measured with two photomultiplier tubes. Linear calibratons for As(III) and As(V)were established over the concentration ranges of 20-60 μg L^{-1}. The limits of detection (signal-to-noise ratio of 3) of As(III) and As(V) were found to be 4 μg L^{-1} and the limits of quantification (signal-to-noise ratio of 10) were found to be 10 μg L^{-1}, respectively. The proposed procedure was successfully applied for the determination of As(III) and As(V) in ground water samples collected from contaminated area of Lampang province.

Second, a sensitive flow injection chemiluminescence procedures was proposed for determination of cadmium in environmental samples. This chapter was focused on the exchangeable cadmium amounts from contaminated soil. A mini column, packed with polystyrene bead as an adsorption material, was used for the pre-concentration of Cd(II) ions based on the complex formation with the ammonium pyrolidinedithiocarbamate (APDC). The Cd-APDC complex adsorbed on polystyrene beads was eluted by methanol and simultaneously determined by the flow injection chemiluminescence system. The chemiluminescence reaction based on Cd(II) catalyze the luminol-H_2O_2 CL reaction in the present of alkaline media was chosen. Under the optimum condition, linear calibration graph was obtained with the limits of detection of 0.6 μg L^{-1} and the limits of quantification of 2.0 μg L^{-1}, respectively.The proposed

procedure was successfully applied for the determination of Cd(II) in soils from nearby zinc mining area.

The final past of the study, a new approach to enhance the electrogenerated chemiluminescence (ECL) of the tris(2,2′-bipyridyl)ruthenium (II)($Ru(bpy)_3^{2+}$) systemusing resonance energy transfer with L-cysteine-capped cadmium telluride quantum dots (CdTe-QDs) in aqueous solution. A possible mechanism to explain the ECL inhibition behavior was proposed which may arise from the competition of cysteine-capped CdTe-QDs and NFs on resonance energy transfer, which strongly enhance the ECL emission in solution. When the $Ru(bpy)_3^{2+}$ ions was oxidized during the anodic sweep by CV. The close contact between $Ru(bpy)_3^{3+}$ excited ions and CdTe-QDs made energy transfer possible to strong excite the luminescence of QDs. The control experiments were performed in the presence and the absence of CdTe-QDs. It was observed that very weak ECL signals could be observed in the presence of only NFs, compared with that in the presence of CdTe-QDs itself and both CdTe-QDs and NFs. Thus, the competition of L-cysteine capped CdTe-QDs and NFs may created imperfections resonance energy transfer, and eventually led to the ECL quenching. The quenching effect of nitrofuran antibiotics on the anodic ECL of $Ru(bpy)_3^{2+}$ CdTe-QDs was found to be selective and concentration dependent and was observed to have a linear relationship over the concentration range $10\text{-}100\times10^{-6}$ M. The detection limits were found to be 0.40, 0.73 and 0.60 μM for furaltadone (FTD), furazolidone (FZD) and nitrofurantoin (NFT), respectively. In addition, the proposed ECL method was successfully applied to detect the total residuals of selected nitrofuran residues in animal feed samples with satisfactory results comparing with high performance liquid chromatography.

6.2 Recommendations for further work

The FI-CL and ECL techniques were successful developed for the determination of arsenic, cadmium in environmental samples and nitrofuran antibiotics in animal feed. These analytical methods are simple and inexpensive method and easy to use. These chemiluminescence detection methods and flow injection systems are environmental friendly for chemical analysis. In the term of economic point of view, the used of the modified instrument for treatment of heavy metals and antibiotics is not only reduce the cost for the imported instrument, but also support in quality monitoring of the exported agricultural products to the oversea countries.

In the case of arsenic, the reported method could be further developed by coupled with HPLC, for an on-line separation procedure to improve the performance of CL detection. The FI-CL analysis of cadmium could be developed or coupled with on-line preconcentration using microfluidic device to improve the detection performance and miniaturized the extraction system with minimal reagent and time consumption. Since ECL detection combines the simplicity and control of electrochemistry with the enhanced sensitivity of chemiluminescence. The proposed ECL result demonstrate the promise of ECL-based detection and could be further develop as paper microfluidic sensors. Moreover, ECL techniques may be further developed by coupled with HPLC, to improve the performance of this technique for the simultaneous analysis.

The proposed FI-CL and ECL method can be both equipped with a computer or timer to automatically control the measurement and the evaluate data. An auto sampler device can be used to obtain accurate and reproducible data. The inexpensive and simple FI-CL and ECL systems described in this thesis could be developed for on-line or portable field analyzers for the determination of certain species in environmental samples. The computing capability of such devices has increased remarkably in recent years and will no doubt continue to do so for the foreseeable future. It is clear that the FI-CL and ECL method is not only a valid analytical method but will continue to provide inexpensive and reliable analytical instruments that will grow in importance both in developed and developing countries in the foreseeable future. This would be able to help the Thai government to improve the economy of Thailand in the near further.

DEVELOPMENT OF MICRO/MESOFLUIDIC CHEMILUMINESCENCE TECHNIQUES USING FLOW BASED TECHNOLOGY FOR MONITORING SELECTED TRACE HEAVY METALS IN ENVIRONMENTAL SAMPLES

NARIN TAOKAENCHAN

DOCTOR OF PHILOSOPHY IN APPLIED CHEMISTRY

MAEJO UNIVERSITY

2014

DEVELOPMENT OF MICRO/MESOFLUIDIC CHEMILUMINESCENCE TECHNIQUES USING FLOW BASED TECHNOLOGY FOR MONITORING SELECTED TRACE HEAVY METALS IN ENVIRONMENTAL SAMPLES

NARIN TAOKAENCHAN

A THESIS SUBMITTED IN PARTIAL FULFILLMENT

OF THE REQUIREMENTS FOR THE DEGREE OF

DOCTOR OF PHILOSOPHY IN APPLIED CHEMISTRY

GRADUATE SCHOOL PROJECT

MAEJO UNIVERSITY

2014

BIBLIOGRAPHY

Adams, C., Y. Wang, K. Loftin and M. Meyer. 2002. Removal of antibiotics from surface and distilled water in conventional water treatment processes. **Journal of Environmental Engineering** 128(3): 253-260.

Adcock, J. L., P. S. Francis and N. W. Barnett. 2007. Acidic potassium permanganate as a chemiluminescence reagent—A review. **Analytica Chimica Acta** 601(1): 36-67.

Agency, U. E. P. 2013. **Arsenic in Drinking Water**. [Online]. Available http://water.epa.gov/lawsregs/rulesregs/sdwa/arsenic/index.cfm (12 April 2013).

Al-Swaidan, H. M. 1994. Microemulsion determination of lead and cadmium in saudi arabian petroleum products by inductively coupled plasma mass spectrometry (ICP/MS). **Science of The Total Environment** 145(1–2): 157-161.

Aly, F. A., S. A. Al-Tamimi and A. A. Alwarthan. 2000. Determination of flufenamic acid and mefenamic acid in pharmaceutical preparations and biological fluids using flow injection analysis with tris(2,2′-bipyridyl)ruthenium(II) chemiluminescence detection. **Analytica Chimica Acta** 416(1): 87-96.

Aly, F. A., N. A. Alarfaffj and A. A. Alwarthan. 1998. Permanganate-based chemiluminescence analysis of cefadroxil monohydrate in pharmaceutical samples and biological fluids using flow injection. **Talanta** 47(2): 471-478.

An-Na, T. and H. Yun-Fei. 2011. Determination of trace cadmium by flow injection on-line microcolumn preconcentration coupled with flame atomic absorption spectrometry using human hair as a sorbent. **Instrumentation Science and Technology** 39(1): 110-120.

Anastos, N., N. W. Barnett, B. J. Hindson, C. E. Lenehan and S. W. Lewis. 2004. Comparison of soluble manganese(IV) and acidic potassium permanganate chemiluminescence detection using flow injection and sequential injection analysis for the determination of ascorbic acid in Vitamin C tablets. **Talanta** 64(1): 130-134.

APHA AWWA. (2005). Standard Methods for Examination of Water and Wastewater. Washington, DC: American Public Health Association.

Ardsoongnearn, C., O. Boonbanlu, S. Kittijaruwattana and L. Suntornsuk. 2014. Liquid chromatography and ion trap mass spectrometry for simultaneous and multiclass analysis of antimicrobial residues in feed water. **Journal of Chromatography B** 945–946: 31-38.

Attiq-Ur-Rehman, M. Yaqoob, A. Waseem and A. Nabi. 2008. Determination of arsenic(V) in freshwaters by flow injection with luminol chemiluminescence detection. **International Journal of Environmental Analytical Chemistry** 88(9): 603-612.

Barbosa, J., S. Moura, R. Barbosa, F. Ramos and M. I. N. d. Silveira. 2007. Determination of nitrofurans in animal feeds by liquid chromatography-UV photodiode array detection and liquid chromatography-ionspray tandem mass spectrometry. **Analytica Chimica Acta** 586(1–2): 359-365.

Barnett, N. and S. Lewis. 1996. Tripping the light fantastic. **Analysis europa**: 28-33.

Barra, C. M., M. L. Cervera, M. de la Guardia and R. E. Santelli. 2000. Atomic fluorescence determination of inorganic arsenic in soils after microwave-assisted distillation. **Analytica Chimica Acta** 407(1–2): 155-163.

Beauchemin, D., K. W. M. Siu, J. W. McLaren and S. S. Berman. 1989. Determination of arsenic species by high-performance liquid chromatography-inductively coupled plasma mass spectrometry. **Journal of Analytical Atomic Spectrometry** 4(3): 285-289.

Behari, J. R. and R. Prakash. 2006. Determination of total arsenic content in water by atomic absorption spectroscopy (AAS) using vapour generation assembly (VGA). **Chemosphere** 63(1): 17-21.

Benito-Pena, E., A. I. Partal-Rodera, M. E. Leon-Gonzalez and M. C. Moreno-Bondi. 2006. Evaluation of mixed mode solid phase extraction cartridges for the preconcentration of beta-lactam antibiotics in wastewater using liquid chromatography with UV-DAD detection. **Analytica Chimica Acta** 556(2): 415-422.

Blazewicz, A., W. Dolliver, S. Sivsammye, A. Deol, R. Randhawa, G. Orlicz-Szczesna and R. Blazewicz. 2010. Determination of cadmium, cobalt, copper, iron, manganese, and zinc in thyroid glands of patients with diagnosed nodular goitre using ion chromatography. **Journal of Chromatography B** 878(1): 34-38.

Broomhead, J. A., C. G. Young and P. Hood. 2007. **Tris(2,2′-Bipyridine)Ruthenium(II) Dichloride Hexahydrate**. John Wiley & Sons, Inc. pp. 338-340.

Camel, V. 2003. Solid phase extraction of trace elements. **Spectrochimica Acta Part B: Atomic Spectroscopy** 58(7): 1177-1233.

Campillo, N., P. Vinas, I. Lopez-Garcıia and M. Hernandez-Cordoba. 1999. Rapid determination of lead and cadmium in biological fluids by electrothermal atomic absorption spectrometry using Zeeman correction. **Analytica Chimica Acta** 390(1–3): 207-215.

Cancela, S. and M.C. Yebra. 2006. Flow-injection flame atomic absorption spectrometric determination of trace amounts of cadmium in solid and semisolid milk products coupling a continuous ultrasound-assisted extraction system with the online preconcentration on a chelating aminomethylphosphoric acid resin. **Journal of AOAC International** 86(1): 185-191.

Carbonell, V., A. Salvador and M. Guardia. 1992. Literature survey of the on-line preconcentration in flow-injection atomic spectrometric analysis. **Fresenius' Journal of Analytical Chemistry** 342(7): 529-537.

Cardellicchio, N., S. Cavalli and J. M. Riviello. 1993. Determination of cadmium and lead at μg/1 levels in aqueous matrices by chelation ion chromatography. **Journal of Chromatography A** 640(1–2): 207-216.

Castro, G. R., V. M. Cristante, C. C. F. Padilha, S. M. A. Jorge, A. O. Florentino, A. G. S. Prado and P. M. Padilha. 2008. Determination of Cd(II), Cu(II) and Ni(II) in aqueous samples by ICP-OES after on-line preconcentration in column packed with silica modified with 2-aminothiazole. **Microchimica Acta** 160(1-2): 203-209.

Cava-Montesinos, P., M. L. Cervera, A. Pastor and M. de la Guardia. 2003. Determination of arsenic and antimony in milk by hydride generation atomic fluorescence spectrometry. **Talanta** 60(4): 787-799.

Changqing, Z., W. Lun, L. Yongxin, C. Maohua and W. Pengsan. 1999. Chemiluminescent system of luminol-8-hydroxy-5-quinolinesulfonic acid-cadmium(II)-hydrogen peroxide. **Chinese Journal of Analytical Chemistry** 27(6): 640-643.

Chen, H., L. Lin, H. Li and J.-M. Lin. 2014. Quantum dots-enhanced chemiluminescence: Mechanism and application. **Coordination Chemistry Reviews** 263–264: 86-100.

Chu, L., G. Zou and X. Zhang. 2012. Electrogenerated chemiluminescence sensor for formaldehyde based on $Ru(bpy)_3^{2+}$-doped silica nanoparticles modified Au electrode. **Materials Science and Engineering: C** 32(8): 2169-2174.

Chumanee, S., S. Sutthivaiyakit and P. Sutthivaiyakit. 2009. New reagent for trace determination of protein-bound metabolites of nitrofurans in shrimp using liquid chromatography with diode array detector. **Journal of Agricultural and Food Chemistry** 57(5): 1752-1759.

Colbert, D., K. S. Johnson and K. H. Coale. 1998. Determination of cadmium in seawater using automated on-line preconcentration and direct injection graphite furnace atomic absorption spectrometry. **Analytica Chimica Acta** 377(2–3): 255-262.

Cornell university genetically engineered machines. 2009. **Cadmium Contamination**. [Online]. Available http://2009.igem.org/Team:Cornell/Project/Background.

Costa, A. C. S., L. Lopes, M. d. G. A. Korn and J. G. Portela. 2002. Separation and pre-concentration of cadmium, copper, lead, nickel and zinc by solid-liquid extraction of their cocrystallized naphthalene dithizone chelate in saline matrices. **Journal of the Brazilian Chemical Society** 13: 674-678.

Cretich, M., V. Sedini, F. Damin, G. Di Carlo, C. Oldani and M. Chiari. 2008. Functionalization of poly(dimethylsiloxane) by chemisorption of copolymers: DNA microarrays for pathogen detection. **Sensors and Actuators B: Chemical** 132(1): 258-264.

Czugala, M., C. Fay, N. E. O'Connor, B. Corcoran, F. Benito-Lopez and D. Diamond. 2013. Portable integrated microfluidic analytical platform for the monitoring and detection of nitrite. **Talanta** 116: 997-1004.

Damin, I. C. F., M. M. Silva, M. G. R. Vale and B. Welz. 2007. Feasibility of using direct determination of cadmium and lead in fresh meat by electrothermal atomic absorption spectrometry for screening purposes. **Spectrochimica Acta Part B: Atomic Spectroscopy** 62(9): 1037-1045.

Daorattanachai, P., F. Unob and A. Imyim. 2005. Multi-element preconcentration of heavy metal ions from aqueous solution by APDC impregnated activated carbon. **Talanta** 67(1): 59-64.

Date, Y., S. Terakado, K. Sasaki, A. Aota, N. Matsumoto, H. Shiku, K. Ino, Y. Watanabe, T. Matsue and N. Ohmura. 2012. Microfluidic heavy metal immunoassay based on absorbance measurement. **Biosensors and Bioelectronics** 33(1): 106-112.

Degroodt, J. M., B. W. De Bukanski, J. De Groof, H. Beernaert and S. Srebrnk. 1992. Chloramphenicol and nitrofuran residue analysis by HPLC and photodiode array detection in meat and fish. **Journal of Liquid Chromatography** 15(13): 2355-2371.

Delaney, J. L., E. H. Doeven, A. J. Harsant and C. F. Hogan. 2013. Reprint of: Use of a mobile phone for potentiostatic control with low cost paper-based microfluidic sensors. **Analytica Chimica Acta** 803: 123-127.

Dmitryenko, L. V. and D. K. Hale. 1965. The sorption of oxytetracycline and chlorotetracycline by sulphonated polystyrene resins. **Journal of the Chemical Society** 1040: 5570-5578.

Dodeigne, C., L. Thunus and R. Lejeune. 2000. Chemiluminescence as diagnostic tool. A review. **Talanta** 51(3): 415-439.

Du, J., L. Hao, Y. Li and J. Lu. 2007. Flow injection chemiluminescence determination of nitrofurazone in pharmaceutical preparations and biological fluids based on oxidation by singlet oxygen generated in N-bromosuccinimide–hydrogen peroxide reaction. **Analytica Chimica Acta** 582(1): 98-102.

Duffy, D. C., J. C. McDonald, O. J. A. Schueller and G. M. Whitesides. 1998. Rapid prototyping of microfluidic systems in poly(dimethylsiloxane). **Analytical Chemistry** 70(23): 4974-4984.

Eteshola, E. and D. Leckband. 2001. Development and characterization of an ELISA assay in PDMS microfluidic channels. **Sensors and Actuators B: Chemical** 72(2): 129-133.

Fan, F., H. Shen, G. Zhang, X. Jiang and X. Kang. 2014. Chemiluminescence immunoassay based on microfluidic chips for α-fetoprotein. **Clinica Chimica Acta** 431: 113-117.

Fang, Z., M. Sperling and B. Welz. 1990. Flow injection on-line sorbent extraction pre-concentration for graphite furnace atomic absorption spectrometry. **Journal of Analytical Atomic Spectrometry** 5(7): 639-646.

Fang, Z., S. Xu, X. Wang and S. Zhang. 1986. Combination of flow-injection techniques with atomic spectrometry in agricultural and environmental analysis. **Analytica Chimica Acta** 179: 325-340.

Fleming, D. 2014. **The Chemiluminescence of Luminol**. [Online]. Available http://www.chm.bris.ac.uk/webprojects2002/fleming/mechanism.htm.

Fletcher, P., K. N. Andrew, A. C. Calokerinos, S. Forbes and P. J. Worsfold. 2001. Analytical applications of flow injection with chemiluminescence detection--a review. **Luminescence** 16(1): 1-23.

Fujiwara, T., K. Kurahashi, T. Kumamaru and H. Sakai. 1996. Luminol Chemiluminescence with Heteropoly Acids and its Application to the Determination of Arsenate, Germanate, Phosphate and Silicate by Ion Chromatography. **Applied Organometallic Chemistry** 10(9): 675-681.

Gaillard, F., Y.-E. Sung and A. J. Bard. 1999. Hot electron generation in aqueous solution at oxide-covered tantalum electrodes reduction of methylpyridinium and electrogenerated chemiluminescence of $Ru(bpy)_3^{2+}$. **The Journal of Physical Chemistry B** 103(4): 667-674.

Gao, Y., F. Y. H. Lin, G. Hu, P. M. Sherman and D. Li. 2005. Development of a novel electrokinetically driven microfluidic immunoassay for the detection of Helicobacter pylori. **Analytica Chimica Acta** 543(1–2): 109-116.

Gao, Z.-X., H.-F. Li, J. Liu and J.-M. Lin. 2008. A simple microfluidic chlorine gas sensor based on gas–liquid chemiluminescence of luminol-chlorine system. **Analytica Chimica Acta** 622(1–2): 143-149.

Garlaschelli, F., G. Alberti, N. Fiol and I. Villaescusa. Application of Anodic Stripping Voltammetry to assess sorption performance of an industrial waste entrapped in alginate beads to remove As(V). **Arabian Journal of Chemistry**.

Gerardi, R. D., N. W. Barnett and S. W. Lewis. 1999. Analytical applications of tris(2,2′-bipyridyl)ruthenium(III) as a chemiluminescent reagent. **Analytica Chimica Acta** 378(1–3): 1-41.

Giokas, D. L., A. G. Vlessidis and N. P. Evmiridis. 2007. On-line selective detection of antioxidants free-radical scavenging activity based on Co(II)/EDTA-induced luminol chemiluminescence by flow injection analysis. **Analytica Chimica Acta** 589(1): 59-65.

Giri, B. and D. Dutta. 2014. Improvement in the sensitivity of microfluidic ELISA through field amplified stacking of the enzyme reaction product. **Analytica Chimica Acta** 810(0): 32-38.

Guo, C., H. Zeng, X. Ding, D. He, J. Li, R. Yang and L. Qu. 2013. Enhanced chemiluminescence of the luminol-$K_3Fe(CN)_6$ system by ZnSe quantum dots and its application. **Journal of Luminescence** 134: 888-892.

Hafez, M. A. H., I. M. M. Kenawy, M. A. Akl and R. R. Lashein. 2001. Preconcentration and separation of total mercury in environmental samples using chemically modified chloromethylated polystyrene-PAN (ion-exchanger) and its determination by cold vapour atomic absorption spectrometry. **Talanta** 53(4): 749-760.

Haslag, C. S. and M. M. Richter. 2012. Electrogenerated chemiluminescence quenching of $Ru(bpy)_3^{2+}$(bpy2,2′-bipyridine) in the presence of acetaminophen, salicylic acid and their metabolites. **Journal of Luminescence** 132(3): 636-640.

Heitkemper, D. T., N. P. Vela, K. R. Stewart and C. S. Westphal. 2001. Determination of total and speciated arsenic in rice by ion chromatography and inductively coupled plasma mass spectrometry. **Journal of Analytical Atomic Spectrometry** 16(4): 299-306.

Hueber, D. M. and J. D. Winefordner. 1995. A flowing electrolytic hydride generator for continuous sample introduction in atomic spectrometry. **Analytica Chimica Acta** 316(2): 129-144.

Husakova, L., T. Cernohorsky, J. Sramkova and L. Vavrusova. 2007. Direct determination of arsenic in beer by electrothermal atomic absorption spectrometry with deuterium background correction (D2-ET-AAS). **Food Chemistry** 105(1): 286-292.

Hutton, E. A., J. T. van Elteren, B. Ogorevc and M. R. Smyth. 2004. Validation of bismuth film electrode for determination of cobalt and cadmium in soil extracts using ICP–MS. **Talanta** 63(4): 849-855.

IARC Monographs on the Evaluation of Carcinogenic Risks to Humans. (2012). **Cadmium and Cadmium Compounds** (Publication.: http://monographs.iarc.fr/ENG/Monographs/vol100C/mono100C-8.pdf

Idowu, M., J. Y. Chen and T. Nyokong. 2008. Photoinduced energy transfer between water-soluble CdTe quantum dots and aluminium tetrasulfonated phthalocyanine. **New Journal of Chemistry** 32(2): 290-296.

Isacsson, U. and G. Wettermark. 1974. Chemiluminescence in analytical chemistry. **Analytica Chimica Acta** 68(2): 339-362.

Ivanova, E., W. Van Mol and F. Adams. 1998. Electrothermal atomic absorption spectrometric determination of cadmium and lead in blood using flow injection on-line sorption preconcentration in a knotted reactor. **Spectrochimica Acta Part B: Atomic Spectroscopy** 53(6–8): 1041-1048.

Javanmard, M. and R. W. Davis. 2011. A microfluidic platform for electrical detection of DNA hybridization. **Sensors and Actuators B: Chemical** 154(1): 22-27.

Jester, E. L. E., A. Abraham, Y. Wang, K. R. El Said and S. M. Plakas. 2014. Performance evaluation of commercial ELISA kits for screening of furazolidone and furaltadone residues in fish. **Food Chemistry** 145: 593-598.

Jing, G., A. Polaczyk, D. B. Oerther and I. Papautsky. 2007. Development of a microfluidic biosensor for detection of environmental mycobacteria. **Sensors and Actuators B: Chemical** 123(1): 614-621.

Jitmanee, K., M. Oshima and S. Motomizu. 2005. Speciation of arsenic(III) and arsenic(V) by inductively coupled plasma-atomic emission spectrometry coupled with preconcentration system. **Talanta** 66(3): 529-533.

Jurado, J. M., M. J. Martín, F. Pablos, A. Moreda-Piñeiro and P. Bermejo-Barrera. 2007. Direct determination of copper, lead and cadmium in aniseed spirits by electrothermal atomic absorption spectrometry. **Food Chemistry** 101(3): 1296-1304.

Kamruzzaman, M., A.-M. Alam, K. M. Kim, S. H. Lee, Y. H. Kim, G.-M. Kim and T. D. Dang. 2012. Microfluidic chip based chemiluminescence detection of L-phenylalanine in pharmaceutical and soft drinks. **Food Chemistry** 135(1): 57-62.

Kanazawa. 2014. **Itai-itai desease**. [Online]. Available http://www.kanazawa-med.ac.jp/~pubhealt/cadmium2/itaiitai-e/itai02.html.

Kang, J., X. Li, J. Geng, L. Han, J. Tang, Y. Jin and Y. Zhang. 2012. Determination of hyperin in seed of Cuscuta chinensis Lam. by enhanced chemiluminescence of CdTe quantum dots on calcein/$K_3Fe(CN)_6$ system. **Food Chemistry** 134(4): 2383-2388.

Kang, J. H. and J.-K. Park. 2005. Development of a microplate reader compatible microfluidic device for enzyme assay. **Sensors and Actuators B: Chemical** 107(2): 980-985.

Kankare, J., K. Fäldén, S. Kulmala and K. Haapakka. 1992. Cathodically induced time-resolved lanthanide(III) electroluminescence at stationary aluminium disc electrodes. **Analytica Chimica Acta** 256(1): 17-28.

Karami, H., M. F. Mousavi, Y. Yamini and M. Shamsipur. 2004. On-line preconcentration and simultaneous determination of heavy metal ions by inductively coupled plasma-atomic emission spectrometry. **Analytica Chimica Acta** 509(1): 89-94.

Karuwan, C., K. Sukthang, A. Wisitsoraat, D. Phokharatkul, V. Patthanasettakul, W. Wechsatol and A. Tuantranont. 2011. Electrochemical detection on electrowetting-on-dielectric digital microfluidic chip. **Talanta** 84(5): 1384-1389.

Kee, J. S., D. P. Poenar, P. Neuzil and L. Yobas. 2008. Monolithic integration of poly(dimethylsiloxane) waveguides and microfluidics for on-chip absorbance measurements. **Sensors and Actuators B: Chemical** 134(2): 532-538.

Keller, N. S., A. Stefánsson and B. Sigfússon. 2014. Determination of arsenic speciation in sulfidic waters by ion chromatography hydride-generation atomic fluorescence spectrometry (IC-HG-AFS). **Talanta** 128: 466-472.

Khorshid, A. F. and Y. M. Issa. 2014. Modified carbon paste sensor for the potentiometric determination of neostigmine bromide in pharmaceutical formulations, human plasma and urine. **Biosensors and Bioelectronics** 51: 143-149.

Kim, J. A., J. Y. Lee, S. Seong, S. H. Cha, S. H. Lee, J. J. Kim and T. H. Park. 2006. Fabrication and characterization of a PDMS–glass hybrid continuous-flow PCR chip. **Biochemical Engineering Journal** 29(1–2): 91-97.

Kim, K.-W., P. Chanpiwat, H. T. Hanh, K. Phan and S. Sthiannopkao. 2011. Arsenic geochemistry of groundwater in Southeast Asia. **Fronters of Medicine** 5(4): 420-433.

Kim, M., W. Choi, H. Lim and S. Yang. 2013. Integrated microfluidic-based sensor module for real-time measurement of temperature, conductivity, and salinity to monitor reverse osmosis. **Desalination** 317: 166-174.

Kim, Y. J., J. E. Jones, H. Li, H. Yampara-Iquise, G. Zheng, C. A. Carson, M. Cooperstock, M. Sherman and Q. Yu. 2013. Three-dimensional (3-D) microfluidic-channel-based DNA biosensor for ultra-sensitive electrochemical detection. **Journal of Electroanalytical Chemistry** 702: 72-78.

Koh, J., Y. Kwon and Y.-N. Pak. 2005. Separation and sensitive determination of arsenic species (As^{3+}/As^{5+}) using the yeast-immobilized column and hydride generation in ICP–AES. **Microchemical Journal** 80(2): 195-199.

Koo, J., J. Ko, H. B. Lim and J. M. Song. 2011. Surface modified microarray chip and laser induced fluorescence microscopy to detect DNA cleavage. **Microchemical Journal** 99(2): 523-529.

Kulmala, S., T. Ala-Kleme, L. Väre, M. Helin and T. Lehtinen. 1999. Hot electron-induced electrogenerated luminescence of Tl(I) at disposable oxide-covered aluminum electrodes. **Analytica Chimica Acta** 398(1): 41-47.

Kumagai, H., Y. Inoue, T. Yokoyama, T. M. Suzuki and T. Suzuki. 1998. Chromatographic Selectivity of Rare Earth Elements on Iminodiacetate-Type Chelating Resins Having Spacer Arms of Different Lengths: Importance of Steric Flexibility of Functional Group in a Polymer Chelating Resin. **Analytical Chemistry** 70(19): 4070-4073.

Kuncova-Kallio, J. and P. J. Kallio. (2006). PDMS and its Suitability for Analytical Microfluidic Devices. **in EMBS Annual International Conference**, New York City, USA.

Kurtz, K. S. and S. R. Crouch. 1991. Design and optimization of a flow-injection system for enzymatic determination of galactose. **Analytica Chimica Acta** 254(1–2): 201-208.

Kwansiririkul, K., F. S. Singharajwarapan, R. Mackay, T. Ramingwong and P. Wongpornchai. 2004. Vulnerability asswaament of groundwater resources in the Lampang basin of northern Thailand . **Journal of Environmental Hydrology** 12: 1.

Lara, R., R. Wuilloud, J. Salonia, R. Olsina and L. Martinez. 2001. Determination of low cadmium concentrations in wine by on-line preconcentration in a knotted reactor coupled to an inductively coupled plasma optical emission spectrometer with ultrasonic nebulization. **Fresenius' Journal of Analytical Chemistry** 371(7): 989-993.

Lemos, V. A. and P. X. Baliza. 2005. Amberlite XAD-2 functionalized with 2-aminothiophenol as a new sorbent for on-line preconcentration of cadmium and copper. **Talanta** 67(3): 564-570.

Lemos, V. A., R. E. Santelli, M. S. de Carvalho and S. L. C. Ferreira. 2000. Application of polyurethane foam loaded with BTAC in an on-line preconcentration system: cadmium determination by FAAS. **Spectrochimica Acta Part B: Atomic Spectroscopy** 55(9): 1497-1502.

Li, B., D. Wang, J. Lv and Z. Zhang. 2006. Chemometrics-assisted simultaneous determination of cobalt(II) and chromium(III) with flow-injection chemiluminescence method. **Spectrochimica Acta Part A: Molecular and Biomolecular Spectroscopy** 65(1): 67-72.

Li, J., J. Liu, H.-C. Zhang, H. Li and J.-P. Wang. 2010. Broad specificity indirect competitive immunoassay for determination of nitrofurans in animal feeds. **Analytica Chimica Acta** 678(1): 1-6.

Li, M. and S. Hak Lee. 2005. Determination of As(III) and As(V) ions by chemiluminescence method. **Microchemical Journal** 80(2): 237-240.

Li, S., S. Cai, W. Hu, H. Chen and H. Liu. 2009. Ionic liquid-based ultrasound-assisted dispersive liquid–liquid microextraction combined with electrothermal atomic absorption spectrometry for a sensitive determination of cadmium in water samples. **Spectrochimica Acta Part B: Atomic Spectroscopy** 64(7): 666-671.

Li, S., J. C. Day, J. J. Park, C. P. Cadou and R. Ghodssi. 2007. A fast-response microfluidic gas concentrating device for environmental sensing. **Sensors and Actuators A: Physical** 136(1): 69-79.

Li, X., J. Hu and H. Han. 2009. Flow-injection Post-chemiluminescence Determination of Furazolidone in Animal Feeds. **American Journal of Biomedical Sciences** 1(3): 260-266.

Li, Y.-S., Y.-D. Du, T.-M. Chen and X.-F. Gao. 2010. A novel immobilization multienzyme glucose fluorescence capillary biosensor. **Biosensors and Bioelectronics** 25(6): 1382-1388.

Liu, W., J. Kou, X. Jiang, Z. Zhang and H. Qi. 2012. Determination of nitrofurans in feeds based on silver nanoparticle-catalyzed chemiluminescence. **Journal of Luminescence** 132(4): 1048-1054.

Liu, W., Z. Zhang and Z. Liu. 2007. Determination of β-lactam antibiotics in milk using micro-flow chemiluminescence system with on-line solid phase extraction. **Analytica Chimica Acta** 592(2): 187-192.

Lomonte, C., M. Currell, R. J. S. Morrison, I. D. McKelvie and S. D. Kolev. 2007. Sensitive and ultra-fast determination of arsenic(III) by gas-diffusion flow injection analysis with chemiluminescence detection. **Analytica Chimica Acta** 583(1): 72-77.

Lv, Y., Z. Zhang and F. Chen. 2003. Chemiluminescence microfluidic system sensor on a chip for determination of glucose in human serum with immobilized reagents. **Talanta** 59(3): 571-576.

M. Featherstone, A., E. C. V. Butler, B. V. O'Grady and P. Michel. 1998. Determination of arsenic species in sea-water by hydride generation atomic fluorescence spectroscopy. **Journal of Analytical Atomic Spectrometry** 13(12): 1355-1360.

Macedo, S. M., R. M. de Jesus, K. S. Garcia, V. Hatje, A. F. de S. Queiroz and S. L. C. Ferreira. 2009. Determination of total arsenic and arsenic (III) in phosphate fertilizers and phosphate rocks by HG-AAS after multivariate optimization based on Box-Behnken design. **Talanta** 80(2): 974-979.

Marchisio, P. F., A. Sales, S. Cerutti, E. Marchevsky and L. D. Martinez. 2005. On line preconcentration of cadmium in commercial tea samples using polyurethane foam as filter associated with ultrasonic nebulization inductively coupled plasma optical emission spectrometric detection. **Instrumentation Science and Technology** 33(4): 449-459.

Marcos, P., M. P. Lué-Merú, R. Ricardo, G. Máximo, V. Maribel, B. J. Luis and B. Marcela. 2004. Pungency evaluation of onion cultivars from the Venezuelan West-Center region by flow injection analysis–UV–visible spectroscopy pyruvate determination. **Talanta** 64(5): 1299-1303.

Marle, L. and G. M. Greenway. 2005. Microfluidic devices for environmental monitoring. **TrAC Trends in Analytical Chemistry** 24(9): 795-802.

Masqué, N., R. M. Marcé and F. Borrull. 1998. New polymeric and other types of sorbents for solid-phase extraction of polar organic micropollutants from environmental water. **TrAC Trends in Analytical Chemistry** 17(6): 384-394.

Matusiewicz, H. and M. Slachcinski. 2012. Development of a new hybrid technique for inorganic arsenic speciation analysis by microchip capillary electrophoresis coupled with hydride generation microwave induced plasma spectrometry. **Microchemical Journal** 102(0): 61-67.

MEMS and Nanotechnology Exchange. 2014. **What is MEMS Technology**. [Online]. Available https://www.mems-exchange.org/MEMS/what-is.html.

Milstein, L. S., A. Essader, E. D. Pellizzari, R. A. Fernando and O. Akinbo. 2002. Selection of a suitable mobile phase for the speciation of four arsenic compounds in drinking water samples using ion-exchange chromatography coupled to inductively coupled plasma mass spectrometry. **Environment International** 28(4): 277-283.

Minamisawa, H., R. Okunugi, M. Minamisawa, S. Tanaka, K. Saitoh, N. Arai and M. Shibukawa. 2006. Preconcentration and determination of cadmium by GFAAS after solid-phase extraction with synthetic zeolite. **Analytical Sciences** 22(5): 709-713.

Mntungwa, N., V. S. Rajasekhar Pullabhotla and N. Revaprasadu. 2013. Facile synthesis of cysteine and triethanolamine capped CdTe nanoparticles. **Colloids and Surfaces B: Biointerfaces** 101: 450-456.

Moreira, C. M., F. A. Duarte, J. Lebherz, D. Pozebon, E. M. M. Flores and V. L. Dressler. 2011. Arsenic speciation in white wine by LC–ICP–MS. **Food Chemistry** 126(3): 1406-1411.

Morita, M., T. Uehiro and K. Fuwa. 1981. Determination of arsenic compounds in biological samples by liquid chromatography with inductively coupled argon plasma-atomic emission spectrometric detection. **Analytical Chemistry** 53(12): 1806-1808.

Mottier, P., S.-P. Khong, E. Gremaud, J. Richoz, T. Delatour, T. Goldmann and P. A. Guy. 2005. Quantitative determination of four nitrofuran metabolites in meat by isotope dilution liquid chromatography–electrospray ionisation–tandem mass spectrometry. **Journal of Chromatography A** 1067(1–2): 85-91.

Ng, J. M. K., I. Gitlin, A. D. Stroock and G. M. Whitesides. 2002. Components for integrated poly(dimethylsiloxane) microfluidic systems. **Electrophoresis** 23(20): 3461-3473.

Nguyen, N.-T. and S. T. Wereley. 2006. **Fundamentals and Applications of Microfluidics**. 2 ed.: Artech House, Incorporated.

Nishijo, M., Y. Suwazono, W. Ruangyuttikarn, K. Nambunmee, W. Swaddiwudhipong, K. Nogawa and H. Nakagawa. 2014. Risk assessment for Thai population: benchmark dose of urinary and blood cadmium levels for renal effects by hybrid approach of inhabitants living in polluted and non-polluted areas in Thailand. **BMC Public Health** 14(1): 702.

O'Sullivan, J. E., R. J. Watson and E. C. V. Butler. 2013. An ICP-MS procedure to determine Cd, Co, Cu, Ni, Pb and Zn in oceanic waters using in-line flow-injection with solid-phase extraction for preconcentration. **Talanta** 115: 999-1010.

Orecchio, S., D. Amorello, M. Raso, S. Barreca, C. Lino and F. Di Gaudio. 2014. Determination of trace elements in gluten-free food for celiac people by ICP-MS. **Microchemical Journal** 116: 163-172.

Pais, T. F. M., S. S. M. P. Vidigal, I. V. Tóth and A. O. S. S. Rangel. 2013. Sequential injection system for the enzymatic determination of ethanol in alcoholic beverages with in-line dilution. **Food Control** 30(2): 616-620.

Palilis, L. P. and A. C. Calokerinos. 2000. Analytical applications of chemiluminogenic reactions. **Analytica Chimica Acta** 413(1–2): 175-186.

Panigati, M., M. Piccone, G. D'Alfonso, M. Orioli and M. Carini. 2002. Determination of lead and cadmium in titanium dioxide by differential pulse anodic stripping voltammetry. **Talanta** 58(3): 481-488.

Park, J.-H., Y. S. Song, J.-G. Ha, Y.-K. Kim, S.-K. Lee and S. J. Bai. 2013. Electrochemical sensing of high density photosynthetic cells using a microfluidic chip. **Sensors and Actuators B: Chemical** 188: 1300-1305.

Paull, B., E. Twohill and W. Bashir. 2000. Determination of trace cadmium in environmental water samples using ion-interaction reversed-phase liquid chromatography with fluorescence detection. **Journal of Chromatography A** 877(1–2): 123-132.

Pittet, P., G.-N. Lu, J.-M. Galvan, R. Ferrigno, K. Stephan, L. J. Blum and B. Leca-Bouvier. 2008. A novel low-cost approach of implementing electrochemiluminescence detection for microfluidic analytical systems. **Materials Science and Engineering: C** 28(5–6): 891-895.

Pohlmann, A., W. W. Stamm, H. Kusakabe and M.-R. Kula. 1990. Enzymatic determination of l-lysine by flow-injection techniques. **Analytica Chimica Acta** 235: 329-335.

Prabakar, S. J. R., C. Sakthivel and S. S. Narayanan. 2011. Hg(II) immobilized MWCNT graphite electrode for the anodic stripping voltammetric determination of lead and cadmium. **Talanta** 85(1): 290-297.

Prakash, S., T. Chakrabarty, A. K. Singh and V. K. Shahi. 2013. Polymer thin films embedded with metal nanoparticles for electrochemical biosensors applications. **Biosensors and Bioelectronics** 41: 43-53.

Purohit, R. and S. Devi. 1997. Determination of nanogram levels of zirconium by chelating ion exchange and on-line preconcentration in flow injection UV—visible spectrophotometry. **Talanta** 44(3): 319-326.

Ranjit Prakash, A., S. Adamia, V. Sieben, P. Pilarski, L. M. Pilarski and C. J. Backhouse. 2006. Small volume PCR in PDMS biochips with integrated fluid control and vapour barrier. **Sensors and Actuators B: Chemical** 113(1): 398-409.

Richter, M. M. 2004. Electrochemiluminescence (ECL). **Chemical Reviews** 104(6): 3003-3036.

Roundhill, D. M. 1994. **Plenum**. New York.

Rubinstein, I. and A. J. Bard. 1981. Electrogenerated chemiluminescence. 37. Aqueous ecl systems based on tris(2,2'-bipyridine)ruthenium(II) and oxalate or organic acids. **Journal of the American Chemical Society** 103(3): 512-516.

Rutyna, I. and M. Korolczuk. 2014. Determination of lead and cadmium by anodic stripping voltammetry at bismuth film electrodes following double deposition and stripping steps. **Sensors and Actuators B: Chemical** 204: 136-141.

Ruzicka, J. and E. H. Hansen. 1975. Flow injection analyses: Part I. A new concept of fast continuous flow analysis. **Analytica Chimica Acta** 78(1): 145-157.

Salinas-Vargas, M. E. and M. P. Cañizares-Macías. 2014. On-line solid–phase extraction using a C18 minicolumn coupled to a flow injection system for determination of caffeine in green and roasted coffee beans. **Food Chemistry** 147: 182-188.

Santhanam, K. S. V. and A. J. Bard. 1965. Chemiluminescence of electrogenerated 9,10-diphenylanthracene anion radical. **Journal of the American Chemical Society** 87(1): 139-140.

Satienperakul, S., P. Phongdong and S. Liawruangrath. 2010. Pervaporation flow injection analysis for the determination of sulphite in food samples utilising potassium permanganate–rhodamine B chemiluminescence detection. **Food Chemistry** 121(3): 893-898.

Schöning, M. J., M. Jacobs, A. Muck, D. T. Knobbe, J. Wang, M. Chatrathi and S. Spillmann. 2005. Amperometric PDMS/glass capillary electrophoresis-based biosensor microchip for catechol and dopamine detection. **Sensors and Actuators B: Chemical** 108(1–2): 688-694.

Sheng, L.-Q., M.-M. Chen, S.-S. Chen, N.-N. Du, Z.-D. Liu, C.-F. Song and R. Qiao. 2013. High-performance liquid chromatography with fluorescence detection for the determination of nitrofuran metabolites in pork muscle. **Food Additives and Contaminants: Part A**: 1-9.

Sheppard, B. S., D. T. Heitkemper and C. M. Gaston. 1994. Microwave digestion for the determination of arsenic, cadmium and lead in seafood products by inductively coupled plasma atomic emission and mass spectrometry. **Analyst** 119(8): 1683-1686.

Som-Aum, W., H. Li, J. Liu and J. M. Lin. 2008. Determination of arsenate by sorption pre-concentration on polystyrene beads packed in a microfluidic device with chemiluminescence detection. **Analyst** 133(9): 1169-1175.

Sukreeyapongse, O., C. Tepwituksakit and N. Notesiri. Arsenic in soil, water and plant at contaminated sites and in agricultural soil of Thailand (Publication.: http://www.niaes.affrc.go.jp/marco/marco2009/english/program/W1-14-2_Sukreeyapongse_Orathai.pdf

Sung, Y.-E., F. Gaillard and A. J. Bard. 1998. Demonstration of Electrochemical Generation of Solution-Phase Hot Electrons at Oxide-Covered Tantalum Electrodes by Direct Electrogenerated Chemiluminescence. **The Journal of Physical Chemistry B** 102(49): 9797-9805.

Tanikkul, S., J. Jakmunee, S. Lapanantnoppakhun, M. Rayanakorn, P. Sooksamiti, R. E. Synovec, G. D. Christian and K. Grudpan. 2004. Flow injection in-valve-mini-column pretreatment combined with ion chromatography for cadmium, lead and zinc determination. **Talanta** 64(5): 1241-1246.

Taokaenchan, N., T. Tanin, P. Pookmanee, S. Satienperakul. 2012. Microfluidic chemiluminescence device for arsenic(III) determination in Thai traditional herbs. **in Paccon 2012**, Chiang Mai , Thailand.

Thongsrisomboon, P., B. Liawruangrath, S. Liawruangrath and S. Satienperakul. 2010. Determination of nitrofurans residues in animal feeds by flow injection chemiluminescence procedure. **Food Chemistry** 123(3): 834-839.

Tokel, N. E. and A. J. Bard. 1972. Electrogenerated chemiluminescence. IX. Electrochemistry and emission from systems containing tris(2,2'-bipyridine)ruthenium(II) dichloride. **Journal of the American Chemical Society** 94(8): 2862-2863.

Tokman, N. and S. Akman. 2004. Determination of bismuth and cadmium after solid-phase extraction with chromosorb-107 in a syringe. **Analytica Chimica Acta** 519(1): 87-91.

Townshend, A. 1990. Solution chemiluminescence-some recent analytical developments. Plenary lecture. **Analyst** 115(5): 495-500.

Trinh, K. T. L., W. Wu and N. Y. Lee. 2014. Planar poly(dimethylsiloxane) (PDMS)–glass hybrid microdevice for a flow-through polymerase chain reaction (PCR) employing a single heater assisted by an intermediate metal alloy layer for temperature gradient formation. **Sensors and Actuators B: Chemical** 190: 177-184.

Tyson, J. F. 1988. Atomic spectrometry and flow injection analysis: a synergic combination. **Analytica Chimica Acta** 214: 57-75.

Ueda, T., K. Wada and M. Hojo. 2001. Voltammetric and Raman spectroscopic study on the formation of Keggin-type V(V)-substituted molybdoarsenate complexes in aqueous and aqueous-organic solution. **Polyhedron** 20(1–2): 83-89.

United States Environmemtal Protection Agency. 2009. **Drinking Water Contaminants**. [Online]. Available http://water.epa.gov/drink/contaminants/.

Van, V., Fleet-Stalder and T. G. Chasteen. 2014. **Using fluorine-induced chemiluminescence to detect organo-metalloids in the headspace of phototrophic bacterial cultures amended with selenium and tellurium**. [Online]. Available http://www.shsu.edu/chm_tgc/publications/JPP/chasteen.htm.

Vass, M., K. Hruska and M. Franek. (2008). Nitrofuran antibiotics: a review on the application, prohibition and residual analysis (Publication., from Veterinarni Medicina: http://www.agriculturejournals.cz/publicFiles/02368.pdf

Villadangos, A. F., E. Ordóñez, M. I. Muñoz, I. M. Pastrana, M. Fiuza, J. A. Gil, L. M. Mateos and A. J. Aller. 2010. Retention of arsenate using genetically modified coryneform bacteria and determination of arsenic in solid samples by ICP-MS. **Talanta** 80(3): 1421-1427.

Viñas, P., N. Campillo, L. Carrasco and M. Hernández-Córdoba. 2007. Analysis of nitrofuran residues in animal feed using liquid chromatography and photodiode-array detection. **Chromatographia** 65(1-2): 85-89.

Visco, R. E. and E. A. Chandross. 1964. Electroluminescence in solutions of aromatic hydrocarbons. **Journal of the American Chemical Society** 86(23): 5350-5351.

Wang, J., M. Aki, D. Onoshima, K. Arinaga, N. Kaji, M. Tokeshi, S. Fujita, N. Yokoyama and Y. Baba. 2014. Microfluidic biosensor for the detection of DNA by fluorescence enhancement and the following streptavidin detection by fluorescence quenching. **Biosensors and Bioelectronics** 51: 280-285.

Wang, J. R. and L. Y. Zhang. 2006. Simultaneous determination and identification of furazolidone, furaltadone, nitrofurazone, and nitrovin in feeds by HPLC and LC-MS. **Journal of Liquid Chromatography and Related Technologies** 29(3): 377-390.

Wei, L., Z. Zhujun and Y. Liu. 2006. Chemiluminescence microfluidic chip fabricated in PMMA for determination of benzoyl peroxide in flour. **Food Chemistry** 95(4): 693-698.

Welna, M. and A. Szymczycha-Madeja. 2014. Effect of sample preparation procedure for the determination of As, Sb and Se in fruit juices by HG-ICP-OES. **Food Chemistry** 159: 414-419.

Wikipedia: the free encyclopedia. 2014. **Electrochemiluminescence**. [Online]. Available http://en.wikipedia.org/wiki/Electrochemiluminescence.

Wordbank. 2008. **Chronic arsenic poisoning: Pictures of sufferers**. [Online]. Available http://users.physics.harvard.edu/~wilson/arsenic/pictures/arsenic_project_pictures2.htm.

Xiang, Q., G. Hu, Y. Gao and D. Li. 2006. Miniaturized immunoassay microfluidic system with electrokinetic control. **Biosensors and Bioelectronics** 21(10): 2006-2009.

Xu, Z.-R., H.-Y. Pan, S.-K. Xu and Z.-L. Fang. 2000. A sequential injection on-line column preconcentration system for determination of cadmium by electrothermal atomic absorption spectrometry. **Spectrochimica Acta Part B: Atomic Spectroscopy** 55(3): 213-219.

Yan, X.-P., X.-B. Yin, X.-W. He and Y. Jiang. 2002. Flow Injection on-line sorption preconcentration coupled with hydride generation atomic fluorescence spectrometry for determination of (ultra) trace amounts of arsenic(III) and arsenic(V) in natural water samples. **Analytical Chemistry** 74(9): 2162-2166.

Yassine, O., P. Morin, O. Dispagne, L. Renaud, L. Denoroy, P. Kleimann, K. Faure, J. L. Rocca, N. Ouaini and R. Ferrigno. 2008. Electrophoresis PDMS/glass chips with continuous on-chip derivatization and analysis of amino acids using naphthalene-2,3-dicarboxaldehyde as fluorogenic agent. **Analytica Chimica Acta** 609(2): 215-222.

Yeh, H.-C., W.-T. Hsu and W.-Y. Lin. 2005. Enhancement in chemiluminescence by carbonate for cobalt(II)-catalyzed oxidation of luminol with hydrogen peroxide. **Journal of the Chinese Chemical Society** 52(4): 657-664.

Yi, W. J., Y. Li, G. Ran, H. Q. Luo and N. B. Li. 2012. Determination of cadmium(II) by square wave anodic stripping voltammetry using bismuth–antimony film electrode. **Sensors and Actuators B: Chemical** 166–167: 544-548.

Yilmaz, V., Z. Arslan, L. Rose and M. D. Little. 2013. Cyanovanadate(III) complexes as novel additives for efficient generation of volatile cadmium species in complex samples prior to determinations by inductively coupled plasma mass spectrometry (ICP-MS). **Talanta** 115: 681-687.

Yin, X.-B., Y. Du, X. Yang and E. Wang. 2005. Microfluidic chip with electrochemiluminescence detection using 2-(2-aminoethyl)-1-methylpyrrolidine labeling. **Journal of Chromatography A** 1091(1–2): 158-162.

Yin, X., Q. Chen, H. Song, M. Yang and H. Wang. 2013. Sensitive and selective electrochemiluminescent detection of nitrite using dual-stabilizer-capped CdTe quantum dots. **Electrochemistry Communications** 34: 81-85.

Yu, J., S. Wang, L. Ge and S. Ge. 2011. A novel chemiluminescence paper microfluidic biosensor based on enzymatic reaction for uric acid determination. **Biosensors and Bioelectronics** 26(7): 3284-3289.

Yu, X., D. Zhang, T. Li, L. Hao and X. Li. 2003. 3-D microarrays biochip for DNA amplification in polydimethylsiloxane (PDMS) elastomer. **Sensors and Actuators A: Physical** 108(1–3): 103-107.

Yu, Y., Z. Chen, S. He, B. Zhang, X. Li and M. Yao. 2014. Direct electron transfer of glucose oxidase and biosensing for glucose based on PDDA-capped gold nanoparticle modified graphene/multi-walled carbon nanotubes electrode. **Biosensors and Bioelectronics** 52: 147-152.

Zhang, J.-W., Y.-K. Wang, X. Du, X. Lei, J.-J. Ma and J.-C. Li. 2011. Ultrasound-assisted emulsification solidified floating organic drop microextraction for the determination of trace cadmium in water samples by flame atomic absorption spectrometry. **Journal of the Brazilian Chemical Society** 22: 446-453.

Zhang, Q. and M. Gong. 2014. Prototyping of poly(dimethylsiloxane) interfaces for flow gating, reagent mixing, and tubing connection in capillary electrophoresis. **Journal of Chromatography A** 1324: 231-237.

Zhang, Y., W. Wang, L. Li, Y. Huang and J. Cao. 2010. Eggshell membrane-based solid-phase extraction combined with hydride generation atomic fluorescence spectrometry for trace arsenic(V) in environmental water samples. **Talanta** 80(5): 1907-1912.

Zhang, Z. F., H. Cui, C. Z. Lai and L. J. Liu. 2005. Gold nanoparticle-catalyzed luminol chemiluminescence and its analytical applications. **Analytical Chemistry** 77(10): 3324-3329.

Zhu, W. W., N. B. Li and H. Q. Luo. 2007. Simultaneous determination of chromium(III) and cadmium(II) by differential pulse anodic stripping voltammetry on a stannum film electrode. **Talanta** 72(5): 1733-1737.

TABALE OF CONTENTS

Page

Page

LIST OF TABLES

LIST OF FIGURES

ABBREVIATIONS

Å	Angstrom
L	Liter
m	meter
mg L^{-1}	milligram per liter
mm	millimeter
nm	nano meter
ppb	parts per billion
µg L^{-1}	Microgram per liter
µFIA	Micro flow injection analysis
µL	Micro liter
µM	Micro molar
µm	Micrometer
AAS	Atomic absorption spectrometer
AFS	Atomic fluorescence spectrometer
ATSDR	Agency for toxic substances and disease registry
CL	Chemiluminescence
ECL	Electrogenerated chemiluminescence
ELISA	Enzyme-linked immunosorbent assay
EPA	Environmental protection agency
EU	European union
ETAAS	Electrothermal atomic absorption spectrometry
FAAS	Electrothermal atomic absorption spectrometry
FDA	Food and drug administration
FIA	Flow injection analysis
FTD	Furaltadone
FZD	Furazolidone
GC	Gas chromatography
HG	Hydride generation

HPLC	High performance liquid chromatography
IC	Ion chromatography
ICP-AES	Inductively coupled plasma with atomic emission spectroscopy
ICP-MS	Inductively coupled plasma mass spectrometry
ICP-OES	Inductively coupled plasma optical emission spectrometry
LC-DAD	Liquid chromatography with diode array
LC-MS	Liquid chromatography–mass spectrometry
LC-UV	Liquid chromatography-ultraviolet visible
LPCVD	Low-pressure chemical vapor deposition
MeCN	Acetonitrile
MEMS	Microelectromechanical system
MLCT	Metal-to-ligand charge-transfer
MRL	Maximum residuals limit
MST	Micro system technology
NFs	Nitrofuran
NFT	Nitrofuratoin
PA	Polyamide
PDMS	Polydimethylsiloxane
PL	Photoluminescence
PMMA	Polymethyl metacrylate
PMT	Photo multiplier tube
PP	Polypropylene
PS	Poly styrene
PTFE	Polytetrafluoroethylene
ROS	Relative oxygen species
SPE	Solid phase extraction
SPEC	Screen print carbon electrode
UV-DAD	Ultraviolet diode array detector
VGC	Vapor generation assmbly
WHO	World health organization